ANALYSIS OF HUMAN VESTIBULAR RESPONSES TO CALORIC STIMULATION

Robert Demers

[redacted] 1975-5

ANALYSIS OF HUMAN VESTIBULAR RESPONSES TO CALORIC STIMULATION

by

ROBERT DEMERS

A thesis submitted to the
Faculty of Graduate Studies and Research
in partial fulfillment of the requirements for
the degree of Doctor of Philosophy

Department of Electrical Engineering
McGill University
Montreal, Quebec
Canada

May, 1975

HUMAN VESTIBULAR RESPONSES TO CALORIC STIMULATION

R. Demers

ABSTRACT

ANALYSIS OF HUMAN VESTIBULAR RESPONSES TO CALORIC STIMULATION

The vestibular response to caloric stimulation is described by a general hypothetical model in which a distributed parameter representation of the relevant thermal processes is coupled to known physiological models of semicircular (s-c) canal dynamics and vestibular adaptation. The transfer function relating torque on the endolymph to irrigating medium temperature is characteristic of a wide band pass filter with distinct components related to heat transfer at the surface, heat conduction through the temporal bone and generation of torque around the s-c canal. An analysis is made of the torque step and pulse responses, of the effects of parameter variations and of the influences of vestibular dynamics. The model responses are compared to slow-phase eye velocity data from human subjects stimulated during continuous irrigation with temperature waveforms (sinusoids, steps and pulses) from a specially designed caloric stimulator. The major characteristics of the experimental responses are qualitatively explainable in terms of the model output torque and reflect the dominant role of thermal dynamics. The responses did not adapt to the extent predicted by the current representation of vestibular adaptation based on rotational studies and the adaptation filter was modified accordingly. The model output which includes both s-c canal dynamics and modified adaptation provided a significantly better fit to step response data than torque alone. The fact that the vestibular component could be separated from the overall caloric response may lead to interesting clinical applications.

RESUME

ANALYSE DE LA REPONSE VESTIBULAIRE A LA STIMULATION CALORIQUE CHEZ L'HOMME

Comme hypothèse de travail, on propose un modèle global de la réponse vestibulaire à la stimulation calorique dans lequel un système à paramètres continus s'appliquant aux phénomènes thermiques en jeu est relié aux modèles simples et connus de la dynamique du canal semi-circulaire (s-c) et de l'adaptation vestibulaire. La fonction de transfert mettant en rapport le couple gravitationnel agissant sur l'endolymphe et la température du fluide irrigant possède une caractéristique "bande passante" et est séparable en trois composantes distinctes d'échange de chaleur à la surface, de conduction de chaleur dans l'os temporal et de génération d'un couple sur le périmètre du canal s-c. L'analyse du modèle porte sur les aspects dynamiques des réponses à l'échelon et à l'impulsion de durée finie, sur l'effet des variations des paramètres et sur l'influence des composantes vestibulaires. Le modèle fut étudié chez l'homme stimulé par des ondes de température (sinusoides, échelon et impulsion) obtenues au moyen d'un stimulateur d'un type nouveau. Dans l'ensemble, les réponses expérimentales mesurées par la vitesse en phase lente du nystagmus oculaire reproduisent les caractéristiques majeures du couple théorique calculé selon le modèle et reflètent la prédominance des phénomènes thermiques. L'adaptation n'est pas aussi importante que prévu par les modèles antérieurs basés sur la réponse à la stimulation rotatoire. Après modification de la fonction représentant l'adaptation, on a obtenu un meilleur ajustement aux réponses expérimentales avec le modèle global qu'avec le modèle thermique simple. La composante vestibulaire peut donc être quantifiée au moyen du modèle global, ce qui permet d'entrevoir un certain nombre d'applications cliniques.

à

COLETTE,

MARIE-JULIE

et

ANNE-MARIE.

ACKNOWLEDGEMENTS

I wish to express my sincere gratitude to my research director, Dr. J. S. Outerbridge for his invaluable guidance, criticism and encouragement throughout the course of this work.

I wish also to acknowledge the support of the technical staff of the Otolaryngological Research Laboratories of the Royal Victoria Hospital. Messrs. John McColl and Leopold van Cleef helped in the construction of the caloric stimulator. Mr. Carmelo Granja advised on computer programming and wrote the software to handle the peripherals. Mrs. Eugenia Sokolowski did the photography work.

The assistance of Mr. M. Cheng in recording some of the experimental caloric step responses was greatly appreciated.

I am thankful to those many volunteers who joyfully accepted to have their ears washed and their vestibular system stimulated.

Miss Gaby Micaleff typed with patience a number of drafts of this thesis and the final copy was typed by Mrs. Elizabeth Wong.

Je suis très réconnaissant à l'HYDRO-QUEBEC pour le généreux octroi d'une bourse d'étude au cours des années 1970-72.

Toute ma gratitude est acquise à mon épouse pour son appui de tous les instants durant ce travail de longue haleine.

This work was conducted in the OTOLARYNGOLOGY RESEARCH LABORATORIES, Royal Victoria Hospital and McGill University, and was supported by Medical Research Council Grant MA-3794.

TABLE OF CONTENTS

CHAPTER 1

INTRODUCTION

In this thesis, the vestibulo-ocular response to caloric stimulation is studied using a quantitative model which is analyzed and tested experimentally. Attention is focused on the dynamic relationship between slow-phase eye velocity and water temperature in the external ear canal, both in the time- and in the frequency domains.

The study has been motivated by the clinical importance of the so-called caloric test which is used to evaluate vestibular functioning in patients with problems of vertigo and dizziness.

A first objective has been to deepen the current understanding of the complex processes involved in the caloric reaction phenomena. A second objective has been the application of the acquired knowledge to reexamine existing clinical procedures and to explore the full potential of caloric testing.

The caloric reaction in man is obtained by a simple procedure in which the ear canal is irrigated with hot or cold (relative to body temperature) water. Heat conducted through the bone acts indirectly on the semicircular canals, the sensing organs of the vestibular system, and generates characteristic eye movements (nystagmus) very similar to those produced by head motion stimuli.

The caloric reaction is usually explained in terms of a theory

proposed by Barany in 1906, some fifty years after the first reported observations of the phenomena by Brown-Sequard. In man and in other animals, the function of the semicircular canals is to transduce head angular motion. Head rotation results in a relative displacement of the fluid ring of endolymph within the canal, and the displaced fluid deflects and stimulates the sensory hair cells projecting into the ring. According to Barany's explanation, after irrigation of the ear canal with hot or cold water, a similar endolymph flow would result due to changes of the endolymph density as a temperature gradient is established across the semicircular canal in the temporal bone. The combined action of gravity and thermal expansion explains in particular the direction reversal of the response when going from hot to cold stimulation or from the prone to the supine position of the head.

Barany was the first to exploit the caloric reaction to examine patients with vestibular disorders. Various testing procedures were subsequently developed but the one originated by Fitzgerald and Hallpike (1942) was adopted as a standard by most clinical laboratories. In the Hallpike test, the ear canal on each side is subjected to two equal but opposite temperature stimuli in a sequence of four irrigations at 30 and 44°C. The eye response is characterized by horizontal nystagmus, an irregular sawtooth-like waveform which consists of a slow movement in one direction interrupted by saccades or quick phases in the other direction. The nystagmic responses are measured usually in terms of the peak velocity of the slow-phase component and from the set of four responses two basic measures of vestibular function

are derived: relative canal sensitivity (labyrinthine preponderance) and directional preponderance (the latter is characterized by nystagmus of greater intensity in one direction than in the other). These measures provide valuable diagnostic signs of organ defects and of lesions in the central nervous system.

The reliability of the caloric test has often been questioned. A major difficulty has been the great variability of sensitivities between subjects and the poor response repeatability in some individuals. This variability causes a significant overlap between normal and abnormal responses so that the test lacks precision as a diagnostic tool. Different measures of nystagmus response as well as new testing procedures have been proposed and evaluated by many clinical researchers but these attempts have not produced any breakthrough that could seriously challenge the Hallpike test as a standard. The lack of progress in the clinical area might be attributed in part to the empirical approach, characterizing the clinical research and to the limited efforts done on basic research concerning the caloric phenomenon.

A research program has been undertaken in this laboratory to evaluate clinical caloric testing within an appropriate theoretical framework centered around a mathematical model of the caloric response. The approach was suggested in part by Steer (1967) who introduced the first model relating slow-phase eye velocity to ear canal temperature. The work was also greatly stimulated by Young (1972) who provided important background material for the present study.

An essential tool of research is a model of the caloric reaction phenomena that can describe in quantitative terms the dynamic aspects

of the response such as rate of rise, time to peak etc. These aspects have received little attention in the past, and it has been widely assumed that a single arbitrarily selected measure such as duration or peak slow-phase velocity could adequately characterize the response.

A caloric response model might be applied to estimate systems parameters from recorded nystagmus by a suitable identification technique and, in principle, the vestibular component could be separated from other influences. A more objective evaluation of the caloric test is also possible with the model. For instance one might consider the interaction between successive irrigations, the significance of measures such as directional preponderance or the effect of parameter variations. Furthermore, a rational basis is provided for developing new testing procedures, and the questions treated might relate to the dynamic range of stimuli, the replacement of successive irrigations in a given ear by a single stimulus the minimization of test duration, etc. An important aspect of the use of the model throughout these applications is that the response variability can be studied and related to the specific parameters with known physical and physiological meaning.

In the context of this clinically oriented research program, the work presented in the thesis has been concerned with the fundamental problem of developing and validating an adequate model of the caloric process. As a starting point, previous models of Steer (1967), Schmaltz (1932) and Young (1972) have been investigated and on the basis of new experimental results, a more general representation of

the caloric reaction phenomenon has been developed that provides a useful working hypothesis.

It has been assumed that the overall nystagmus response to caloric stimulation is influenced by three different dynamic processes. The first process is that which generates a torque on the endolymph when a temperature stimulus is applied in the ear canal according to the theory of Barany. The second process involves the hydromechanical events in the semicircular canal that usually follow angular acceleration stimuli. The third process is neural adaptation, a high-pass filtering mechanism acting on the canal signal before it appears as nystagmus.

The overall caloric response model represents the dynamic relationship between irrigating water temperature and slow-phase eye velocity, respectively viewed as the input and the output variables of the system. The model is hypothetical since neither canal dynamics nor neural adaptation have been shown to exert significant influences on the caloric response, which is generally believed to be dominated by the sluggish thermal events. The new model extends and modifies the original representation of Steer that consisted only of the thermal process coupled to canal dynamics. Neural adaptation has since been emphasized in vestibular models and it has been included here as a possible component of the caloric response.

Mathematical representations of the processes underlying the caloric reaction phenomena have already been obtained in different contexts by a number of authors. In the present work, these representations have been coupled together without any major modification

to yield the overall caloric response model. On the one hand, the models of Schmaltz (1932) and of Young (1972) provide a quantitative description of the thermal phenomena that has been used in preference to Steer's because they offer a better explanation of new experimental data obtained in this study. On the other hand, the classic description of semicircular canal dynamics (van Egmond, Groen and Jongkees, 1949) has been simplified and combined with a first order high-pass "adaptation" filter, following here the approach of Malcolm and Melvill Jones (1970).

The caloric response model has been studied both theoretically and experimentally. In particular, an extensive analysis has been done of the basic models of Schmaltz (1932) and Young (1972) to clarify the dynamic characteristics of the caloric stimulation process. Experiments of a new type involving prolonged caloric stimulation have been conducted and the data applied to verify the general model. The results have indicated that both canal dynamics and neural adaptation exert significant influences on the overall caloric response.

Thesis Outline

In Chapter 2, further details are given concerning the relevant anatomical and physiological basis of vestibular system functioning and a critical review is made of the literature on caloric stimulation to give a proper perspective to the work presented here.

Chapter 3 is mainly theoretical. It begins with a detailed presentation of the models of Schmaltz and Young. A transfer function

relating torque on the endolymph to ear canal temperature is derived which has the characteristics of a wide band-pass filter and is mathematically separable into three components, each related to a physical process. The transfer function provides simple explanations for certain features of the pulse and step responses as well as for the effects of parameter variations. Also, it is shown that the temperature difference across the canal is very closely related to the torque and this provides the basis for an experimental verification of the model and for an approximate and simpler method of calculating the response. The overall model is then examined, and the possible roles of canal dynamics and adaptation are discussed.

The experimental section begins in Chapter 4 with a description of the apparatus and techniques. In particular, a fast-response thermal stimulator of new design is described. Chapter 5 reports experiments performed on human subjects. In contrast to the usual technique of caloric stimulation by short irrigations, precisely controlled periodic and transient temperature stimuli were delivered during sustained continuous irrigation.

First, the response to sinusoidal inputs was examined to determine the linearity of the system and its general characteristics in a frequency range extending from 0.0005 to 0.02 Hz.

Second, the response to step temperature changes was studied. Step responses recorded over 15 minutes exhibited sustained nystagmus and the corresponding slow-phase velocity output was analyzed quantitatively by a curve fitting program to determine the model parameters.

Finally two other experiments of an exploratory nature are

described. First, step responses were again recorded, but the water flow rate of the irrigation stream was varied to study the role of this parameter on heat transfer. The output curves were also fitted to the model to estimate the variation in the heat transfer coefficient.

Secondly, the responses to both temperature pulses and temperature pulses followed by a slow return to baseline temperature (tail) were recorded and compared. The temperature pulses "with tail" were intended to approximate the stimuli generated by the short irrigations used in the standard caloric test. The objective was to determine the relative importance of the uncontrolled "tail" part of the stimuli. Responses from the true pulses were also fitted to the model.

The final chapter summarizes the results and indicates a number of areas for future research.

CHAPTER 2

ANATOMICAL AND PHYSIOLOGICAL BASIS OF THE VESTIBULO-OCULAR REFLEX IN RELATION TO CALORIC STIMULATION

This chapter introduces the essentials of the anatomy and physiology of the vestibular system required for the understanding of the caloric vestibular response. The subject has been divided into the following general headings (a) anatomy and dynamic functioning of the semicircular canal, (b) the vestibulo-ocular system,and (c) associated phenomena due to neural processing mechanisms. The process of caloric stimulation is then discussed and a review of existing theoretical models is made. Finally, current trends in the development of caloric testing procedures are examined.

2.1 The Semicircular Canal: Anatomy and Function

The vestibular apparatus (figure 2.1) consists of three membranous semicircular ducts arranged in orthogonal planes and connected to a common sac, the utricle. The saccule is the other important structure of the vestibular labyrinth. All these components communicate with each other by various ducts and are filled with a fluid, the endolymph. They are encased in a system of corresponding cavities within the petrous portion of the temporal bone. Both the saccule and the utricle are found within a common central chamber, the vestibule; each possesses one otolith, an organ

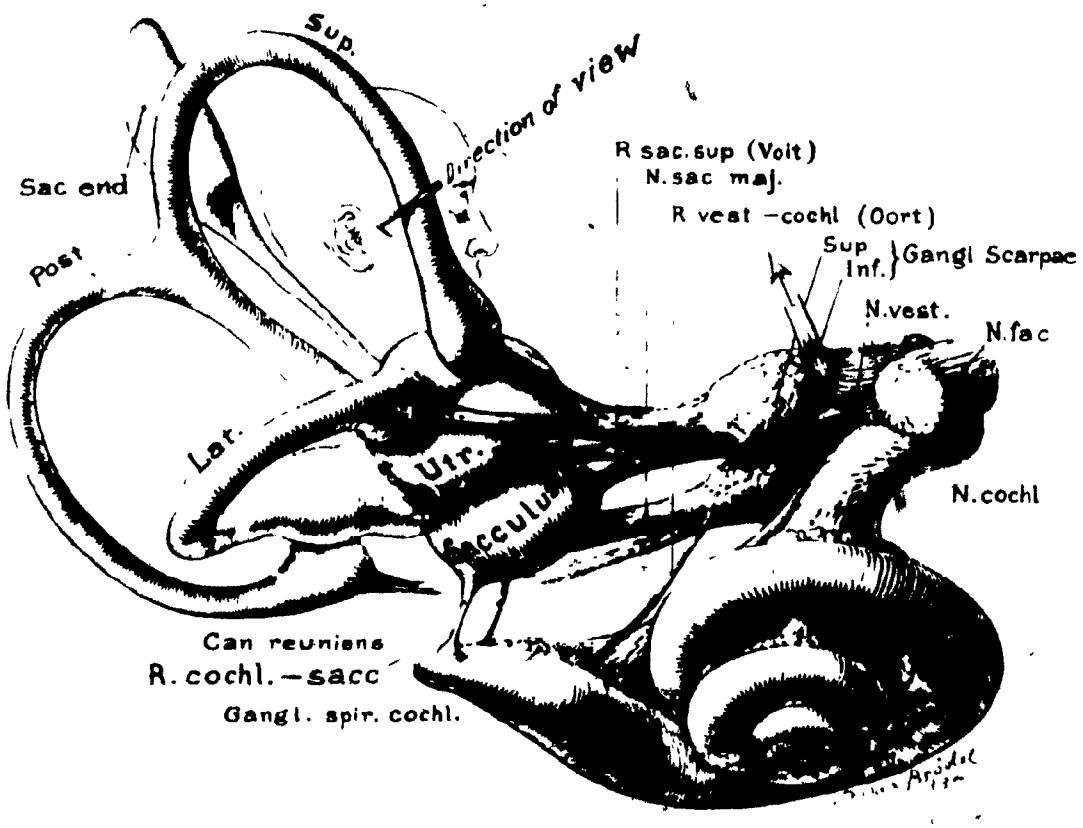

Fig. 2.1. Semi-diagrammatic drawing of the human vestibular apparatus (from M.Hardy, Anat. Rec. 59:412, 1934)

sensitive to linear acceleration. The membranous semicircular canals are of much smaller cross section than the corresponding bony canals in which they are supported by fibers and a fluid, the perilymph. An enlargement of the circular cross section called the ampulla is found at one end of each canal near the utricle; it contains the crista, a transverse crest of sensory hair cells, which supports the cupula, a gelatinous water-tight flap extending to the opposite wall of the ampulla.

Consider the schematic representation of a semicircular canal in figure 2.2. During angular acceleration of the skull, an inertial reaction torque is applied to the endolymph fluid ring within the semicircular canal, according to an elementary physics principle. This torque is opposed by viscous forces of the flow through the small cross section of the duct and by the weak elastic torque of the cupula. If laminar flow and small deviations are assumed, the dynamic equilibrium of these forces may be expressed in a differential equation (van Egmond, Groen and Jongkees, 1949) relating the angle of the deflected cupula θ_c to head angular acceleration $\ddot{\theta}_H$:

$$\ddot{\theta}_c + \frac{b}{J}\dot{\theta}_c + \frac{k}{J}\theta_c = a\ddot{\theta}_H \qquad (2.1)$$

where J is the moment of inertia of the fluid ring, b is the moment of viscous retardation per unit relative angular velocity of the fluid, and k is the moment of elastic retardation per unit relative angular displacement of the fluid. The factor a is a proportionality constant

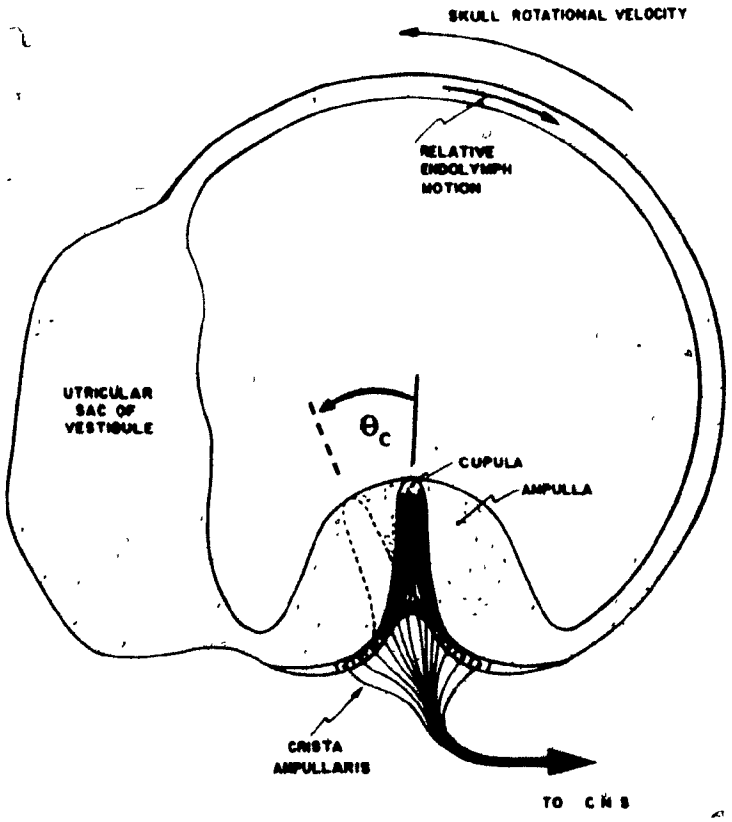

Fig. 2.2. Diagrammatic representation of an idealized semicircular canal (from Melvill Jones, G. & Milsum, J.H., IEEE Trans. Biomed. Eng. BME-12: 54-62, 1965).

between the cupular deflection angle and the relative angular displacement of the fluid.

Since $k \ll b$ and $J \ll b$, a transfer function may be written as

$$\frac{\Theta_c(s)}{\ddot{\Theta}_H(s)} = \frac{a \tau_1 \tau_2}{(\tau_1 s + 1)(\tau_2 s + 1)} \qquad (2.2)$$

where

$$\tau_1 \simeq \frac{b}{k} \qquad (2.3)$$

and

$$\tau_2 \simeq \frac{J}{b} \qquad (2.4)$$

J and b may be estimated from physical dimensions of the canal and fluid properties. The odd shape of the utricle is neglected and a uniform circular duct is assumed. However, appropriate circumferential lengths are considered when estimating the effective moment of inertia and viscous damping. According to the recent estimates of Money et al. (1971) the ratio J/b is 1/289 sec in man. Values around 1/200 sec have been suggested in the past by Schmaltz (1932) and Mayne (1965). Since k is unknown, τ_1 can only be estimated by experiments. When factors involving neural adaptation are taken into account, the time constant of the canal appears to be about 21 seconds in man (Young

and Oman 1969, Malcolm and Melvill Jones, 1970).

Because of the wide separation between the values of the canal time constants, the semicircular canal seems to function as a velocity transducer (Jones and Milsum, 1965). Indeed, in response to a velocity input (let $\ddot{\theta}_H = -s\dot{\theta}_H$ in equation 2.2) the cupula deflection yields approximately constant amplitude ratio and no phase shift over a wide range of frequencies (0.01 - 30 Hz) that probably spans the frequency spectrum of normal head movements (Jones and Spells, 1963).

2.2 The Vestibulo-Ocular System

The signal generated at the cupula gives rise to eye movements by what is called the vestibulo-ocular reflex. The most direct connections between the semicircular canal receptors and the eye muscles are shown in figure 2.3 to illustrate the case of horizontal eye movement. The receptors of the cristae are connected by the vestibular nerve to the several vestibular nuclei located in the brain stem of the central nervous system. There are two major pathways from the vestibular nuclei to the eyes, one to the oculomotor nucleus related to the medial rectus and the other to the abducens nucleus related to the lateral rectus. The two rectus muscles act on the eyeball in a push-pull fashion.

In figure 2.4, the neuro-anatomical pathways that are concerned with oculomotor control are shown in greater detail. They are introduced to illustrate the complexity of the system and to emphasize the interaction of the vestibular system with vision. It should also be noted that the vestibular system participates in many other reflexes

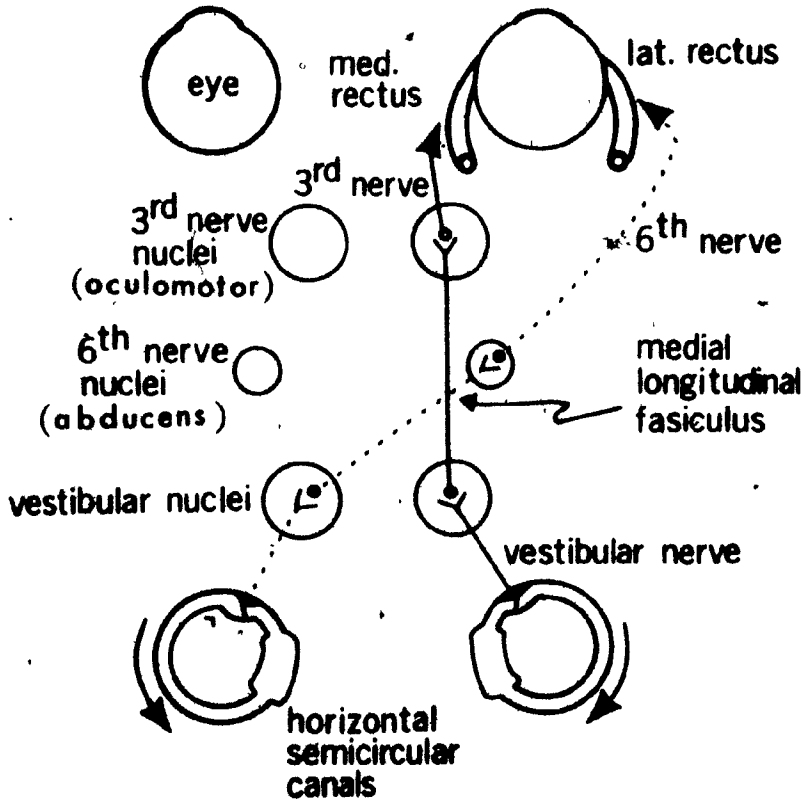

Fig. 2.3. Diagrammatic representation of neural connections in the horizontal plane from left and right semicircular canals to lateral and medial rectus muscles of the right eye. (Modified from Milsum, J.H. & Melvill Jones, G., Annals N.Y. Acad. Sci. 156: 851-871, 1969).

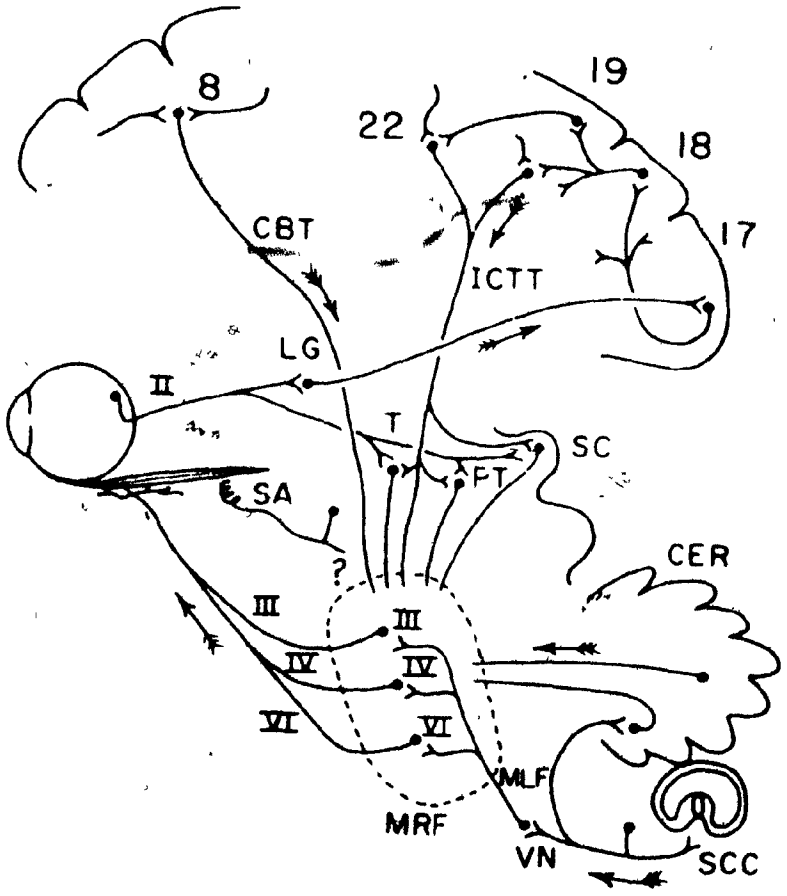

Fig. 2.4. Diagrammatic representation of the major known elements of the oculomotor system. SCC, semicircular canals; VN, vestibular nuclei; MLF, medial longitudinal fasciculus; MRF, mesencephalic and pontine reticular formation; III, IV, VI, the oculomotor, trochlear, and abducens nuclei and nerves; II, optic nerve; LG, lateral geniculate body; ICTT, internal corticotectal tract; 17, 18, 19, 22, primary and association visual areas; occipital and parietal; 8, frontal eye field; CBT, corticobular tract; T, tegmental nuclei; PT, pretectal nuclei; SC, superior colliculi; CER, cerebellum; SA, stretch afferents from extraocular muscles. (from Robinson, D.A. IEEE Proceedings 56: 1032-1049, 1968).

through additional connections from the vestibular nuclei to the spinal cord, the cerebellum and other nervous centers. These reflexes play an important role especially in postural control but they are not discussed further since they have no particular relevance to the problem considered in this thesis.

The eye position nystagmus signal recorded during stimulation of the vestibular system has often been considered as the sum of a continuous, slowly varying component and a staircase-like component with a position step change at every saccade. Such a decomposition has been justified by the fact that these components originate in different anatomical locations. Indeed, the slow-phase component appears to be related to the neural signal arising from the receptors in the cristae (figure 2.3) whereas the saccades come from one or more "generators" within the central nervous system (Monnier, 1967). The time derivative of the continuous position signal called the eye slow-phase velocity has first been used as an index of vestibular response by Buys (1924) and it has subsequently been found to be directly proportional to the deflection angle of the cupula as calculated from the torsion pendulum model of the semicircular canal (Hallpike and Hood, 1953). However, this very simple relationship does not hold quite true as will be seen below when discussing adaptation.

From figure 2.3, one may wonder how the signals from the receptor cells on both sides are integrated to provide the resultant slow-phase eye movement. An important principle of the functioning of the vestibular system is that the brain stem treats these signals as if

it were a differential amplifier, the differential output being directed to the push-pull eye muscle system. In absence of any stimulation, there exists a continuous neural tone transmitted from each canal and kept in balance with the other. During a rotation stimulus, the firing frequencies in the two vestibular nerves vary in a push-pull mode, i.e., one increases while the other decreases. In bilateral caloric stimulation the same temperature stimulus applied simultaneously to both ears yields no response as the state of balance is maintained by the increasing frequency levels on both sides.

In man, the vestibulo-ocular reflex appears to play an important role in visual image fixation (Jones and Milsum, 1965). The visual tracking system by itself performs satisfactorily only at relatively low frequencies of angular head movement and in the absence of vestibular effects considerable image slip would occur during the ordinary head movements of everyday life. However, the vestibulo-ocular reflex produces eye slow-phase movements that are compensatory and hence the retinal image slip is considerably reduced during the intervals between saccades. Thus, the semicircular canal in monitoring head angular velocity seems to provide a predictive "feed forward" signal to keep the eyes on target (Milsum, 1966).

2.3 Neural Processing Mechanisms

The vestibulo-ocular response is modified by neural processing mechanisms known mostly by the characteristics of the response under certain experimental conditions. Three different phenomena related

to such neural influences are mentioned: habituation, adaptation and inhibition due to reduced arousal.

Habituation

According to Monnier, Belin and Pole (1970), habituation is a general phenomenon that has been discovered by vestibular specialists and which is characterized by a response decline to repeated stimulation. An introduction to a number of concepts related to habituation as well as an extensive bibliography are given in the above reference.

Examples of studies of habituation to caloric stimulation may be found in Lidvall (1961a, 1961b), Henriksson et al. (1961) and Collins (1965). In man, vestibular habituation may depend on visual fixation and this is discussed in particular by Collins (1965) for caloric stimulation. This author showed that caloric testing repeated at one day intervals did not affect slow-phase velocity if the subjects had their eyes open in complete darkness, whereas a response decline was observed in a corresponding group with visual fixation. Collins' results seemed to contradict those obtained by Forssmann, Henriksson and Dolowitz (1963) who reported a significant decline of the peak slow-phase velocity when caloric stimuli were repeated at 5 minute intervals in similar conditions of recording with eyes open in the dark. However, it now seems that such habituation experiments involving a sequence of closely spaced caloric stimuli (Forssman et al., 1963; Fluur and Mendel, 1962a, 1962b), should perhaps be interpreted as if a single prolonged stimulus had been applied to the cupula. Indeed it is probable that after a 40 second irrigation the thermal stimulus acting on the endolymph persists for at least 10 minutes (Hood, 1973). Therefore, the response decline in such

experiments could also be attributed to thermal effects or to some form of adaptation.

Neural Adaptation

Adaptation has been introduced in the previous chapter as a component of a hypothetical model of caloric vestibular response. It is therefore appropriate to treat this question in greater detail.

The term adaptation is loosely defined as a response decline to a prolonged stimulus. In the vestibular system, the concept of adaptation has been expressed explicitly in the form of a mathematical model (Young and Oman, 1969; Malcolm and Melvill Jones, 1970) which has been found to account for a number of phenomena unexplainable by the classic torsion pendulum model of van Egmond and coworkers. Figure 2.5 is an example of such a phenomenon. The response shown follows a step change in head angular velocity, but instead of decreasing monotonically to zero after the initial rise as predicted by equation 2.2 the response becomes negative and is further prolonged beyond the expected duration.

The adaptation model of Malcolm and Melvill Jones (1970) is based upon two major assumptions: first, a shifting central reference level L is assumed to exist, which is continuously compared to the cupula signal. The rate of shifting is given by

$$\frac{dL}{dt} = \frac{1}{\tau_a}(\theta_c - L) \qquad (2.5)$$

where τ_a is the adaptation time constant.

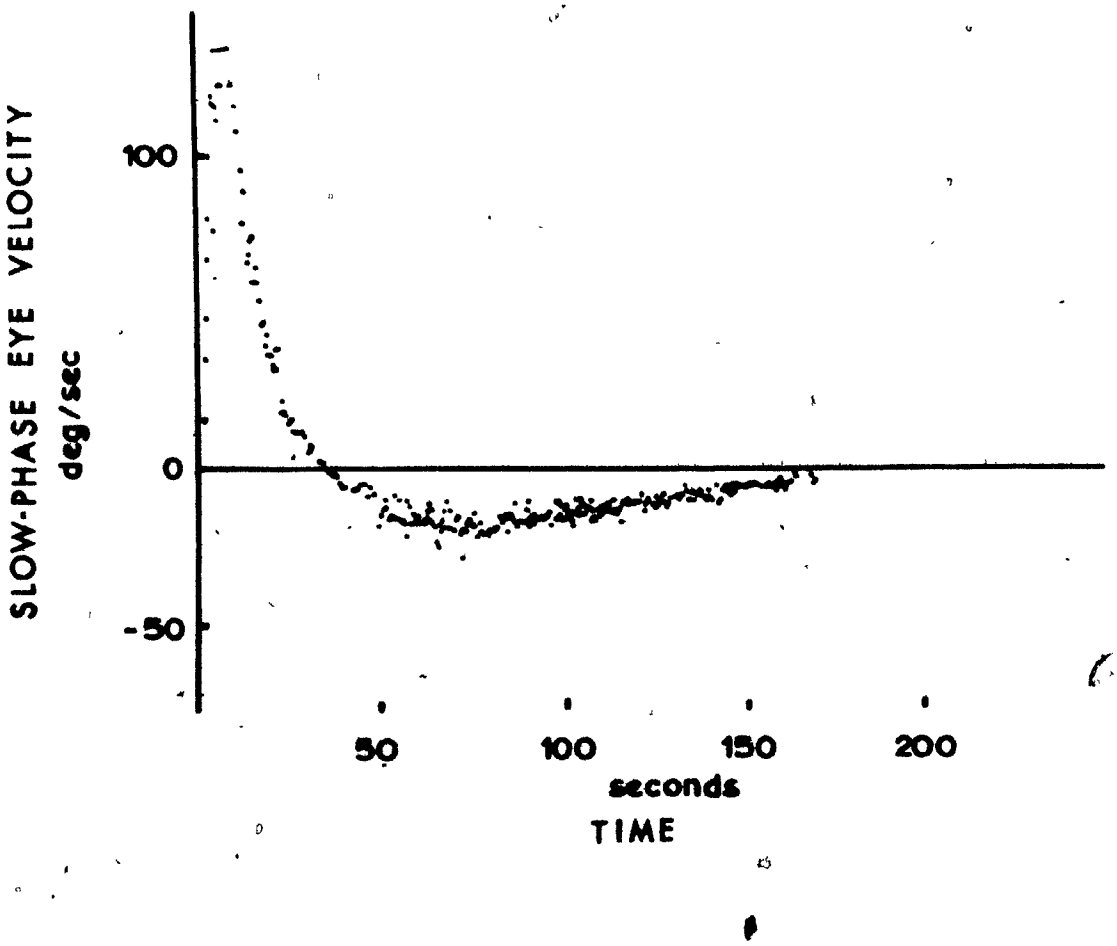

Fig. 2.5. The response to a step change in angular velocity of the head. The classic model of semicircular canal dynamics predicts an exponential decay to zero, after the initial peak. The negative overshoot of the response is explained by the adaptation phenomenon (from Malcolm, R. & Melvill Jones, G. Acta Otolaryng. 70: 126-135, 1970).

Second, slow-phase eye velocity is assumed to be proportional to the difference between the reference level and the cupula signal.

$$\dot{\theta}_e \propto (\theta_c - mL) \qquad (2.6)$$

where $\dot{\theta}_e$ is the eye slow-phase velocity and m is a so-called directional preponderance factor, set to 1 for normal subjects.

The associated transfer function given by Malcolm and Melvill Jones may be reduced to:

$$\frac{\dot{\theta}_e(s)}{\theta_c(s)} = \frac{\tau_a s + 1 - m}{\tau_a s + 1} \qquad (2.7)$$

with $0 \leq m \leq 1$

Equation 2.7 with $m = 1$ becomes

$$\frac{\dot{\theta}_e(s)}{\theta_c(s)} = \frac{\tau_a s}{\tau_a s + 1} \qquad (2.8)$$

which is identical to that derived by Young and Oman (1969).

Malcolm and Melvill Jones determined τ_a experimentally and obtained 82 seconds; on the other hand, Young and Oman used a τ_a value of 120 seconds. Young and Oman also modelled adaptation of the subjective sensation for which the time constant was 30 seconds. This lower value is consistent with the repeated observation that sensation

vanishes more rapidly than eye nystagmus. Stockwell, Gibson and Guedry (1973) gave further support to the value of the adaptation model and they discussed additional methods of identifying the time constant.

The existence of adaptation in the response to caloric stimulation has not been investigated previously. Young (1972) noted that in the response of some subjects to a temperature pulse, there was a decline which occurred before the theoretically predicted decline of pressure on the cupula. This was interpreted qualitatively as evidence of adaptation. Hood (1973) described an experiment in which subjects were submitted to a standard irrigation in the supine position and nystagmus was recorded until it vanished after about 4 minutes. The subjects were then turned into the prone position, following which nystagmus reappeared in the opposite direction for another 4 minutes. The sequence was repeated with a progressively attenuating response. The results indicate that the thermal effects on the canal endolymph from a 40 second irrigation may extend over 10 minutes. The disappearance of the nystagmic response after four minutes suggests that some adaptation took place.

Arousal Factors

Another central factor influencing vestibular nystagmus is the level of arousal of the subject. It is common experience that rapid changes in the nystagmus pattern may occur as a drowsy subject becomes alert. In vestibular testing in general, a current practice is to have the subject perform mental arithmetic or other intellectual activities that maintain the arousal level sufficiently high. Collins (1963) has investigated arousal factors during caloric stimulation and shown that

slow-phase eye velocity is decreased during reverie, as if the system gain were turned down. Torok (1970) has advocated simple relaxed attention rather than forced mental alertness and he has indicated that reverie does not affect the peak nystagmus frequency of the caloric response.

2.4 The Process of Caloric Stimulation

It is appropriate to recall how Barany explained the process of caloric stimulation. During and after irrigation of the ear canal, a temperature gradient is set up within the bone across the semicircular canal. Because of the changes in endolymph density, the equilibrium of the gravity forces acting on the fluid is perturbed and hence, endolymph flow is produced. It is generally believed that the heat from the thermal stimulus is conducted preferentially through a short bony ridge which connects the horizontal semicircular canal to the posterior and upper part of the auditory meatus near the tympanic membrane. The distance from the bone surface to the canal center is approximately 0.76 cm in man (Young, 1972).

In order to verify the extent of temperature changes occurring during caloric stimulation, a number of experimenters have inserted sensitive thermocouples close to or inside the semicircular canal in cadavers (Schmaltz and Volger, 1924), in temporal bone preparations (Dohlman, 1925), in human skulls (Young, 1972) and in patients undergoing surgery of the labyrinth (Cawthorne and Cobb, 1954; Kleinfelt and Dahl, 1968). Generally, the results obtained by these authors have demonstrated that significant temperature changes occur in the temporal bone or in the semicircular canal. The most quoted reference is probably Cawthorne and Cobb (1954) who measured in man the time course of the temperature difference

between opposite points within the perilymphatic space of the horizontal canal. The importance of these measurements of temperature gradient across the canal lies in the fact that such measurements have been so far the only direct method to assess the validity of Barany's theory.

Harrington (1969) has challenged the concept of the bone as a main heat pathway and he claims that heat can travel just as well or even better through the air-filled middle ear. However, this conclusion is difficult to accept from a physical viewpoint since Dohlman (1925) has shown that bone thermal conductivity is 4 to 8 times greater than that of air. Harrington's data should therefore be interpreted cautiously, and perhaps new experiments done since the basis of existing theoretical models of caloric stimulation is seriously questioned by these data and since no other similar work is reported in the literature.

The interpretation of semicircular canal or bone temperature measurements usually brings up the question of vascular influences. In principle at least, heat could be carried away from the temporal bone site by the vessels in the skin of the auditory meatus, in the bone itself or on the walls of the membranous ducts and sacs of the labyrinth.

A debate has always existed in the literature on the greater sensitivity to cold stimuli than to hot, due presumably to a vasoconstrictive effect of the cold (Jongkees, 1948; Steer, 1967; Brunner and Norris, 1971). On the other hand, Aschan, Bergstedt and Stahle (1956) and Henriksson (1956) have noted that such a difference could arise from a systematic error in delivering exactly opposite temperature stimuli, since the hot stimulus

might be smaller than the cold one because of greater heat losses along the hot cannula carrying the water to the ear. These authors recorded no difference between hot and cold responses when temperatures were very carefully controlled.

The question of vascular influences has also appeared to account for variation of caloric response due to changes in body position (Jongkees, 1948; Das and Mehra, 1969). On the whole, blood flow seems to have a relatively minor influence on the caloric response and therefore it is not discussed in any further detail.

2.5 Previous Theoretical Works

The phenomenon of caloric stimulation in man has been treated analytically by Schmaltz (1932), Steer (1967) and Young (1972) and the contribution of these authors will be emphasized in forthcoming paragraphs. Other related works have been published by Gusev (1970) and Lebovitz (1973). Gusev developed a mathematical theory to explain experimental data from pigeons who had their semicircular canal simultaneously rotated and heated by a point source. Lebovitz discussed the theoretical basis of vestibular stimulation by absorption of (VHF) microwaves within the human semicircular canal. The interest of these works lie mainly in the illustration of unusual phenomena of caloric stimulation.

Schmaltz (1932) was the first to express the theory of Barany in a quantitative model using mathematical equations derived from basic physical laws. In particular, he applied the well known heat conduction equation to estimate the temperature variations across a semicircular canal within a semi-infinite solid bone. He also calculated endolymph density

changes according to the principle of thermal expansion of fluid and then used Poisseuille's law to obtain the resultant velocity of endolymph flow. Unfortunately, he did not take into account the cupula reaction, which he considered as negligible.

Steer (1967) made the simplifying assumption that a linear temperature gradient was generated across the semicircular canal as if the input temperature at the ear canal was filtered through a first order lag. The gradient produced a torque on the endolymph which was looked at as an equivalent angular acceleration, that was fed to the input of the classic semicircular canal model discussed previously.

Young (1972) extended Schmaltz's model and in particular included the important boundary condition of limited heat transfer at the bone surface. Furthermore, he validated the assumption of unidimensional heat flow in the representation of heat conduction through bone by the following experiment. Steady state temperature measurements were performed at increasing distances from the surface in temporal bones of human skulls using sinusoidally varying temperatures at the external auditory meatus. The amplitudes and the phases were shown to be linear functions of distance, as predicted by the steady state solutions of the heat conduction equation (figure 2.6). Young also derived the output pressures applied to the cupula for pulse and sinusoidal inputs which he then qualitatively compared to slow-phase eye velocity responses from human subjects.

These theoretical works will be discussed further in the next chapter where an analysis of Young's model is carried out in detail.

2.6 Current Trends in Caloric Testing

There have been few attempts to depart from the standard caloric test

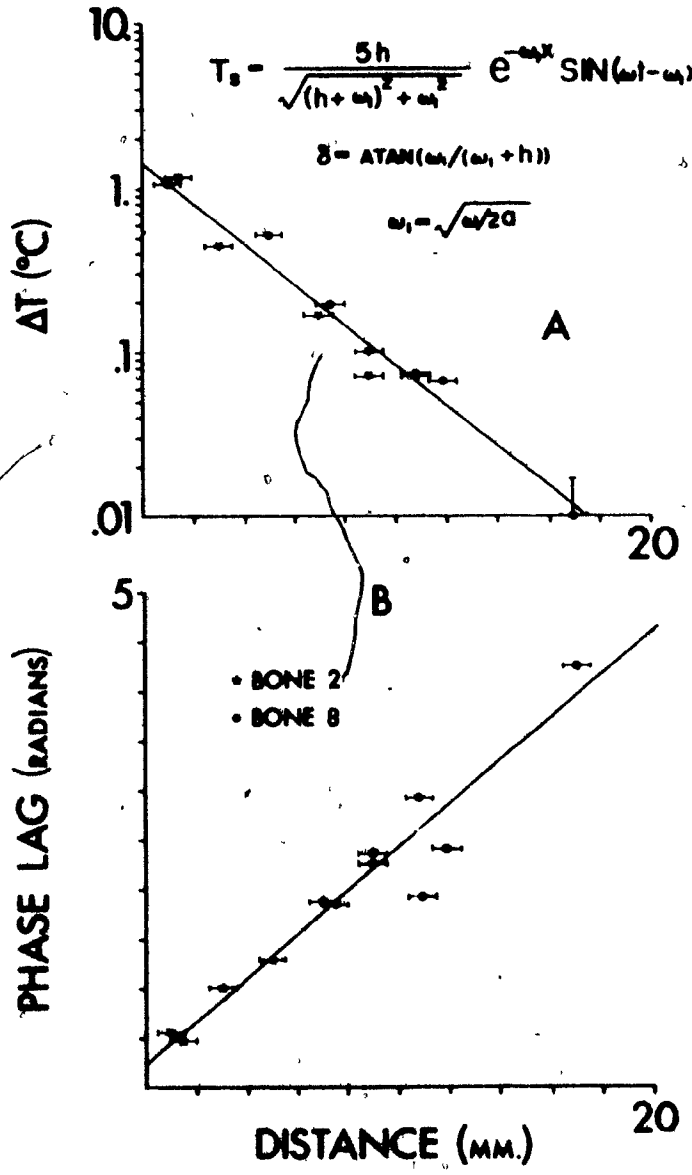

Fig. 2.6. Amplitude and phase of temperature (T_s) recorded at various distances within the temporal bone of human skulls. The period of the input temperature signal within the external ear canal was about 200 seconds. Amplitude decreased exponentially and phase increased linearly with increasing distance from the temporal bone surface as predicted by the model equation. (from Young, J.H., Ph.D. Thesis, University of Michigan, 1972).

procedure, and in most cases they have met with limited success. A hot caloric test with only one irrigation per ear has been proposed (Bernstein, 1965; Halama and Hinchcliffe, 1970; Barber et al. 1971) but according to Dayal and coworkers (1973), the test is not to be recommended as it further complicates the problem of interpretation. An interesting approach has been tested by Litton and McCabe (1967) who used a sequence of gradually increasing cold stimuli in order to obtain some measure of the response linearity. These authors assumed that departures from linearity might be due to neural fatigue or "recruitment" depending on the shape of the curve recorded. They found in a few clinical cases that these nonlinearities were the only abnormal findings. Steffen, Linthicum and Churchill (1970) claimed that the Litton and McCabe's technique could be automated by delivering a ramp of temperature from 37° to 19°C over a 5 minute period. This application of a continuous temperature waveform is an interesting one but it has unfortunately been done without an appropriate theoretical basis.

New temperature-controlled air stimulators have been produced that may eventually replace the classic water baths. Their main advantages lie in the ease of manipulation and the tolerance by all subjects including those with perforated tympanic membrane (Gates, Young and Winegar, 1970; Baertschi and Allison, 1972; Albernaz and Guananca, 1973). However, according to Capps and Preciado (1973), much higher air temperatures must be used to obtain response levels comparable to those obtained with water. In this respect, it should be noted that due to the different thermal characteristics of air and water, gas flow rate

must be very high to provide a thermal stimulus equivalent to that of water irrigation. One may compare for instance the results of Aantaa(1967) and Young (1972) respectively obtained at 2 and 5 L/min air flow. The responses at 2 L/min are approximately half those obtained at 5 L/min and the latter are closer to responses obtained with standard water irrigation (250 ml/min).

Obviously, further studies are needed before gas stimulators can be used on a routine basis. The gas flow rate factor is in fact related to the more general question of heat transfer in the caloric stimulation process which will be discussed in this work.

CHAPTER 3

THEORETICAL ANALYSIS OF A VESTIBULAR RESPONSE MODEL

3.1 Introduction

In this chapter, a detailed analysis of a model relating thermal torque on the endolymph to ear canal temperature is presented. The model has been taken from the recently published thesis of Young (1972) who extended the original work of Schmaltz (1925). Young's model has been further developed into a more general representation of the vestibulo-ocular response by addition of the well known models of semicircular canal dynamics and neural adaptation.

Our main objectives have been first, to describe the fundamental characteristics of the caloric stimulation process, and secondly, to make a number of predictions which will be used in next chapter to interpret experimental vestibulo-ocular responses.

The model of Young and Schmaltz is introduced formally in section 3.2. The work presented in the following sections is original and has been published in part as a conference abstract (Demers and Outerbridge, 1974).

In sections 3.3 and 3.4, attention is focused on two inter-connected aspects, the transfer function relating output torque to ear canal temperature and the torque response to a step change in temperature. The emphasis put on these elementary aspects can be justified from

basic concepts of systems theory. Indeed, the characteristics of any process described by a linear differential equation are completely described by the corresponding transfer function in the frequency domain and by the system impulse response (or its time integral, the step response) in the time domain. The step response has been preferred here since it applies more readily to the experimental work of next chapter.

In section 3.5, the effects of varying the model parameters are examined to provide basic material for practical analysis of experimental caloric responses. This is also a first step in tackling the basic problem of the variability of the caloric response between subjects that has made the clinical test somewhat unreliable.

In section 3.6, the theoretical relation between output torque and the temperature difference across the semicircular canal is derived and analyzed. The question is particularly relevant since the measurement of the temperature difference across the canal has widely been considered as a direct measure of the stimulus acting on the endolymph. The validity of this interpretation is assessed, since the torque on the endolymph in fact depends on the temperature distribution around the canal, and a simplified method of torque calculation is described.

In section 3.7 an overall model is described which relates vestibulo-ocular response to input temperature at the ear canal. The thermal process transfer function is now coupled to a simplified

representation of canal dynamics in series with a neural adaptation filter. The mathematical formulation of the model is discussed and theoretical output curves are examined which are used to interpret the experimental results of next chapter.

3.2 The Semi-Infinite Solid Model

The complex geometries of the external ear canal and of the temporal bone are simplified by assuming a semi-infinite solid of homogeneous material with uniform conditions over the plane surface of heat exchange with the irrigating medium (figure 3.1). In this solid, unidimensional heat flow occurs according to the classic heat conduction equation,

$$\frac{\partial^2 T}{\partial x^2} = - \frac{\rho_B c_B}{\kappa_B} \frac{\partial T}{\partial t} \qquad (3.2.1)$$

where $T = T(x,t)$ is the temperature at time t(sec) and distance x(cm) from the surface. The parameters ρ_B, c_B and κ_B represent the density, the specific heat and the thermal conductivity of the temporal bone. The group

$$\alpha = \frac{\kappa_B}{\rho_B c_B} \qquad (3.2.2)$$

is defined as the thermal diffusivity and has the dimension $cm^2 sec^{-1}$.

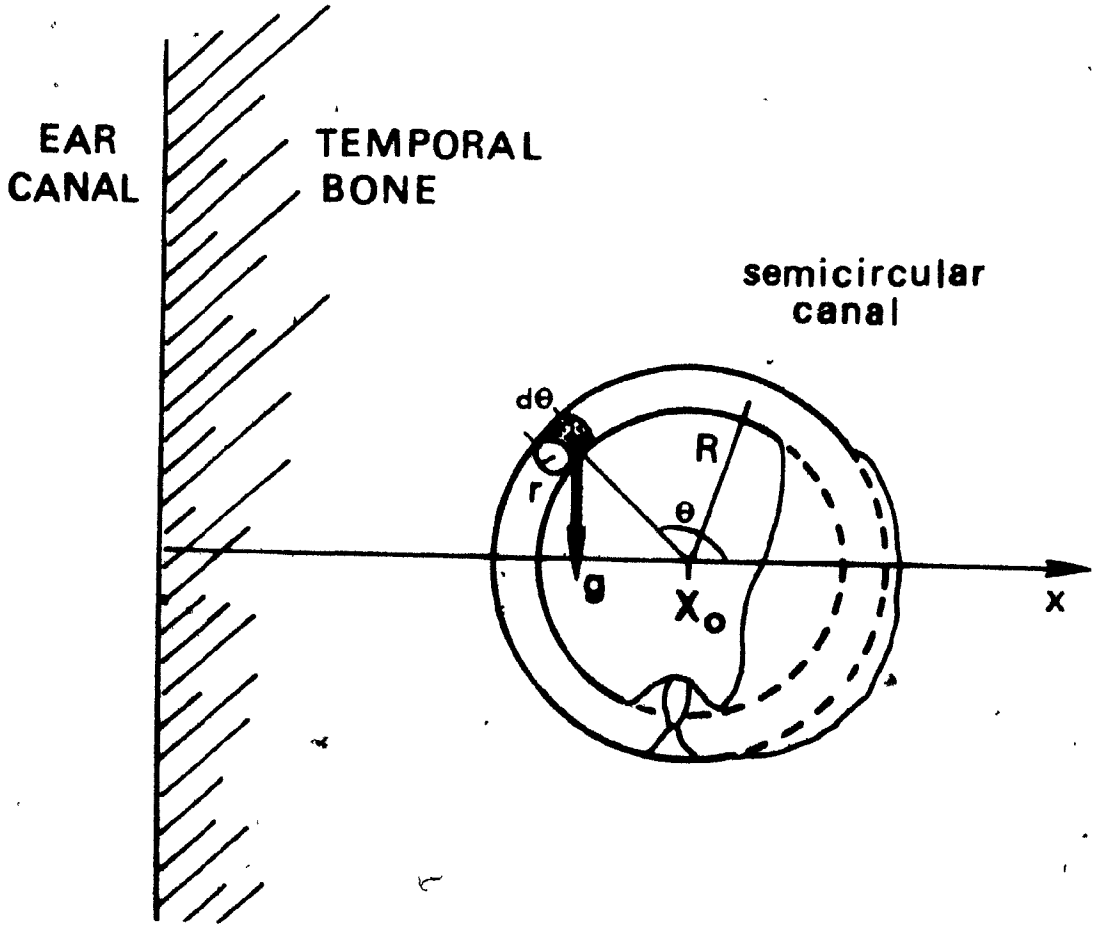

Fig. 3.1. Diagrammatic representation of the semicircular canal within the temporal bone represented as a semi-infinite solid. R = large radius of the semicircular canal; r, small radius; X_o, distance to canal center from surface; g, gravitational constant.

Boundary conditions are defined as follows:

(1) at infinity, a constant temperature is assumed, equal to body temperature and for convenience taken here as the zero temperature level

$$T(\infty,t) = T_o = 0 \qquad (3.2.3)$$

(2) at the surface, a linear process is assumed to govern the rate of heat transfer (Young, 1972), i.e.,

$$\kappa_B \frac{\partial T}{\partial x} = H \cdot (T_w - T) \Bigg]_{x=0} \qquad (3.2.4)$$

where T_w is the temperature of the irrigating medium (water) and H is the heat transfer coefficient. H depends on a number of factors such as surface conditions and flow characteristics, and in practice can only be determined by experiment. Equation 3.2.4 is better expressed as

$$\frac{\partial T}{\partial x} = h\,(T - T_w) \Bigg]_{x=0} \qquad (3.2.5)$$

where

$$h = \frac{H}{\kappa_B} \qquad (3.2.6)$$

The initial conditions are defined by uniform body temperature throughout the solid at $t = 0$:

$$T(x,0) = T_o \qquad (3.2.7)$$

The solution of 3.2.1 given these initial and boundary conditions is a classic problem treated in the theory of heat conduction in solids and solutions may be found in many textbooks, e.g. Carslaw and Jaeger (1959) and Miller (1956).

Torque Generation

Consider the idealized lateral semicircular canal as a toroid of circumference $2\pi R$ and cross-section πr^2, embedded within the bony solid with its center at a distance X_o from the surface. The gravity force acts on the elementary mass $\pi r^2 R d\theta$ and the force component tangential to the canal circumference produces a torque dM on the endolymph with respect to canal center axis, given by

$$dM = \pi \rho_F g r^2 R^2 \cos\theta \, d\theta \qquad (3.2.8)$$

Equation 3.2.8 pertains to the case where the gravity force is in the canal plane and perpendicular to the direction of heat flow. A more general case is the one in which the gravity vector is at arbitrary angles with both canal plane and direction of heat flow. This case is not discussed since it introduces additional multiplicative factors without changing the basic nature of the results. The net overall torque M is obtained by integration over the circumference;

$$M = \pi g r^2 R^2 \int_0^{2\pi} \rho_F \cos\theta \, d\theta \qquad (3.2.9)$$

From the basic experimental definition of thermal coefficient of expansion β, the endolymph density ρ_F may be written as a function of temperature around T_o,

$$\rho_F(T) \simeq \rho_F(T_o) \left[1 - \beta (T - T_o)\right] \qquad (3.2.10)$$

Denoting by $T(\theta,t)$ the temperature on the canal circumference and taking 3.2.10 into 3.2.9, one obtains

$$M = -\beta\rho_F(T_o)\, g\, \pi\, r^2\, R^2 \int_0^{2\pi} T(\theta,t) \cos\theta\, d\theta \qquad (3.2.11)$$

Letting

$$C_1 = -\beta\rho_F(T_o)\, g\, \pi\, r^2\, R^2 \qquad (3.2.12)$$

3.2.11 becomes

$$M = C_1 \int_0^{2\pi} T(\theta,t) \cos\theta\, d\theta \qquad (3.2.13)$$

Now since pressure = force ÷ area, the pressure differential ΔP across the cupula may also be calculated by 3.2.13 except that C_1 is replaced by C_2

where $$C_2 = -\beta\rho_F(T_o)\, g\, R \qquad (3.2.14)$$

Young (1972) used the exact temperature distribution $T(\Theta,t)$, obtained by solving the heat conduction equation to calculate the pressure differential across the cupula. On the other hand, Schmaltz (1932) assumed that the temperature gradient was sufficiently linear across the canal to allow calculating the endolymph velocity from $\partial T/\partial x$ evaluated at the center of the canal. Using this assumption in the above equations, one can indeed show that

$$M \simeq C_1 \pi R \frac{\partial T}{\partial x} (X_o,t) \qquad (3.2.15)$$

Finally, Steer (1967) avoided computing $\partial T/\partial x$ from the heat conduction equation as Schmaltz did. He simply assumed that the temperature gradient followed the time course of a first order lag. However, such a representation poorly describes the system, as will be shown below.

The model contains a large number of parameters, listed for convenience in Table 3.1, along with the estimated values for man. In particular, one may note that the thermal properties of the temporal bone are not very well known. For a long time, the only measurements of bone conductivity were those made by Dohlman (1925) on slices of ox femur, for which he obtained values of $2.4 - 4.8 \times 10^{-4}$ gm-cal/cm-sec-C°. The bone conductivity values shown in Table 3.1 were derived by Young (1972) from equation 3.2.6 using both measurements of figure 2.6 and estimates of H based upon approximating models from heat transfer technology. Similarly, prior to Young's work, the only figure for thermal diffusivity was 0.00175 cm^2-sec^{-1} given by Schmaltz (1925).

TABLE 3.1

ρ_B	density of bone	?	$gm\ cm^{-3}$	
c_B	specific heat of bone	?	$cal\text{-}^oC^{-1}$	
κ_B	thermal conductivity of bone	$1.2 - 4.2 \times 10^{-4}$	$\frac{gm\text{-}cal}{sec\text{-}cm\text{-}^oC}$	Young (1972)
α	thermal diffusivity of bone	0.0025	$cm^2\text{-}sec^{-1}$	Young (1972)
ρ_F	specific gravity of endolymph	1.008	$gm\text{-}cm^{-3}$	Money (1971)
β	thermal expansion coefficient of endolymph	4.4×10^{-4}	$^oC^{-1}$	Steer (1967)
r	small s-c canal radius (figure 3.1)	0.014	cm	Jones and Spells (1963)
R	large s-c canal radius	0.315	cm	Igarashi (1966)
X_o	distance to s-c canal center	0.76	cm	Young (1972)
h	ratio - $\frac{\text{heat transfer coefficient}}{\text{bone thermal conductivity}}$	5.0	cm^{-1}	Young (1972)

The constant C_1 calculated from Table 3.1 values is

$$C_1 = 2.65 \times 10^{-5} \text{ dyne } -\text{cm}^{\circ}\text{C}^{-1} .$$

and

$$C_2 = 0.136 \text{ dyne - cm}^{-2} \ ^{\circ}\text{C}^{-1}.$$

The values from Table 3.1 will be referred to as normal in the following paragraphs.

3.3 Torque/Temperature Transfer Function

Laplace transformation of 3.2.1, 3.2.5 and 3.2.7 yields

$$T(x,s) = \frac{h}{h + \sqrt{\frac{s}{\alpha}}} e^{-x\sqrt{\frac{s}{\alpha}}} T_w(s) \qquad (3.3.1)$$

In 3.3.1, s denotes the complex frequency variable. It is also clear from the context that T (x,s) stands for the Laplace transform of T (x,t) and this simple notation will be applied to other variables whenever necessary. The derivation of 3.3.1 is again found in many textbooks, e.g. Carslaw and Jaeger (1959).

Applying the Laplace transformation to 3.2.13, one obtains

$$M(s) = C_1 \int_0^{2\pi} T(\theta,s) \cos\theta \, d\theta \qquad (3.3.2)$$

From figure 3.1

$$x = X_o + R \cos \Theta \qquad (3.3.3)$$

From the above, one obtains

$$\frac{M(s)}{T_w(s)} = C_1 \frac{h}{h + \sqrt{\frac{s}{\alpha}}} e^{-X_o\sqrt{\frac{s}{\alpha}}} \int_0^{2\pi} e^{-\sqrt{\frac{s}{\alpha}} R \cos \Theta} \cos \Theta \, d\Theta \qquad (3.3.4)$$

The above expression is the transfer function describing the relationship between the output torque applied to the endolymph fluid and the input temperature of the irrigating fluid.

Now, given the general form of the modified Bessel function of order N

$$I_N(z) = \frac{1}{\pi} \int_0^{\pi} e^{z \cos \Theta} \cos n\Theta \, d\Theta \qquad (3.3.5)$$

where z is a complex variable, and, since cos Θ is symmetric relative to the x axis, it is easy to verify that

$$\int_0^{2\pi} e^{-\sqrt{\frac{s}{\alpha}} R \cos \Theta} \cos \Theta \, d\Theta = 2\pi I_1 \left(-R\sqrt{\frac{s}{\alpha}}\right) \qquad (3.3.6)$$

From a basic property of the Bessel function

$$I_1(z) = -I_1(-z) \qquad (3.3.7)$$

and the transfer function is finally expressed as

$$\frac{M(s)}{T_w(s)} = -2C_1 \frac{h}{h + \sqrt{\frac{s}{\alpha}}} e^{-X_o\sqrt{\frac{s}{\alpha}}} \pi I_1\left(R\sqrt{\frac{s}{\alpha}}\right) \qquad (3.3.8)$$

The above transfer function has quite a remarkable form. It consists of three mathematically separable components that can be related to different physical processes, and they will be discussed separately in the forthcoming paragraphs. In all components, the frequency variable s is always under the square root sign and appears associated with the diffusivity parameter, thus allowing definition of a generalized frequency variable.

$$s' = \frac{s}{\alpha} \qquad (3.3.9)$$

The dimensions of s' are cm^{-2}.

In addition, each of the three components has its own characteristic parameter, h, X_o and R respectively. The transfer function $M(s)/T_w(s)$ and its components are double valued functions, because of the fractional power of s; these functions are therefore non-analytic and require

special treatment for their inverse transformation (De Russo, Roy, Close, 1967).

The first component

$$\frac{h}{h + \sqrt{s'}}$$

is related to the heat transfer process due to forced convection at the temporal bone surface within the ear. It may be considered as the transfer function relating the surface temperature $T(0,s)$ to the temperature of the irrigating fluid, as made evident by letting $x = 0$ in 3.3.1. Except for the square root operator, the form is that of a first order lag. This is apparent in the Bode plot of figure 3.2 and one may observe a high frequency asymptote with a negative slope of 10 db/decade, and a maximum phase shift of 45^{o}.

The second component

$$e^{-X_o \sqrt{s'}}$$

is associated with the heat conduction process within the semi-infinite solid. It is the transfer function relating the temperature at the center of the semi-circular canal to the surface temperature. The operator $e^{-\sqrt{s}}$ is often called the diffusion operator and has been discussed in other contexts e.g. Jones (1969). The Bode plot (figure 3.3) is characterized by infinite attenuation and phase lag at high frequencies.

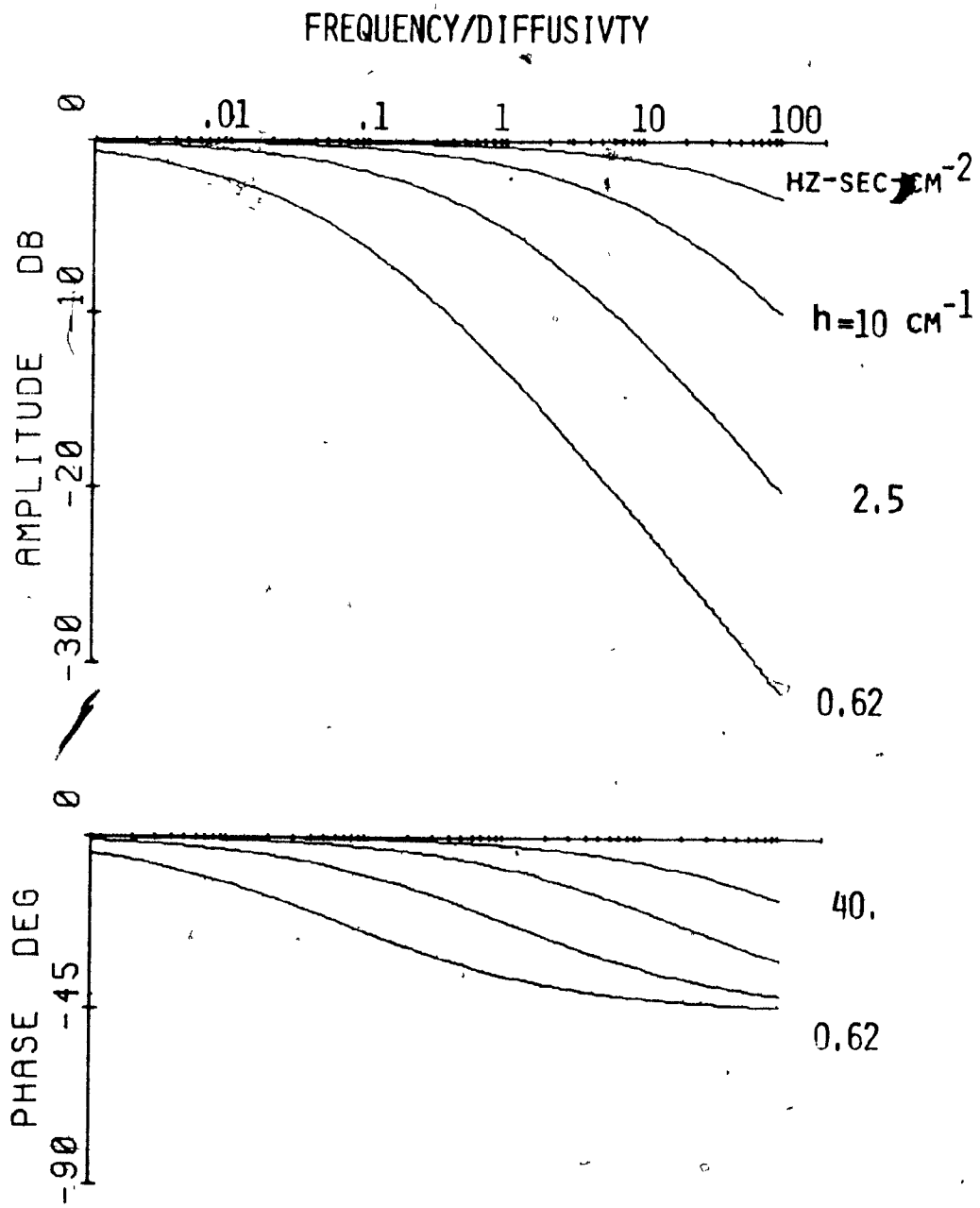

Fig. 3.2. Frequency characteristics of $h/(h + s/\alpha)$ describing the linear heat transfer process at the surface of the semi-infinite solid bone. The function relates the surface temperature to the temperature of the irrigating medium. h = heat transfer coefficient/bone thermal conductivity. α = thermal diffusivity of bone.

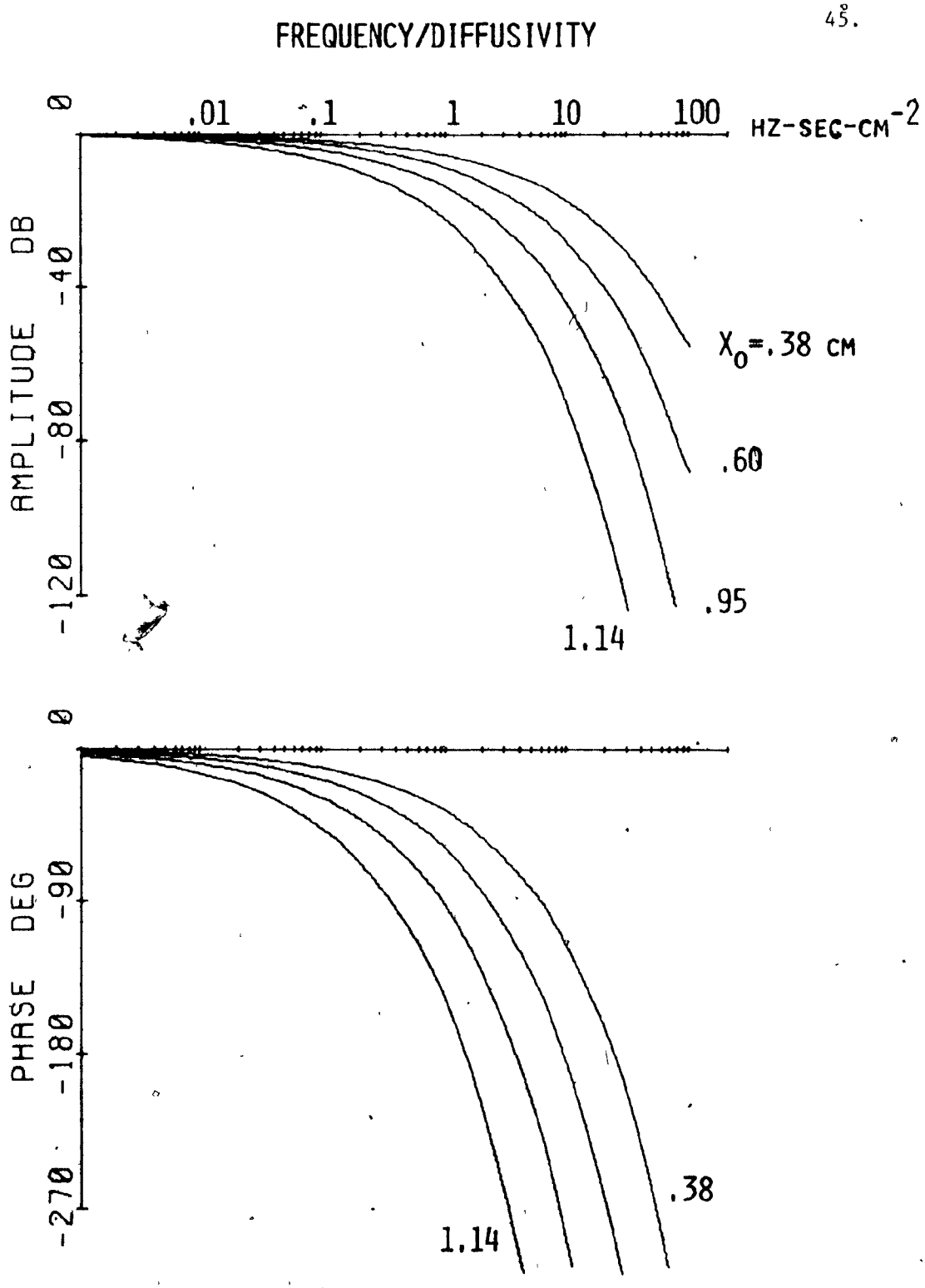

Fig. 3.3. Frequency characteristics of the diffusion operator $\exp(-X_o\ s/\alpha)$ describing the heat conduction process. The function relates temperature at distance X_o (canal center) to surface temperature. α = thermal diffusivity of bone.

The third component

$$I_1 (R \sqrt{s'})$$

describes the torque generating process around the canal as shown by the integral form of I_1. The modified Bessel function with complex argument can be evaluated by direct integration (two real integrals must then be computed) or by the complex series expansion (Olver, 1964).

$$I_1 (z) = \frac{z}{2} \sum_{j=0}^{\infty} \frac{\left(\frac{z}{2}\right)^{2j}}{j!\,(j+1)!} \tag{3.3.10}$$

For large values of the argument ($Im(z) > 60$) good accuracy is obtained with the asymptotic expansion

$$I_N (z) = \frac{e^z}{\sqrt{2\pi z}} \left\{ 1 - \frac{(\mu - 1)}{8z} + \frac{(\mu - 1)(\mu - 9)}{2!\,(8z)^2} + \cdots \right\} \tag{3.3.11}$$

where $\mu = 4n^2$.

Details on Bessel functions may be found in a number of texts, for example McLachlan (1955). The Bode plot of $I_1(R\sqrt{s'})$ is shown in

figure 3.4. It exhibits increasing amplitude and phase with increasing frequency, behaviour typical of a "differentiation" operation. For $s' < 1.0$, the amplitude various linearly with a 10 db/decade positive slope and there is a constant phase lead of 45^{o}. This is predicted from the series expansion which reduces to

$$I_1 (R \sqrt{s'}) \simeq \frac{R}{2} \sqrt{s'} \qquad (3.3.12)$$

as $s' \to 0$. At high frequencies, both amplitude and phase lead increase to infinity.

The overall transfer function is shown in figure 3.5 along with the individual components, for "normal" parameter values. The Bessel function dominates at low frequency but as frequency increases the exponential diffusion operator eventually overrides all other terms as can be shown mathematically. Indeed, consider the limiting case (not met in practice) where R is at its maximum permissible value i.e. $R = X_o$. If $I_1(R\sqrt{s'})$ is replaced by the first term of the asymptotic expansion given by 3.3.11, then

$$\frac{M(s)}{T_w(s)} \simeq \frac{h}{h + \sqrt{s'}} \frac{1}{\sqrt{s'}} \qquad (3.3.13)$$

for large values of s' and $R = X_o$.

The heat transfer process acts as a "trimming" factor in the

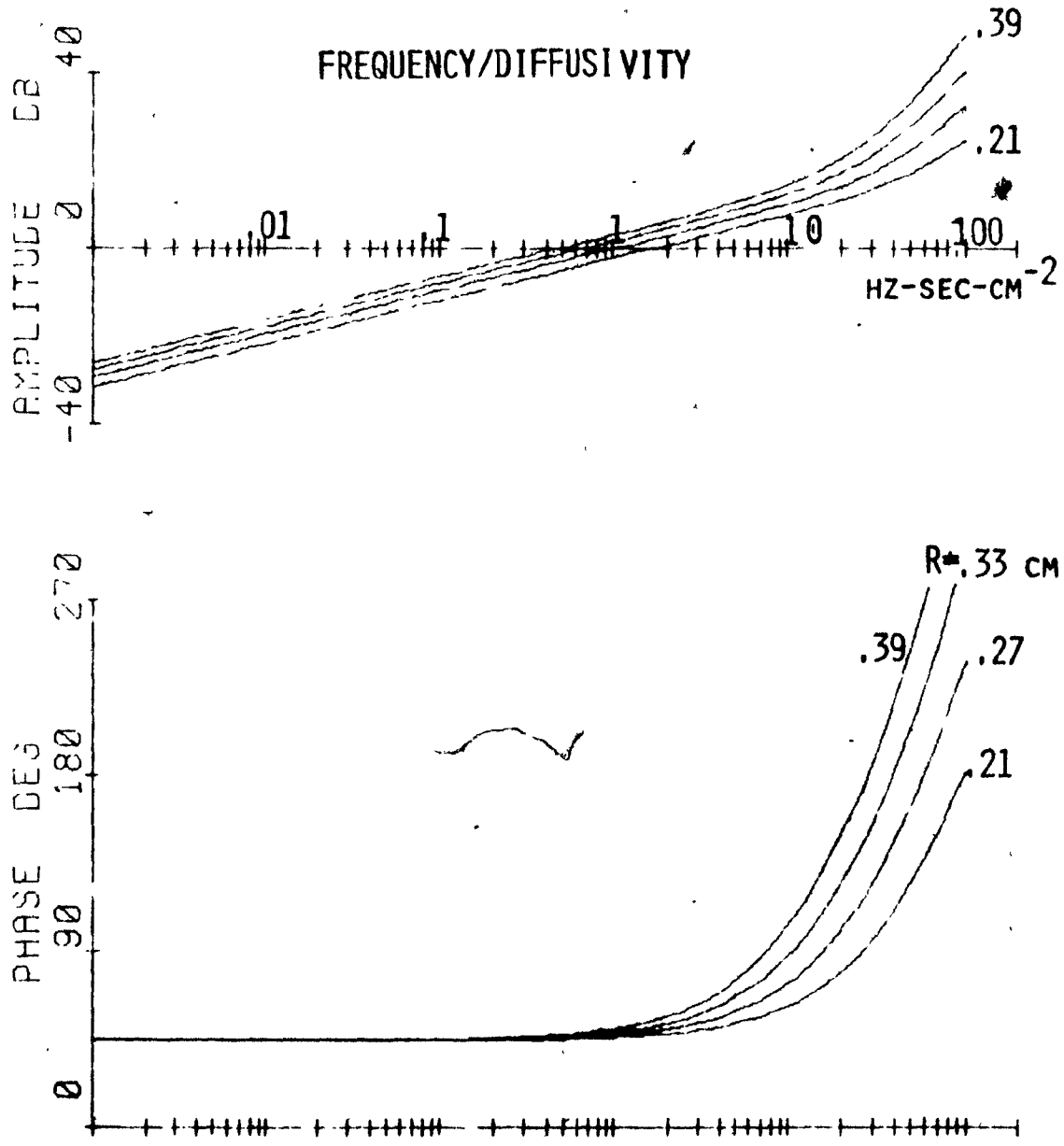

Fig. 3.4. Frequency characteristics of I_1 ($R\sqrt{s/\alpha}$) describing the torque generating process. The function relates torque acting on the canal endolymph to temperature at the canal center. R, large canal radius; α, thermal diffusivity of bone.

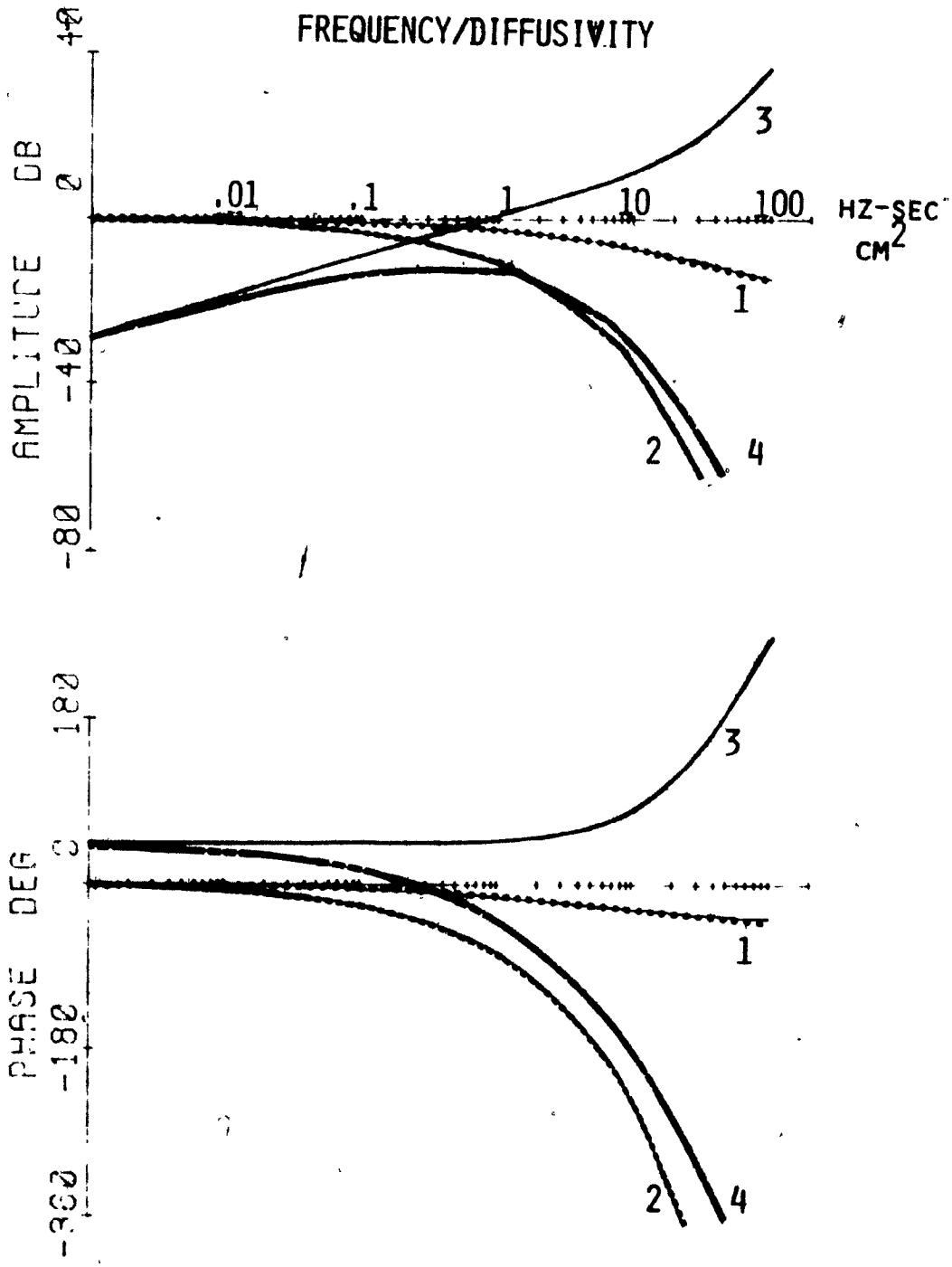

Fig. 3.5. The torque/temperature transfer function and its components. 1, $h/(h + \sqrt{s'})$; 2, $\exp(-X_o \sqrt{s'})$; 3, $I_1 (R\sqrt{s'})$: s' = frequency divided by thermal diffusivity.
Curve 4 is the overall transfer function relating torque applied to the semicircular canal endolymph to temperature of the irrigating medium. $h = 5cm^{-1}$, $R = 0.3cm$, $X_o = 0.76cm$.

overall transfer function without changing the major characteristics imposed by the other two components. The influence of the h parameter will, however, become more evident when considering parameter variations in the time domain.

The behaviour of the overall transfer function relating torque to input temperature may be summarized by looking at it as a wide band-pass filter with a sharp cut-off on the high frequency side only. The peak amplitude is located around 0.001 Hz (period of 16 minutes) and accelerated attenuation appears past 0.25 Hz. Below the peak frequency, positive phase shift is present with a maximum theoretical value of +45 degrees only. The process is also characterized by attenuation taking place throughout the frequency range, and at normal parameter values, the maximum amplitude ratio taken from figure 3.5 is 0.25. In absolute values, the peak output torque calculated for a $1^{o}C$ sinusoidal input at the ear canal is therefore $2C_1 \times 0.25 = 1.3 \times 10^{-5}$ dyne-cm and the corresponding pressure is 0.068 dyne cm^{-2}.

3.4 Time Domain Solutions: Step and Pulse Response

The solution of the heat conduction equation to a unit step temperature change with boundary conditions as given in section 3.2 can be found in Carslaw and Jaeger (1959):

$$T(x,t) = \operatorname{erfc}\left(\frac{x}{2\sqrt{\alpha t}}\right) - e^{hx + h^2\alpha t} \operatorname{erfc}\left(\frac{x}{2\sqrt{\alpha t}} + h\sqrt{\alpha t}\right) \qquad (3.4.1)$$

where

$$\text{erfc}\,(u) = \frac{2}{\sqrt{\pi}} \int_{u}^{\infty} e^{-\xi^2}\, d\xi \qquad (3.4.2)$$

and is called the "co-error" function. Note that

$$\text{erfc}\,(u) = 1 - \text{erf}\,(u) \qquad (3.4.3)$$

where erf is the "error" function.

To evaluate the "co-error" function, a rational approximation due to Hastings (1955) has been found very useful:

$$\text{erf}\,(u) \approx 1 - e^{-u2} \sum_{j=1}^{5} d_j \left(\frac{1}{1 + pu}\right)^j \qquad (3.4.4)$$

where p and the d_j's are constants (see Appendix 1 for values of p and d_j's).

From the above,

$$M(t) \simeq 2 C_1 \int_0^{\pi} e^{-\frac{x^2}{4\alpha t}} \left[\sum_{j=1}^{5} d_j \left(y_1^j - y_2^j \right) \right] \cos\theta \, d\theta \qquad (3.4.5)$$

where

$$y_1 = \left[1 + p \frac{x}{2\sqrt{\alpha t}} \right]^{-1} \qquad (3.4.6)$$

and

$$y_2 = \left[1 + p \frac{x}{2\sqrt{\alpha t}} + h\sqrt{\alpha t} \right]^{-1} \qquad (3.4.7)$$

Note that 3.4.5 does not contain the exponential term with positive arguments found in 3.4.1 and therefore presents fewer problems in computing for large values of h or t. Furthermore, the symmetry of the function with respect to the x axis allows one to consider only the integral over the interval $(0,\pi)$.

The step responses shown below were calculated from 3.4.5 and 3.3.3 using a standard integration subroutine. In practice, the summation over the j's must be carried out with double precision. Also,

the generalized time variable t'

$$t' = \alpha t \qquad (3.4.8)$$

in cm^2 was used. A listing of the computer program is given in Appendix 1.

Figure 3.6 illustrates the torque step response at normal parameter values. For comparison, the corresponding temperature at the canal center has also been plotted. The most noticeable characteristic of the torque curve is a peak at about $t' = 0.3$ (120 seconds in real time with $\alpha = 0.00125$) followed by a very slow decay. At $t' = 3.0$, (1200 seconds or 20 minutes) the output is still approximately 50% of the peak value. Over the time interval shown in figure 3.6, the response appears to have a steady state component. In theory, however, as $t' \to \infty$ the response must tend to zero as required by 3.4.5. The slow decay corresponds to the $\sqrt{s}$ low frequency asymptote in the Bode plot of figure 3.5. The peak or "overshoot" of the step response may also be attributed to the "band pass" nature of the transfer function.

In figure 3.7A and B, torque pulse responses have been plotted at various pulse widths. The peak amplitude rises with pulse width in almost a linear fashion up to $t' = 0.1$ and thereafter continues to increase up to the peak of the step response. The termination of the pulse is marked by a fast decay of the torque followed by a prolonged negative tail. The level and the duration of the negative "overshoot" increase with pulse duration. In figure 3.7B, details

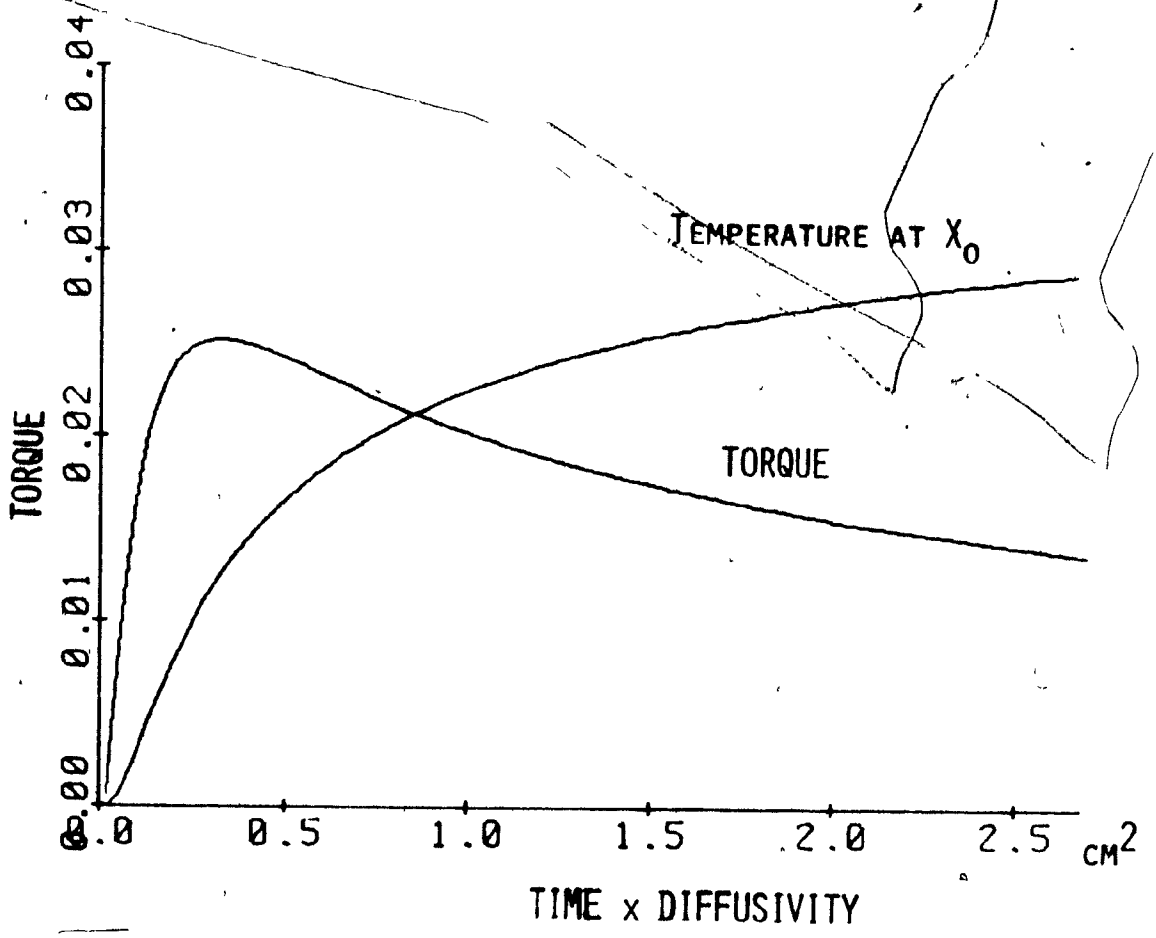

Fig. 3.6. Output torque and temperature at the center of the semicircular canal following a unit step change of the irrigating medium temperature. Parameter values: $h = 20\ cm^{-1}$, $R = 0.3$ cm, $X_o = 0.76$ cm. N.B.: The curve shown is the calculated $\int$ of equation 3.4.5 multiplied by R^2. Hence, to obtain torque in dyne-cm, a multiplicative factor is required which is equal to $2.C_1 / R_1^2 = 5.88 \times 10^{-4}$ where $R_1 = 0.3$.

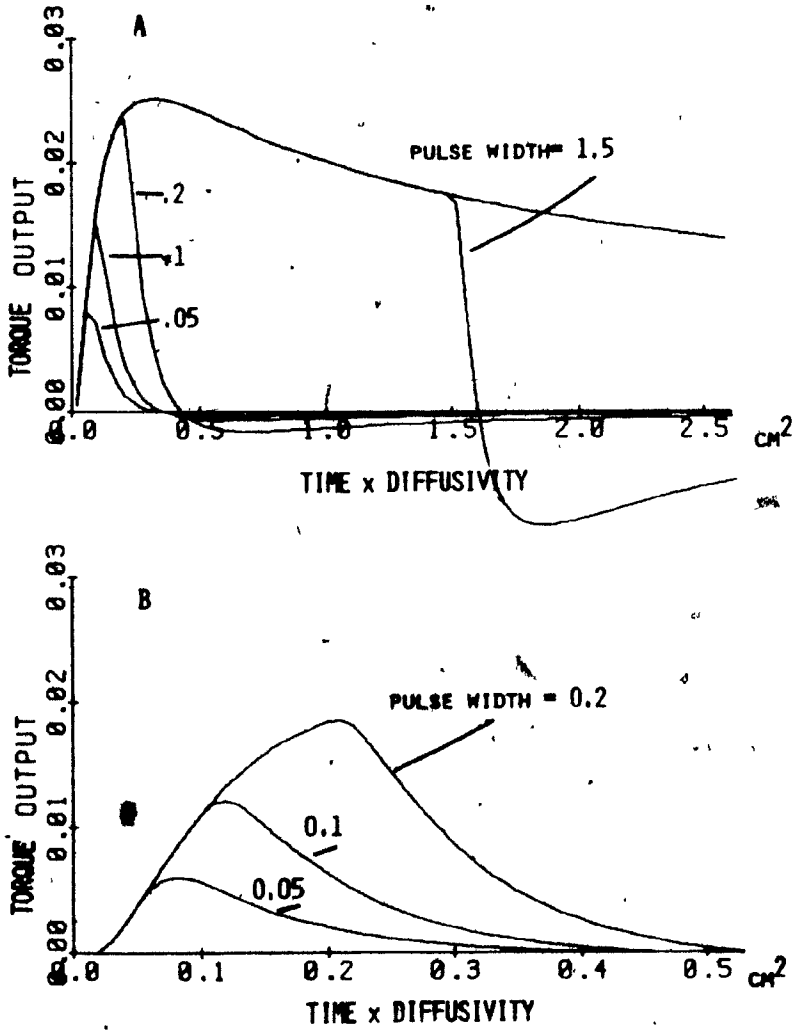

Fig. 3.7. Model output torque from unit temperature pulses of varying widths. The pulse width is given in normalized time i.e. time x diffusivity. Parameter values, A: $h = 20cm^{-1}$; R = 0.3cm; X_o = 0.76cm; B: same as in A except h = 5. For torque units, see fig. 3.6.

near the origin have been emphasized. A time delay of about 0.025 cm^2 (10 sec) is noticeable before the initial response rise. The peak torque of a 0.1 wide pulse is a little more than half the peak torque of the corresponding step input. At normal diffusivity, a 0.1 cm^2 width is equivalent to the 40 second duration of a standard irrigation. However, in the caloric test, the peak torque reaches a greater percentage of the step response peak as shown in the experimental chapters because of an added tail in the temperature stimulus.

3.5 Parameter Variation Study

The effects of parameter variations in the transfer function will be discussed here only qualitatively. Changes in the diffusivity are reflected as shifts of the transfer function $M(s)/T_w(s)$ along the frequency axis. The individual components of the transfer function undergo a somewhat similar horizontal shift of their amplitude and phase when their characteristic parameter varies (figure 3.2 to figure 3.4). Whenever, the transfer function of a given component is shifted relative to the others, the overall transfer function is of course modified except for the Bessel function term. In the latter case, as R is varied in the overall transfer function, the only major change is a vertical shift, i.e. a change of the total gain, which is due to the lineraity of the amplitude curve over the range of R values considered. However, minor modifications are found in the high frequency region.

In the time domain, parameter variations will be considered by looking at changes produced in the step responses. First the effect of diffusivity changes may be visualized as a compression or extension

in time of a given output curve without changing the amplitude. This behaviour corresponds to the horizontal shift of the overall transfer function in the frequency domain. In figure 3.8, three groups of step responses are shown in which the parameters h, X_o and R are varied, in turn, around their normal values.

The h coefficient has been varied over two orders of magnitude from 40 to 0.625, mainly because a great variability is expected in this parameter associated with heat transfer at the bone surface. Indeed, related factors such as the thermal resistance of the skin, skin blood flow and geometry of the ear cavity are likely to vary more than other anatomical parameters. As shown in figure 3.8a, with increasing h values, the peak amplitude of the torque step response increases, the time to reach the peak becomes shorter and the decay more rapid. The characteristic "overshoot" disappears at around h = 1.25 and an overdamped step response is observed for smaller h values. Note, however, that the magnitude does not vary by more than a factor of about 6 in the region of the peak and by a factor of 2 at the end of the interval considered, which is consistent with the relatively small amplitude attenuation of the corresponding transfer function. On the other hand, as h increases to infinity, the torque output tends to a limit as may be noted from figure 3.8a. Indeed, let $h \to \infty$ in 3.4.7, then y_2 vanishes in 3.4.5 which reduces to

$$M(t) = C_1 \int_0^{2\pi} \operatorname{erfc}\left(\frac{x}{2\sqrt{\alpha t}}\right) \cos\theta \, d\theta \qquad (3.5.1)$$

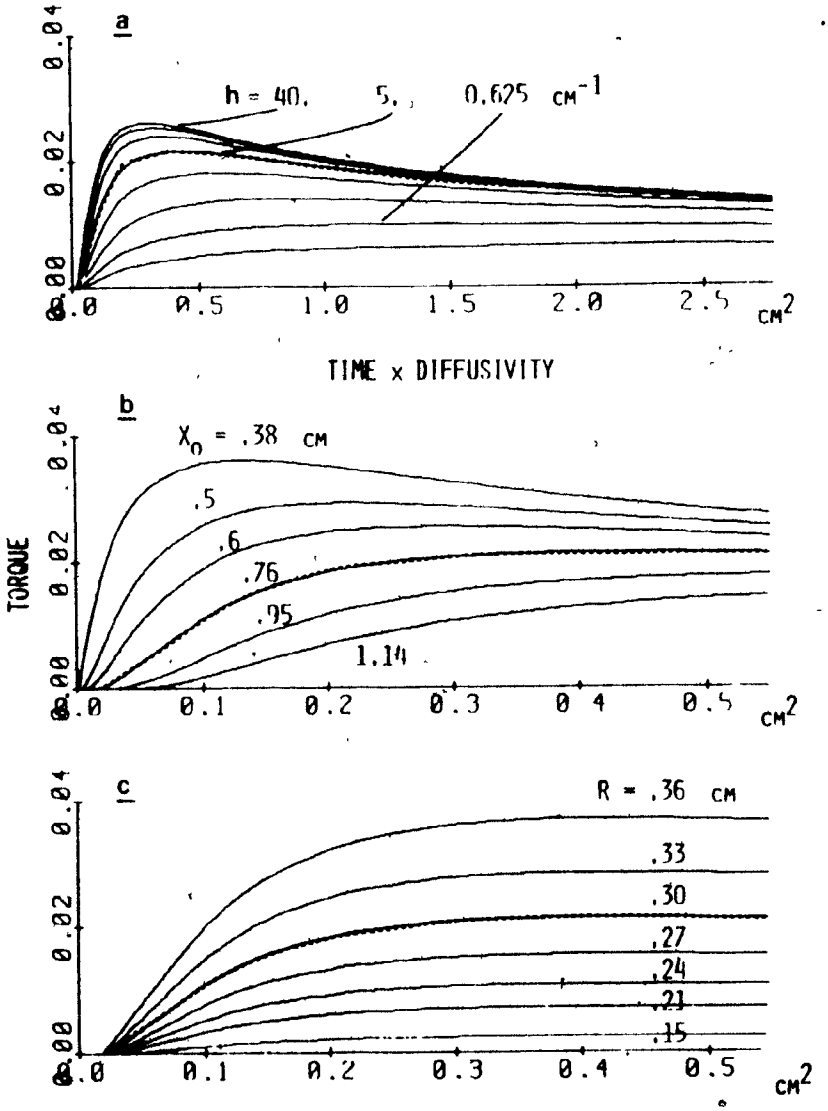

Fig. 3.8. The effect of parameter variations on the model output torque. In panels a, b and c, the parameters h, X_o and R are respectively varied around normal values. The dotted line indicates the output at normal parameter values i.e. h = 5.0cm^{-1}, X_o = 0.76cm, R = 0.3cm. For torque units, see fig. 3.6.

The latter equation is the solution obtained when the boundary condition at the surface is one in which the surface temperature is prescribed to a given value. This case corresponds to unlimited heat transfer rate at the surface.

Increasing values of X_o produce effects similar to those observed for decreasing values of h, i.e. reduction in peak amplitude and larger time to peak. In figure 3.8b, the torque step response is plotted over the interval 0 - 0.6, (240 seconds in real time) to emphasize details near the origin. The initial time delay increases with increasing X_o which corresponds to larger phase lag brought by X_o changes in the overall transfer function.

Finally, the effects of variations in the canal large radius R are illustrated in figure 3.8c. The shape of the output curve is practically unaffected and only the amplitude changes. The integral in equation 3.4.5 has been found to vary linearly with R and the constant C_1 contains R^2 so that in practice the overall torque is proportional to the cube of the radius as can be shown from figure 3.8c. However, this effect on the torque is compensated by corresponding increases of the moment of inertia J of the fluid which also varies as the cube of the radius. Therefore, the equivalent angular acceleration of the endolymph is in fact independent of R since it is proportional to the ratio of torque to moment of inertia M/J (see section 3.7 below).

3.6 Relationship between Output Torque and Temperature Difference Across the Canal

In this section, the relationship between output torque and

temperature difference across the canal will be studied.

From figure 3.1, the temperature difference ΔT across the canal is given by

$$\Delta T\ (t) = T\ (X_o - R,t) - T\ (X_o + R,t) \qquad (3.6.1)$$

or, after Laplace transformation

$$\Delta T\ (s) = T\ (X_o - R,s) - T\ (X_o + R,s) \qquad (3.6.2)$$

Consider the transfer function $T(s)/T_w(s)$ obtained by applying 3.3.1 to 3.6.2

$$\frac{\Delta T\ (s)}{T_w(s)} = \frac{h}{h+\sqrt{s'}}\ e^{-X_o\sqrt{s'}}\ 2\ \sinh\ (R\sqrt{s'}) \qquad (3.6.3)$$

The above expression differs from the torque transfer function $M(s)/T_w(s)$ of equation 3.3.8 mainly by an hyperbolic sine function found in place of the Bessel function. The sinh and modified Bessel functions are compared in the Bode plot of figure 3.9 and a remarkable similarity is observed. Both functions expand in odd powers of z and for $z < 1$,

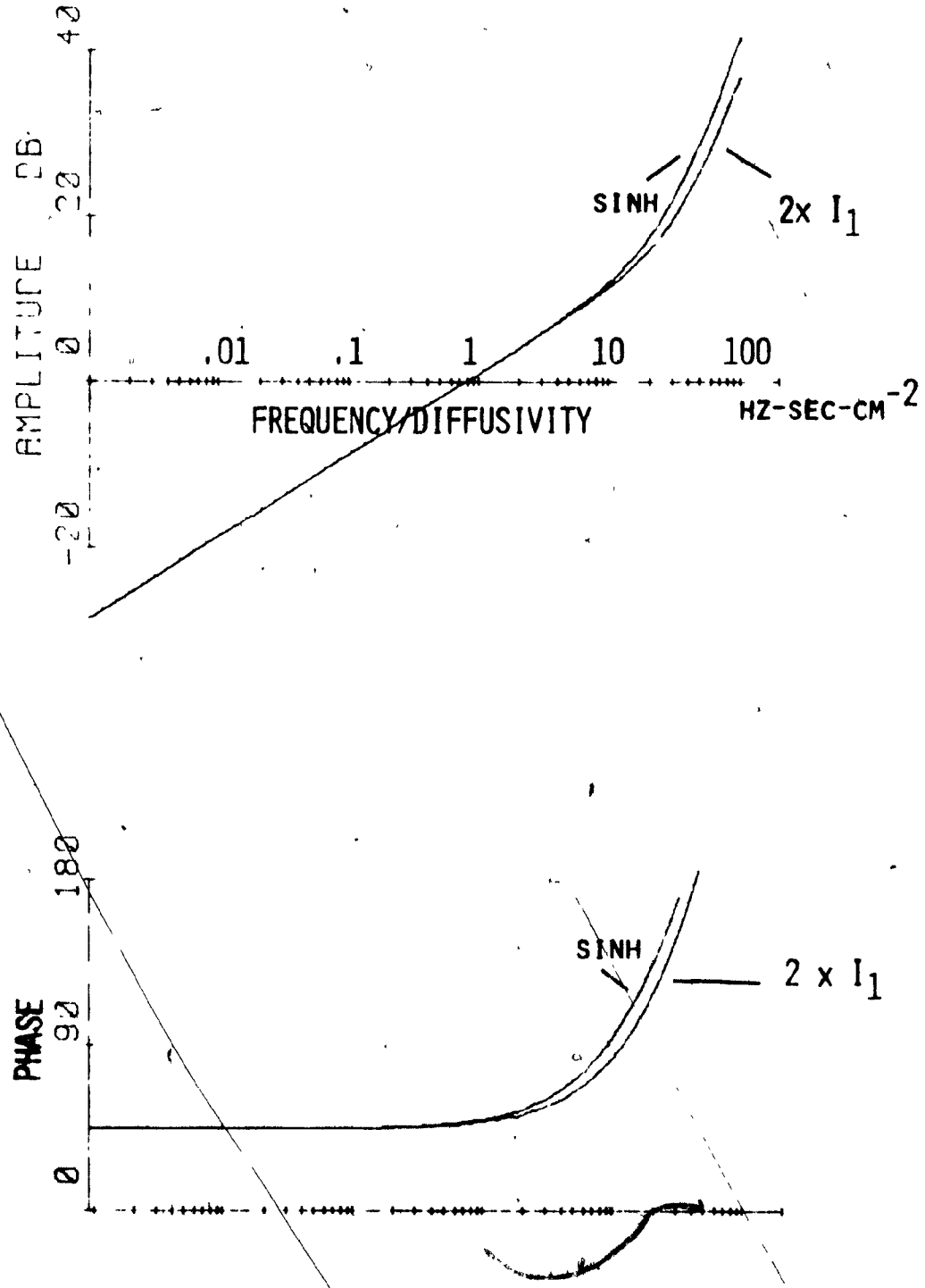

Fig. 3.9. Frequency characteristics of the function Sinh ($R\sqrt{s/\alpha}$) relating the temperature difference across the canal to the temperature at the canal center. The Bessel function I_1 ($R\sqrt{s/\alpha}$) (multiplied by 2) is shown for comparison. R = 0.3cm.

$$\sinh(z) \simeq 2 I_1(z) \qquad z < 1 \qquad (3.6.4)$$

with

$$\sinh(z) - 2 I_1(z) \simeq \frac{z^3}{24!} \qquad (3.6.5)$$

On the basis of 3.6.4, one may write

$$M(s) \simeq \frac{\pi C_1}{2} \Delta T(s) \qquad (3.6.6)$$

to express the relationship between the torque and ΔT.

In figure 3.10, the normalized step responses, for both torque and ΔT are compared at various parameter values. In many cases, the curves are almost superimposed. However, there are, minor differences and for instance ΔT always leads the torque as predicted from the Bode plot of figure 3.9.

It may be concluded that over a wide range of parameter values, the temperature difference across the canal is closely related to the thermal torque and that in practice, these two variables have the same dynamics. This relationship offers the basis for a direct experimental validation of the present model, making it possible to verify the response characteristics that were emphasized in the previous sections.

Another advantage is, of course, a marked simplification of the computational procedures since one needs only to calculate the

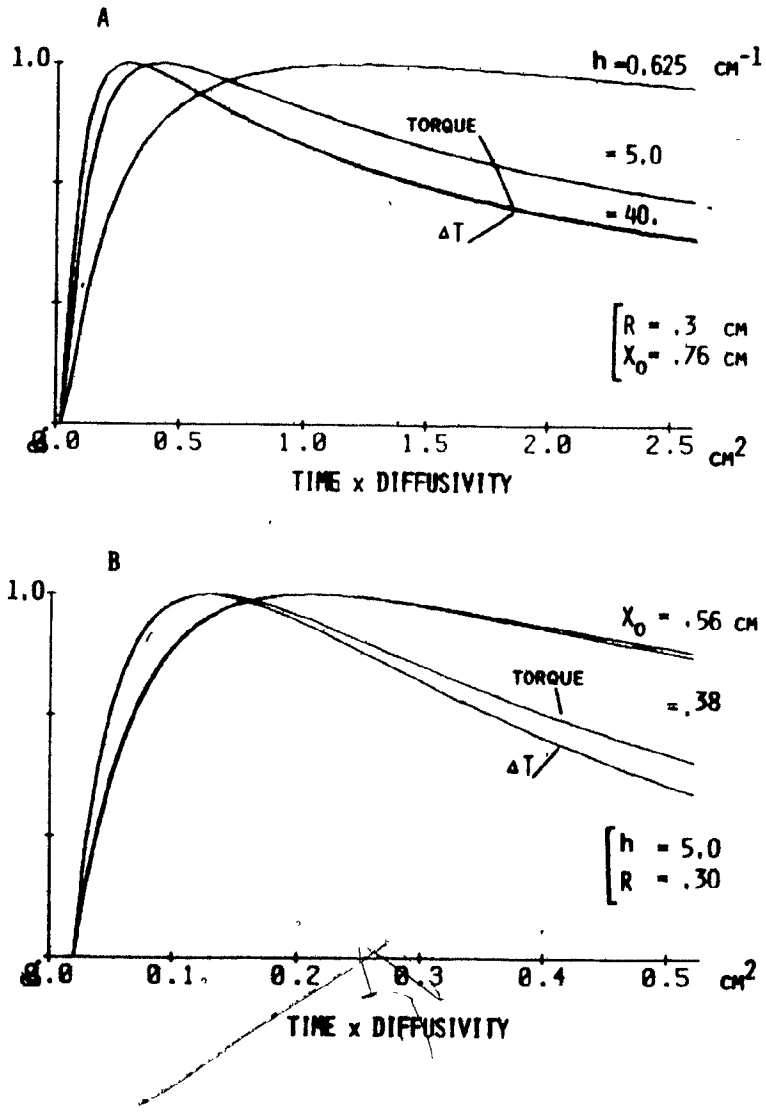

Fig. 3.10. Model output torque and temperature difference across the canal (ΔT) following a step change of the irrigating medium temperature. The curves are normalized relative to peak values. Note that ΔT always leads torque. The deviations between torque and ΔT are the largest at small values of X_o e.g. X_o = .38 in B.

temperature at two points instead of performing an integration. This approach is different than the one used by Schmaltz (equation 3.1.15) and based on $\partial T/\partial x$ evaluated at the canal center. It can easily be shown that, except for a multiplicative factor, Schmaltz's method is equivalent to replacing the Bessel function by $\sqrt{s/\alpha}$ i.e. the low frequency asymptote of I_1. Schmaltz's method should yield curves always lagging the true torque but still representative of the latter. It would appear, however, that the variable ΔT is a closer approximation and, in any case, is the only one that can be measured.

As made evident by equation 3.6.3, Steer's representation of the dynamics of the temperature difference across the canal by a first order lag is an oversimplification. In particular, it ignores the characteristic attenuation at low frequencies. Steer based his assumption on the recordings of temperature gradients across the human canal obtained by Cawthorne and Cobb (1954). However, these data originated from standard short duration irrigations and were unsuitable to provide good estimates of the system's behaviour at very low frequencies.

3.7 General Model of Vestibular Response to Caloric Stimulation

The general caloric response model proposed in the introduction chapter as a working hypothesis is now discussed quantitatively from a theoretical viewpoint. The model is presented in block diagram form in figure 3.11 and consists of the thermal process, discussed in the previous sections, followed by the hydromechanical and neural components of the vestibular dynamics that have been introduced in the previous chapter. The two models have been coupled together by defining (Steer, 1967)

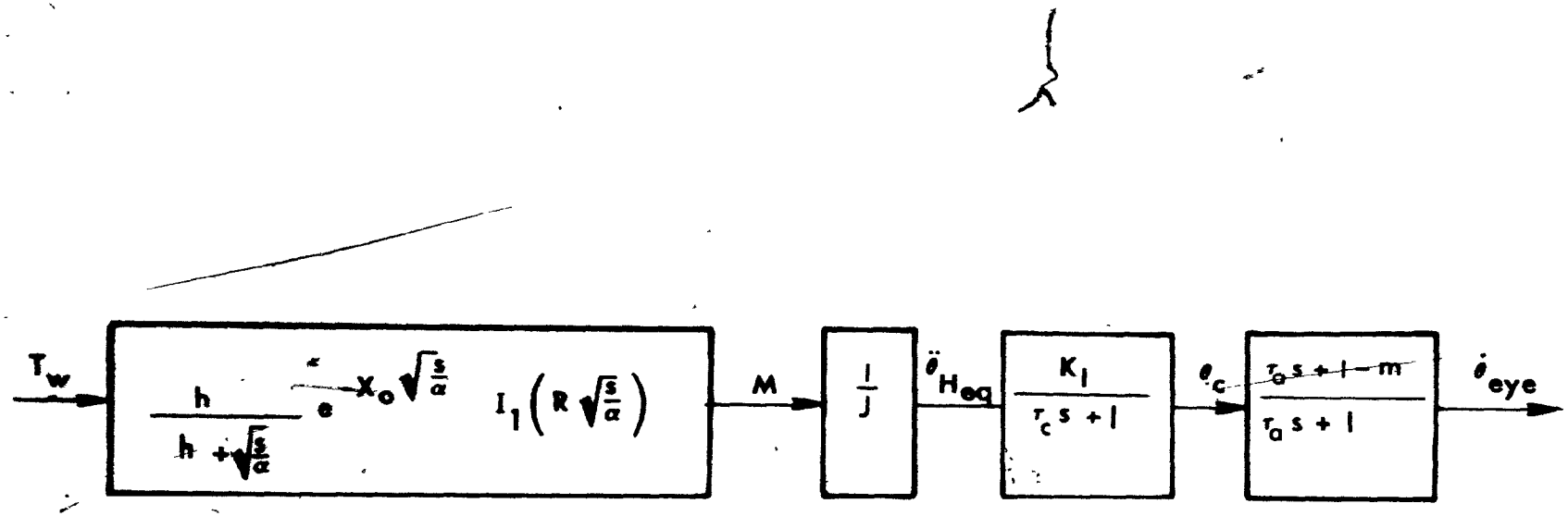

Fig. 3.11. The general caloric response model obtained by coupling torque model (first block) to semicircular canal dynamics (third block) and to neural adaptation (fourth block). The second block is a gain factor relating thermal torque M to equivalent angular acceleration of the head $\ddot{\theta}_{H\ eq}$. T_w, temperature of the irrigating medium; θ_c, theoretical cupula deflection; $\dot{\theta}_{eye}$, theoretical slow-phase velocity or adapted response.

an equivalent head angular acceleration $\ddot{\theta}_{Heq}$ as

$$\ddot{\theta}_{Heq} = \frac{M(s)}{J} \qquad (3.7.1)$$

where M(s) is the thermal torque defined by 3.3.2 and J, the moment of inertia of the endolymph ring given by

$$J = 2\pi^2 r^2 R^3 \rho_F (T_o) \qquad (3.7.2)$$

It is assumed that J and other constants of the hydromechanical model do not vary significantly with temperature.

Canal dynamics have been simplified since the frequency range of interest is located below 1 Hz. The canal transfer function from chapter 2 is therefore written as

$$\frac{\theta_c(s)}{\ddot{\theta}_{Heq}} \simeq \frac{K_1}{\tau_1 s + 1} \qquad (3.7.3)$$

where K_1 is a constant.

For convenience, the transfer function of the neural adaptation component

is repeated

$$\frac{\theta_E(s)}{\theta_c(s)} = \frac{\tau_a s + 1 - m}{\tau_a s + 1} \qquad (3.7.4)$$

In the above, the parameter m will be left unspecified since we are involved here with adaptation from unilateral stimulation. The following normal value will be used

$$\tau_a = 82 \text{ sec and } \tau_1 = 21 \text{ sec}$$

obtained by Malcolm and Melvill Jones (1970). The break frequencies associated with these time constants are 0.00196 Hz and 0.00757 Hz for τ_a and τ_1 respectively. For convenience, these values are given in terms of the generalized time constants τ_a' and τ_1'. Thus $\tau_a' = 0.205$ and $\tau_1' = 0.0525$ cm^2 with corresponding break frequencies at 0.783 and 3.02 cm^{-2} respectively.

First, the effect of these components on the thermal torque will be discussed in the frequency domain. The combination of canal and neural adaptation dynamics (figure 3.12) produces a filter with a band pass located in the region of maximum amplitudeof the thermal torque/ temperature transfer function.

The transfer function $\theta_E(s)/T_w(s)$ relating slow-phase eye

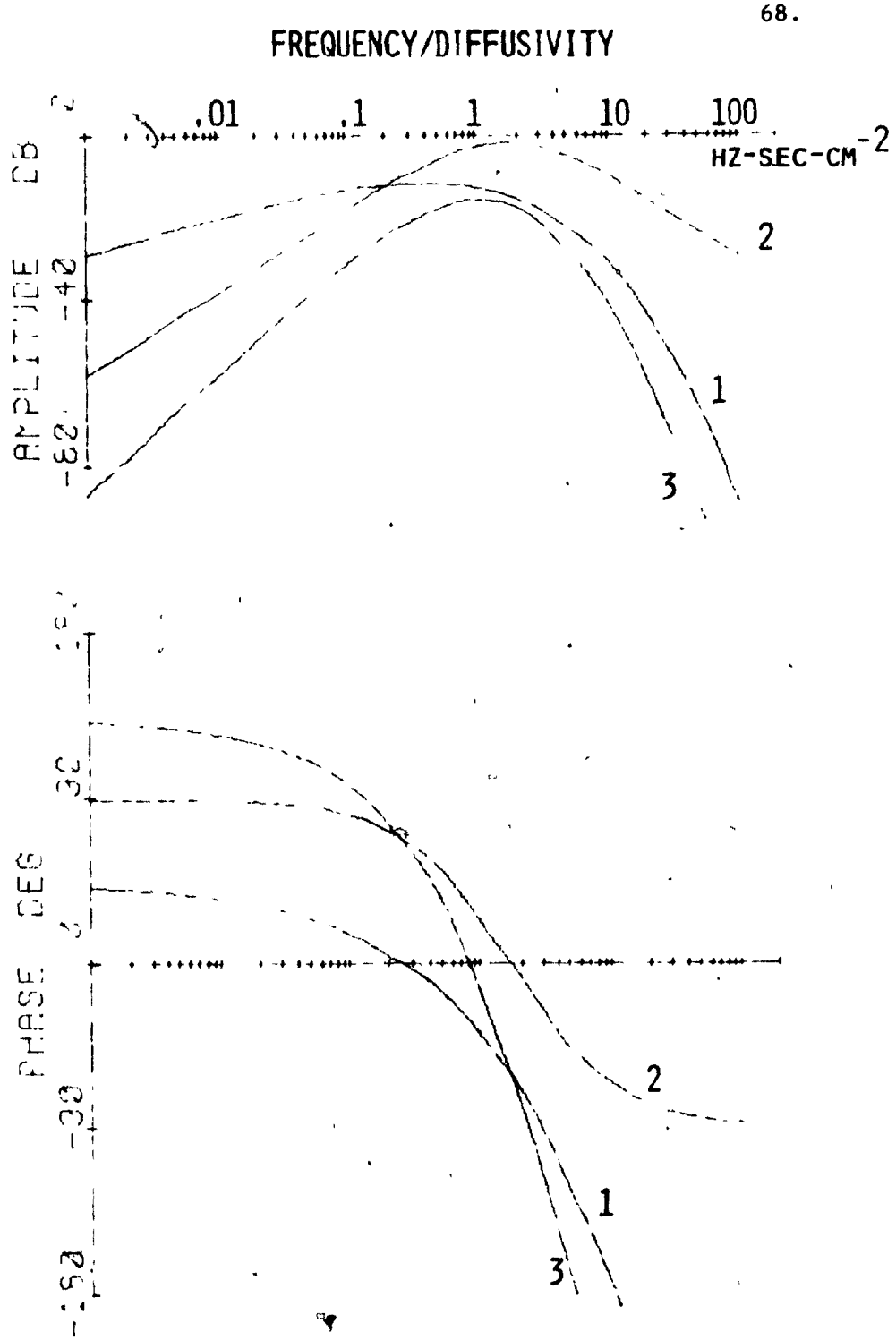

Fig. 3.12. The effect of canal dynamics and neural adaptation on the torque/temperature transfer function. 1:torque function (see fig. 3.5) 2: semicircular canal lag (τ_c = 21 sec) in series with adaptation filter (m = 1, τ_a = 82 sec). The time constants are normalized (i.e. x 0.0025 cm^2/sec. 3: overall transfer function).

velocity to ear canal may now be discussed. Neural adaptation substantially increases the attenuation and phase lead already present in the thermal torque transfer function and a maximum slope of 3/2 and phase lead of 135^{o} are now seen in the low frequency asymptote. These effects are progressively reduced as the parameter m is decreased from 1 to 0. The canal first order process adds attenuation and phase lag at high frequencies above 2.0 cm^{-2} but is definitely not a dominating factor since the exponential term of the torque function is overriding all other terms in that region.

In the time domain, both step and pulse responses have been studied. The time course of the slow-phase eye velocity θ_E was calculated by filtering the torque response through digital filters equivalent to the canal and neural adaptation transfer functions; the method is briefly described in Appendix 2.

Step responses are shown in figure 3.13 for increasing values of m. The adaptation filter sharpens the peak already present in the torque responses and precipitates the return towards the baseline. The maximum effect takes place for m = 1; the peak is reached in about half the time - 80 sec instead of 160 - and the response reaches zero level at t' ≈ 0.75, (5 minutes) to continue in the reverse direction at a lower level but for a prolonged duration. Thus adaptation would eliminate from the eye response the nearly steady state component applied by the thermal torque.

In figure 3.14A, the cupular deflection θ_c is compared to the

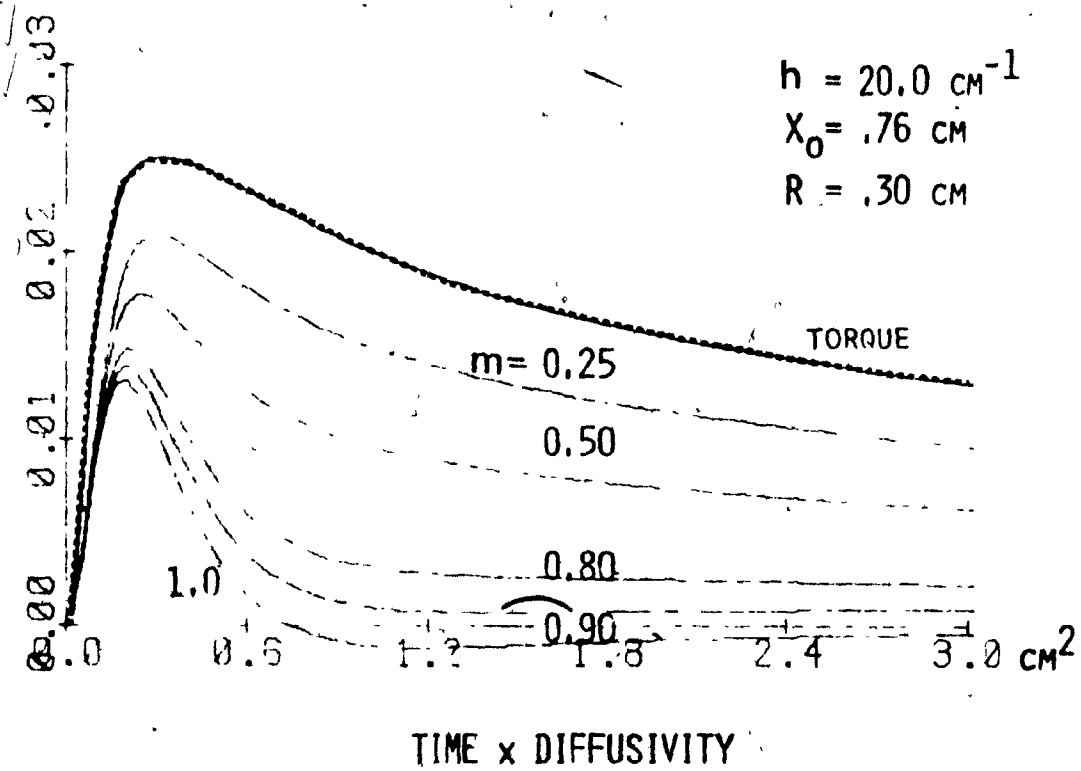

Fig. 3.13. The effect of canal dynamics and neural adaptation on the torque step response. The adapted response (solid curves) is shown in arbitrary units for various values of m of the adaptation filter. τ_c = 21sec and τ_a = 82sec. The dotted line is torque.

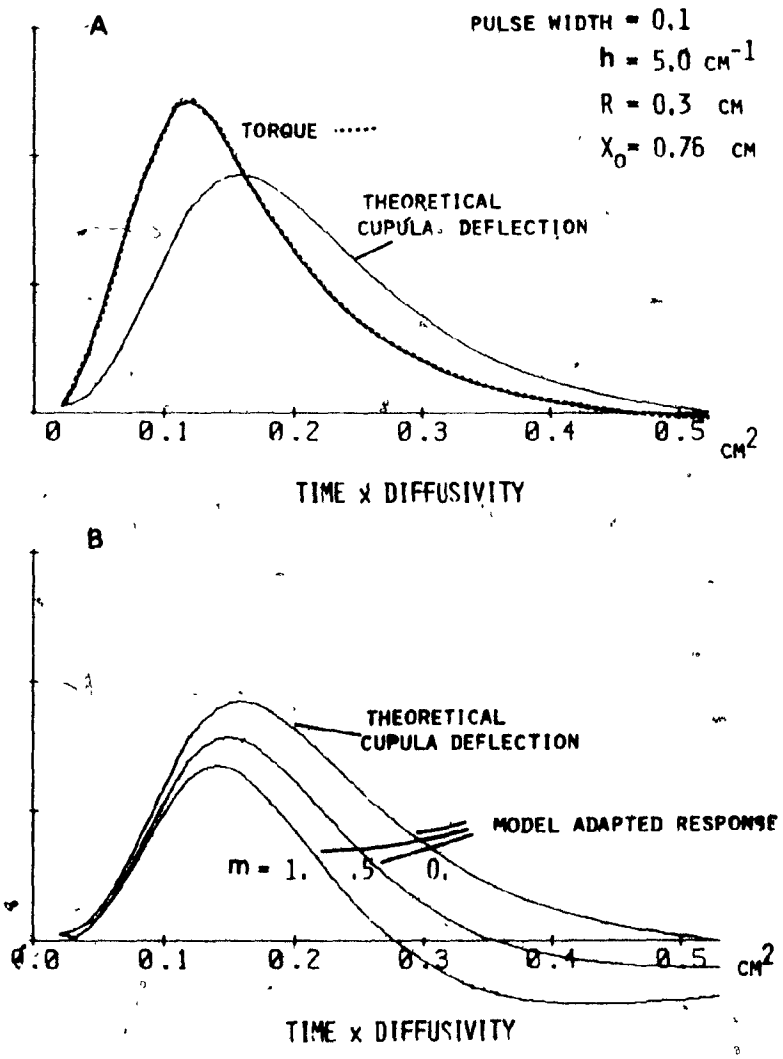

Fig. 3.14. A: The effect of canal dynamics (τ_c = 21sec) on the torque pulse response.

B: The effect of neural adaptation (τ_a = 82sec) at various values of m.

applied torque M when the input is a pulse of width 0.1 (40 seconds). The canal long-time constant widens the output pulse, the peak occurs later and a 25% reduction in the amplitude occurs. When adaptation is added (figure 3.14B), the peak amplitude Θ_E is further reduced but is brought back towards the peak torque time. The secondary negative overshoot is accentuated and the response reverses its sign earlier in time.

3.8 Discussion

The semi-infinite solid model of the caloric response is based upon a number of assumptions and simplifications which could be justified by the mere fact that the problem becomes otherwise mathematically untractable. Very fortunately, the theoretical predictions derived from the model are partly supported by Young's experiment (figure 2.6) in which the fundamental hypothesis of unidimensional heat flow has been so nicely confirmed. However, the process of caloric stimulation is essentially defined by the torque (or pressure) integral equation (3.2.13) and therefore is not validated by Young's experiment.

A major result of the study is a transfer function for the output torque which consists of three mathematically separable components representative of the underlying physical processes. In particular, the torque generating process is described by a "differentiating" operation which dominates the system's behaviour at frequencies below 0.001 Hz. The presence of this term is not entirely unexpected since from a physical viewpoint the caloric effect takes place by a difference in the gravitational

pull exerted on both sides of the fluid ring within the semicircular canal. At first sight, the mathematical representation of this phenomenon by a modified Bessel function may appear unusual; in fact this is but one of many other examples of irrational functions involving fractional power of the complex variable that are usually found with distributed parameter systems described by partial differential equations. It should be noted that the same physical process of the torque generation may equally be represented by other mathematical functions arising through the solution of models with different geometry and boundary conditions, e.g. the infinite slab model (solid limited by two infinite planes separated by a finite width). In any case, "differentiator-like" functions, whatever they are, are always likely to appear to describe the torque generating process.

In the time domain, the typical step response exhibits a peak between 2 and 3 minutes after the start. The peak is followed by a prolonged drift-like decline such that the output level is still at 50% of the peak value after 15 minutes. The corresponding features observed for a short pulse input is an initial positive peak followed by a prolonged negative and low amplitude secondary output.

These observations from the pulse response in particular are of some significance in caloric testing since the return to pre-stimulation conditions appear to take much longer than is generally assumed. The typical 5 - 8 minutes interval between irrigations in the standard test has been based on the assumption that the temperature effect on the canal is

completed when the nystagmic response vanishes. Hood's experiment (1973) discussed in the previous chapter has shown that the nystagmic response decline is partly due to adaptation and that the thermal stimulus persists for 11 minutes. The theoretical results shown here are in general agreement with Hood's conclusion.

The step response just described as "typical" is only one of a rather wide spectrum of "damped" and "underdamped" responses revealed by the study of parameter variation. Thermal diffusivity and distance to the canal center are important intrinsic factors determining the shape of the response. A third anatomical parameter, the canal radius, has been found to produce only amplitude variation of the torque and furthermore has no effect on the magnitude of equivalent angular acceleration.

Thermal diffusivity depends in particular on the density of the temporal bone, which appears to be quite variable in the region between the ear canal cavity and the bony semicircular canal. For instance, Ishiyama and Keels (1970) have discussed the case of a hyperactive squirrel monkey that was later found to have an unusually dense temporal bone. As already noted, little is known on bone thermal properties in general and even less on the range of variation encountered. On the other hand, the only source of data concerning the canal center distance is Young (1972) who failed to indicate the spread around the average value of 0.76 cm obtained in five human skulls. There exists a need to collect data on those parameters to estimate their importance in the variability of caloric responses.

Finally, the parameter h depends on two factors, the heat transfer

coefficient and bone conductivity. The value of the heat transfer coefficient is mainly determined by the physical properties of the irrigating medium and the characteristics of the flow within the ear cavity. Two basic types of fluids have been used in caloric stimulation: gases and water (section 2.6, chapter 2). Based upon the large differences in the thermal properties between these fluids, it is not unrealistic to consider h values that differ by one or even more orders of magnitude. Hence, both "damped" and "underdamped" response may be encountered depending on the conditions in which irrigation is performed. This point will be further examined in experiments on the effect of flow rate (Chapter 5).

The value (5.0 cm^{-1}) of the h coefficient quoted before as "normal" refers to the case of a gas stimulator at 5 L/min flow rate. It cannot, of course, be applied to the case of water irrigation without some reserve and, in fact, the results described later on indicate that the h coefficient for water at flow rates above 150 cc/min is at least ten times higher. Comparative studies conducted on the same preparation would, however, be more appropriate to examine this aspect more rigorously.

The brief analysis of parameter variation introduces to us some of the difficulties involved in applying the model to a given experimental response. Indeed, the problem of parameter identification is complicated by the fact that a number of combinations of parameter values may give closely resembling shapes. Parameters may be simultaneously varied in directions that either amplify or nullify the effect obtained when only one is changed; for example, increasing h and shortening X_o or vice versa. Furthermore, if one can only consider relative shapes, as is usually

the case in nystagmic responses, the effects of diffusivity variation will appear similar to those of X_o and h.

Of course, the magnitude of this identification problem is reduced if independent measures of the parameters can be obtained or if they can be estimated within reasonable limits, e.g. X_o. Furthermore, one can make use of the fact that the response tends to a limit for high h values, and consequently arrange for experimental conditions providing elevated heat transfer rates. (In practice, a minimum value of 50 seems adequate.) In these conditions, the parameter h can be eliminated as a variable parameter of the response.

The extension of the model to include semicircular canal dynamics and neural adaptation has allowed us to predict "theoretical" vestibulo-ocular responses. In this more general model, the torque variable is considerably modified by the adaptation high-pass filtering which practically eliminates the sustained torque output level in less than 5 minutes. This effect is attenuated if a model of adaptation is considered that exhibits some "directional preponderance" as shown by varying the parameter m. In the literature, the response to prolonged caloric step inputs has rarely been discussed, and there exist no published records from which one could derive the time course of the slow-phase eye velocity response. It would appear, however, that caloric stimulation maintained even for one or more hours produces a continuous nystagmus. Some indications to that effect are provided by Schmaltz (1932, p. 380, 3rd para), Spiegel and Aronson (1934) and van Egmond and Tolk (1954). On the other hand, the presence of adaptation in caloric responses from

short irrigation is indicated by Young (1972) and Hood (1973). In the absence of any useful data from the literature, the question of adaptation is left and will be resumed however in Chapter 5 after presenting the results of the experimental work.

CHAPTER 4

EXPERIMENTAL STUDIES ON THE CALORIC VESTIBULAR RESPONSE: METHODS AND TECHNIQUES

An experimental study of the caloric vestibular response is reported in the following two chapters. Human volunteers were connected to a special apparatus and selected temperature stimuli were delivered during sustained irrigation of the external ear canal with water. Eye movements were recorded by electro-oculography and analyzed in terms of slow-phase eye velocity from the eye position recording. Methods and techniques are introduced in the present chapter; the specific experiments and the results are discussed in Chapter 5.

In section 4.1, a new caloric stimulator is described that has been designed and developed by the author as a necessary step to carry on the experimental program. It is intended for use in a number of clinical projects to be run in the clinical laboratory in addition to its use in basic research.

Section 4.2 is concerned with the experimental set up, methods and measuring techniques common to all experiments.

In Section 4.3, a slow-phase velocity analyser is described and the method of sampling slow-phase eye velocity from the recording is discussed.

4.1 A New Caloric Stimulator*

Only two caloric stimulators using water as a heat carrier have been described in the literature, by Steffen, Linthicum and Churchill (1970) and by Maffei, Zini and Bottazi (1967). Steffen et al used a device in which custom-made valves driven mechanically by a geared motor produced temperature ramps by mixing water from two baths. Maffei and coworkers built an apparatus in which saline was heated directly by an electrical current under the control of a rheostat. Both the above devices lacked flexibility and it was felt that a general purpose stimulator to provide arbitrary temperature waveforms and amplitudes should be developed.

In the following paragraphs the basic design philosophy and operating principles of the new stimulator are discussed, leaving out simple technical details and standard circuitry. The aspects related to safety are considered in some depth to show that the stimulator can be safely used on human subjects.

4.1.1 Operating Principles and Basic Description

A functional diagram of the caloric stimulator is given in figure 4.1. The device consists of an hydraulic circuit in which tap water is pumped at a constant flow rate across an electrical heater and flows out through a cannula to be inserted into the subject's ear.

The heater is a central component of the system and its design was approached by considering a number of basic principles. First, the maximum required electrical power E_{max} depends on the

---

* The technical help of Messrs. L van Cleef and J. McColl was greatly appreciated.

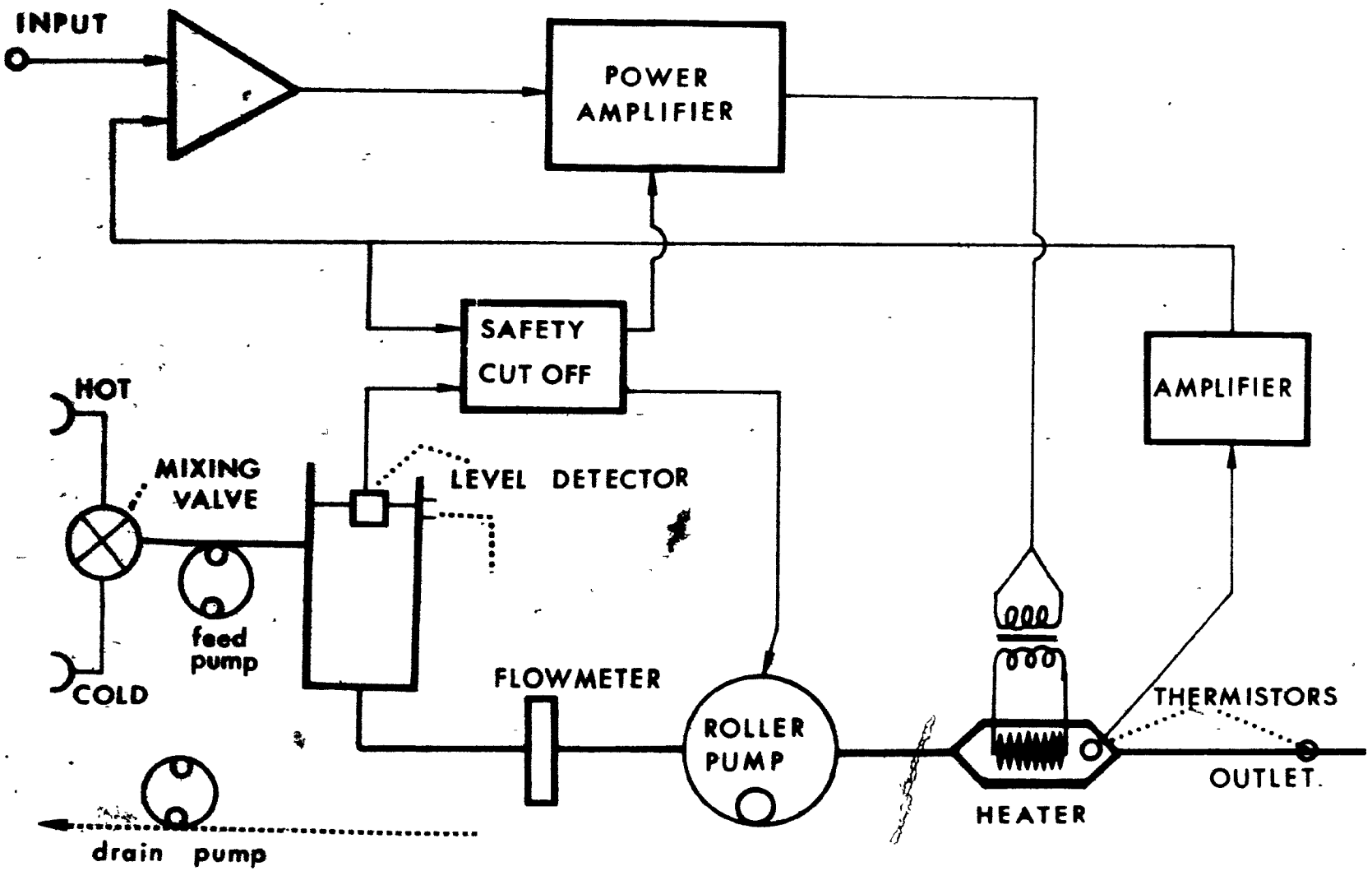

Fig. 4.1. Schematic diagram of the caloric stimulator.

temperature range and on the water flow rate F as

$$E_{max} = 4.18\ F(T_{e\ max} - T_i) \qquad 4.1$$

where $T_{e\ max}$ is the upper temperature limit and T_i the water temperature at the inlet. A decision was made to limit the power at 300 watts, making it possible to cover a $20^{o}C$ range around body temperature, at 150 cc/min flow rate, with a wide margin for heat losses and inefficiencies. This range was found adequate for the experimental work and it also included the temperature levels used in standard caloric tests.

The flow rate was selected arbitrarily since no precise indication could be found in the literature concerning the minimum required flow rate in caloric stimulation. The results of next chapter indicate that efficient heat transfer may occur at 150 cc/min.

The output temperature is dynamically related to both E and T_i by the approximating transfer function

$$T_e(s) = \frac{1}{\frac{F}{V}S \pm 1}\ T_i(s) \pm \frac{E(s)}{4.18\ F} \qquad 4.2$$

where V is the volume of fluid around the heater. Hence, the ratio F/V is the time constant of the heater and a fast response requires small values of V. The size of the heater element is a major factor determining the volume and it can be minimized by lowering the element's electrical resistance, reducing the operating voltage and selecting high resistivity material, as can be shown

from simple physical considerations.

The following configuration was chosen after a few trials. The heater element is a 2.5 cm #22 Nichrome wire (R = 80 milliohms) crimped inside brass tubing and positioned along the axis of a 1/8 inch diameter hole within a block of Plexiglass. The water enters simultaneously near both extremities of the heater wire and leaves through a single central outlet (Fig. 4.2).

The power control unit is shown in greater detail in figure 4.3. The heater element represented by a pure resistive component is connected across the secondary of a 110V-5V current transformer controlled on the primary by a triac switch. A commercially available trigger circuit (µA742 supplied by Fairchild Semiconductor*) delivers the trigger pulses to the triac. Power is applied to the heater in short bursts of 60 cycles at a frequency of about 3Hz. The corresponding sequence of input pulses to the triac trigger is provided by a pulse width modulator consisting of a triangular waveform generator feeding into a comparator.

The pulse width is directly proportional to the signal applied at the second input of the comparator. At frequencies sufficiently below the modulating frequency, the power delivered is directly proportional to the modulator input signal and the circuit behaves as a linear power amplifier. The technique sometimes called "time proportionating" is commonly used for handling large AC power loads at relatively low cost and is described in a number of application notes from various manufacturers (e.g. Fairchild Semiconductor).

* Fairchild Semiconductor, Mountain View, California, U.S.A.

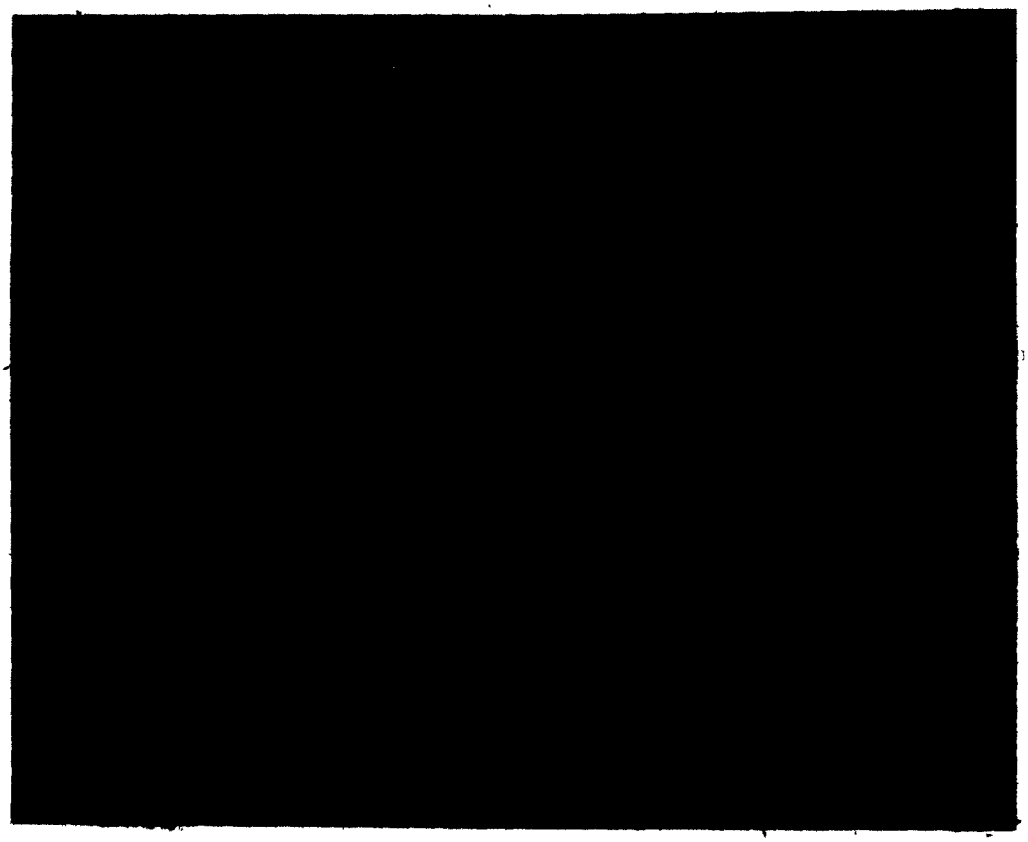

Fig. 4.2. Photograph of the heater block. The heater element is shown separately above the heater block.

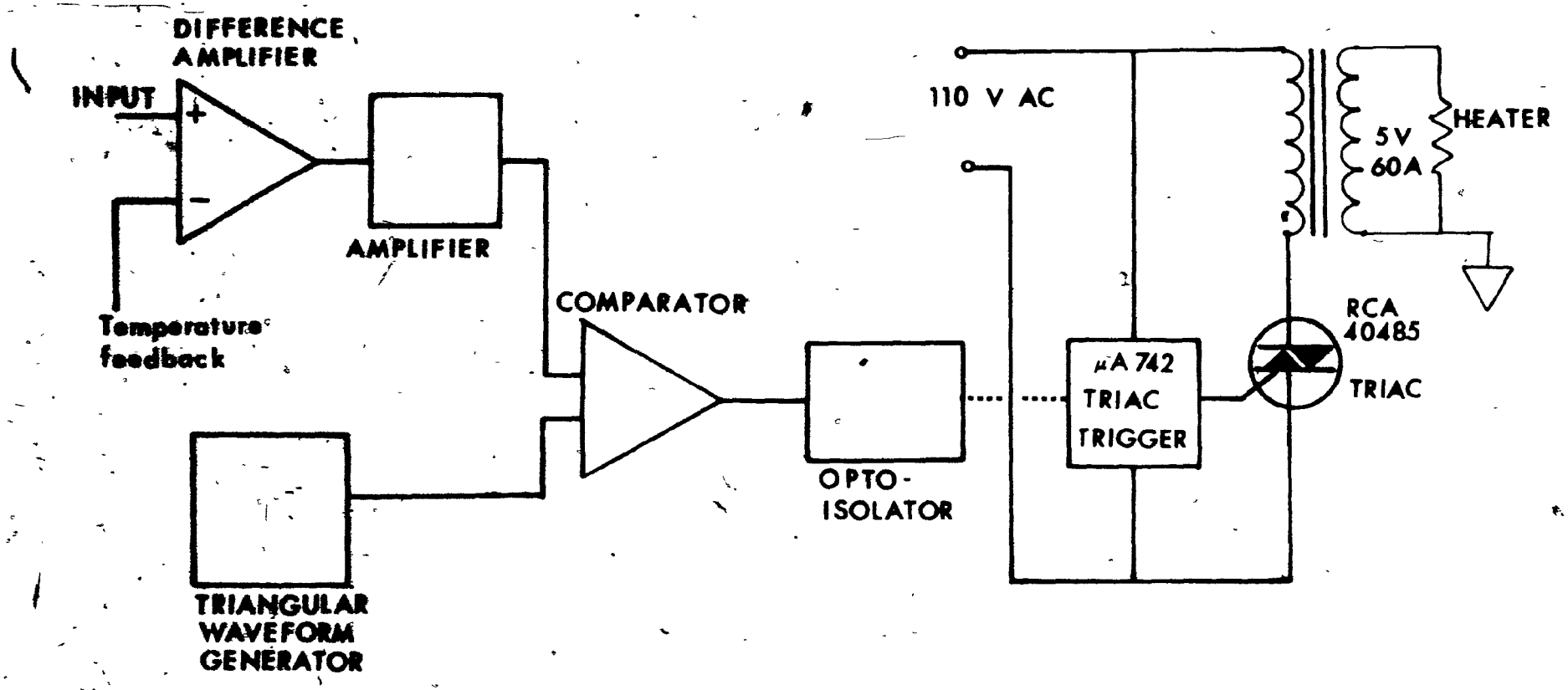

Fig. 4.3. Block diagram of the heater power control unit.

The "power amplifier" is part of a simple temperature control system. The signal driving the caloric stimulator is applied to the input of a difference amplifier and compared to the output temperature signal fedback from a thermistor amplifier. The error signal is amplified and fed to the pulse width modulator to generate the power pulse across the heater.

The temperature sensor at the heater outlet consists of an assembly (Thermilinear Component)[a] made of two thermistors mounted in a single 1/8" diameter bead. It is incorporated in a network of high precision resistors to provide a linear output with ± 0.16°C maximum deviation in the 0 - 50°C range.

Hydraulic Components

Water is obtained at 28°C from a thermostatic valve (Powers 440 Fotoguard)[b] connected to both the hot and cold taps and it runs continuously into a one gallon reservoir on the main instrument. The reservoir ensures complete debubbling of the mixed water and is kept filled to overflowing. A magnetic float level detector connected to a safety control circuit is installed on the reservoir. Water is circulated through the heater block by an adjustable-speed roller pump[c] and the flow rate is monitored by a Gilmont ball flowmeter[c]. The outlet tube consists of a 3 ft. long Teflon spaghetti tubing[d] within an envelope of corrugated plastic.

---

a. supplied by Yellow Springs Instrument, Yellow Springs, Ohio, U.S.A.
b. supplied by Powers Corp., Skokie, Illinois, U.S.A.
c. supplied by Cole-Parmer, Chicago, Illinois, U.S.A.
d. supplied by Polymer Corporation of Pennsylvania, Reading, Pa., U.S.A.

The very thin wall of the Teflon tubing (0.012") has a low heat capacity that minimizes damping; the envelope protects the tube from cooling drafts around the apparatus since this part is not included in the temperature feedback. Finally, a double-head pump[c] run by a single motor has been added to the system. One pump regulates the inflow to the supply reservoir from the mixing valve, the other returns the excess water to the drain.

4.1.2. Performance

The performance of the caloric stimulator is summarized in figure 4.4. A recording (A) of the outputs of both the heater feedback and the tube outlet thermistors shows that a 0.4°C peak-to-peak temperature ripple at the heater is smoothed down to within 0.1°C by the thermal capacitance and resistance of the outlet tube walls. Temperature linearity in relation to input voltage is illustrated by the stimulator response to a 0.002 Hz triangular waveform (C). The step response (B) has a time constant of about 3 seconds and from frequency response measurements the output is 3 db down at 0.1 Hz.

With very high gain of the error signal amplifier, the sensitivity of the apparatus in °C/volt should be close to the reciprocal of the gain of the thermistor amplifier in volt/°C. In practice, stability problems have limited the gain and the sensitivity is about 1.6°C/volt for a thermistor gain of 0.5 V/°C. Because of the limited gain, the output temperature varies with the temperature of the supply reservoir (approximately 0.25°C/°C). The latter

c. supplied by Cole-Parmer, Chicago, Illinois, U.S.A.

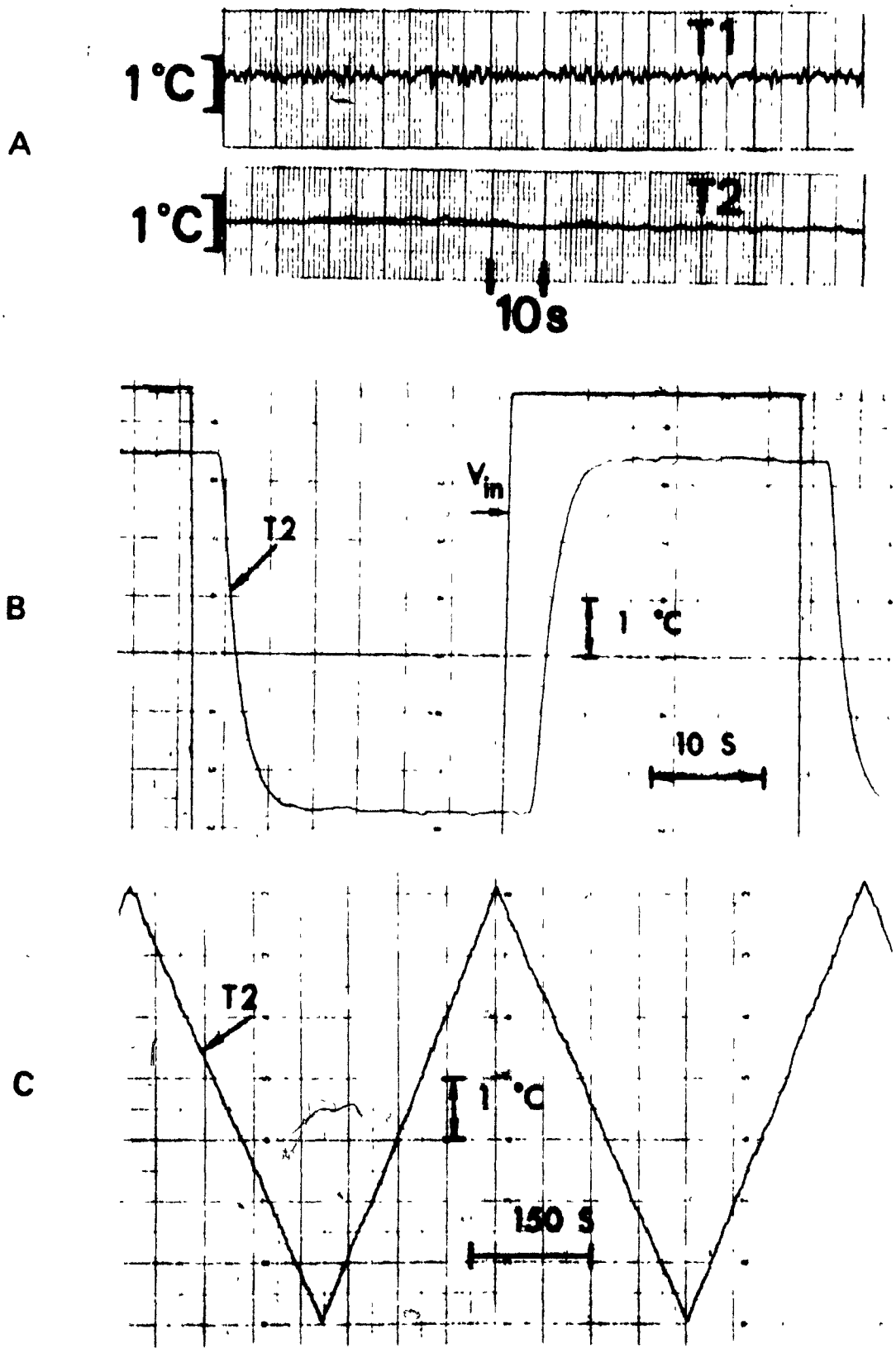

Fig. 4.4. A: simultaneous recordings of temperature at the heater outlet and at the cannula outlet (T_2) at constant input voltage. B: T_2 response to a square wave input. C: T_2 response to a triangular waveform. V_{in}: voltage input signal.

is however maintained within 0.25°C by the mixing valve so that the output temperature drift is negligible after the initial warm-up period. The output temperature is also dependent on the square of the line voltage and in any location where the power line is fluctuating, the instrument does not perform satisfactorily unless a voltage regulator is used.

4.1.3. Safety Aspects

Particular attention was given to potential thermal and electrical hazards throughout the development of this apparatus (which was intended for caloric testing in humans). During sustained irrigation of the ear canal, the cannula is located in very close proximity to the tympanic membrane. The irrigation per se has no harmful effect as shown by years of clinical caloric testing. However, one may point out that because of malfunctioning very high water temperatures could be produced and, in the extreme case, steam could be ejected into the subject's ear. Such dangerous effects could only occur under conditions of reduced or stoppped flow with maximum power applied to the heater (equation 4.2). A number of safeguarding mechanisms were therefore incorporated into the design, in particular a safety cut-off relay and a roller pump in the hydraulic circuit (fig. 4.1). The safety cut-off is triggered by signals from either the reservoir level detector or the heater thermistor. The temperature signal is viewed through a window circuit to detect high temperature above 46°C or conditions such as disconnected

or damaged thermistor. Both the pump and the heater are disconnected when the relay is activated and the instrument must be reset manually to resume operation. The roller pump was selected in place of other less expensive pumps to insure constant flow despite variation of the hydraulic resistance within the tubing or at the tip of the cannula.

Destructive testing was used to investigate the worst case. In special tests, the effect of stopping the water pump with full power applied to the heater was examined. Some boiling then occurred but a large bubble was rapidly formed, the element turned red hot and fused in 2 seconds or less. No temperature increase was recorded at the tip of the patient's cannula, the outlet tube apparently acting as a protective buffer. The tests thus confirmed that the instrument is intrinsically safe under all conditions.

Finally, the electrical safety aspects are discussed. The current transformer isolates the heater from the power line and only low voltages appear across the heater. Furthermore, the transformer secondary is grounded on one side to provide a current pathway in case of an insulation breakdown between the primary and secondary windings. In an ideal set-up, the subject should be isolated from ground, but if it were necessary to ground the subject, then minimal AC current (< 5 microamperes) might flow from the heater through the water in the tube. Indeed, the resistivity of tap water is high under most circumstances and typically, the electrical resistance

between the outlet tube extremities was of the order of 4 Megohms.

4.2 Methods and Measurements

The subjects were male and female volunteers between 20 and 35 years old with no history of vestibular disturbance.

The subjects were first fitted with electrodes to detect eye movements using the well-known principles of electro-oculography (Schackel, 1967). Three silver-silver chloride electrodes (Beckman 3509 8 mm^2 surface area) were covered with electrolyte jelly and applied to the external canthi and the mid-front position after vigorous rubbing of the skin with alcohol. This was followed by a 30 minute waiting period in the dark or wearing red goggles to allow for electrode stabilization and adaptation of the retinal potential to darkness (Gonshor and Malcolm, 1971).

The subjects were then seated comfortably (figure 4.5) and adjustments were made to have the head at an angle of 30 degrees with the horizontal so that the lateral semicircular canals were in the vertical plane. As much as possible, the head was kept in its natural position relative to body axis.

The external ear canal was first examined and a short cannula made of silicone rubber tubing was carefully introduced inside the ear canal deeply enough to have the tip of the cannula within one or two millimeters of the tympanic membrane without touching it. The cannula was immobilized with tape, or using a special holder made of steel wire and encircling the pinna. In both cases, the cannula remained fixed relative to the head to allow for possible head

Fig. 4.5. The experimental set-up. The subject is shown with the electrodes fixed on the canthi and the cannula inserted into the ear canal. The caloric stimulator is on the left.

movements. The free end of the cannula could be manipulated safely and was connected to a three-way stopcock at the end of the stimulator outlet tube. The other arm of the stopcock was used to circulate water in the tube during the preparatory phase of the experiment. A funnel was conveniently positioned to collect the water coming out of the ear canal.

Before starting the irrigation, calibration of eye position signal was done and a short recording was obtained with eyes closed to detect the presence of any spontaneous nystagmus.

Irrigation always started at normal body temperature and was maintained at that level for a time to allow the subject to become accustomed to the irrigation. The temperature was often readjusted slightly since many subjects had detectable nystagmus at 37°C. The adjustment never exceeded one degree centigrade in practice.

Throughout the preparatory phase and during the experiment itself the room was kept dark except for a red light required for the operator's convenience. After the period of habituation to irrigation, the subject was asked to keep his eyes closed unless instructed otherwise.

Control of Arousal

Great care was taken to maintain the arousal level of the subject to a sufficiently high level during the prolonged periods of stimulation. Contrary to what was expected, the continuous irrigation was not an arousing factor and most subjects habituated rapidly to the sensation which was described by many as pleasant. Some even

tended to fall asleep. Mental arithmetic was not found to be particularly useful in maintaining arousal during these long recordings (up to 30 min). It was however found that subjects could readily be kept aroused through conversation on a subject of special interest to the individual. For instance, medical students responded very well when asked to review human anatomy or to discuss diseases and various therapies. Other preferred mathematical games or kitchen recipies. It was also found that some subjects could maintain a brisk nystagmus without any conversation whereas others had occasional periods of dysrhythmia and suppression of nystagmus even during mental activity. As a whole however, the control of arousal could be achieved satisfactorily in most cases. This required continuous monitoring of the nystagmus waveform on the recorder and continuous interaction with the subject.

Measurements

(a) Eye Position

The potential difference across the two outer electrodes was measured by a high input impedance (10^{14} ohms) Burr Brown model 3061/25 differential amplifier with a fixed gain of 100 and an adjustable output offset. The output of this first stage was carried to a second general purpose amplifier and the total gain varied between 500 and 1000 to yield a signal in the volt range. In a few cases to be indicated, an AC amplifier was used. Calibration was performed in the usual way using light sources subtending a known arc.

(b) Temperature

The temperature of the irrigating medium was sensed prior to the ear cannula tubing with the linear thermistor assembly described in section 2.1.2. This measurement was in error by a small time delay and a negligible temperature drop along the cannula. Calibration was done in constant temperature water baths by comparison of the thermistor output with a mercury thermometer having a $0.1^{o}C$ resolution.

(c) Recording

Both the eye position and temperature signals were recorded on a two-channel recorder continuously driven at 10mm/sec. In a number of cases the data was stored on a FM magnetic tape recorder.

4.3. Slow-phase Eye Velocity Measurements

A semi-automated technique to measure slow-phase eye velocity was developed. A chart reader was constructed* (figure 4.6) which included a specially designed goniometer that measured the angle of a line on the chart with respect to the time axis. The goniometer consisted of a standard one-turn 2.5" diameter wire-wound potentiometer in which the shaft had been replaced by a 1" diameter transparent core with a reference cursor on the face close to the paper. The goniometer was mobile in both directions across the chart and another potentiometer fixed to the sliding assembly measured the displacement along the time axis. Both the angle and time potentiometer were connected to a computer via a small signal conditioning

---

* The assembly was built by Mr. A. Hagemann.
The goniometer was modified with the help of Mr. J. McColl.

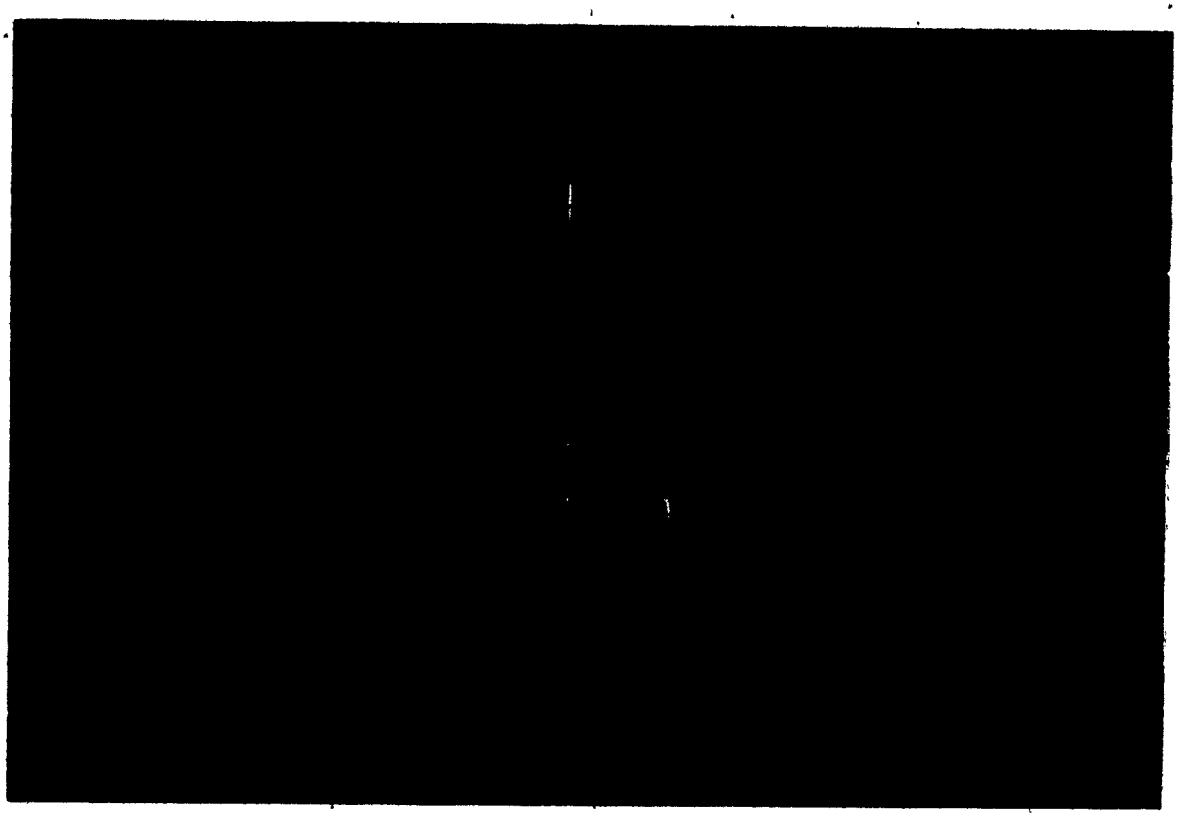

Fig. 4.6. Slow-phase eye velocity analyser. The potentiometer with a transparent core measures the angle of the cursor relative to the time axis of the recording. Slow-phase velocity is proportional to the tangent of that angle.

box and a suitable program calculated the time and slow-phase velocity.

The accuracy of the output angle was checked by repeated measurements of a series of known angles traced by a digital plotter. The relative error of the computed tangent was 0.8% at 45° and 5% at 5° and 85°, the error being symmetric about 45°. For long recordings, the time potentiometer had to be reset every 60 cm, but with sufficient care the accuracy could be maintained within one second over periods of 1500 seconds or more.

To measure slow-phase velocity, the center of the cursor was conveniently located at the mid-point of the intersaccadic interval and the cursor was aligned on the best line fitting the eye position within the interval. In some cases, slow-phase velocity varied continuously within the interval. The average slope was then determined by aligning the cursor on the chord joining both extremities of the interval. During the period of direction reversal, nystagmus is absent and the eyes may remain relatively steady or jump in a stepwise fashion in either one or the other direction. During such periods, slow-phase velocity was sampled as the slope of the eye position tracing, despite the absence of saccades. As a rule, each intersaccadic interval was sampled except in the case of high frequency nystagmus beating at more than one per second, when only representative saccades were sampled. The average time interval between samples was in the range 1-2 seconds. Prolonged periods of artifacts and dysrhythmia were marked and left blank in plots of slow-phase velocity.

In figure 4.7, a sequence of slow-phase eye velocities

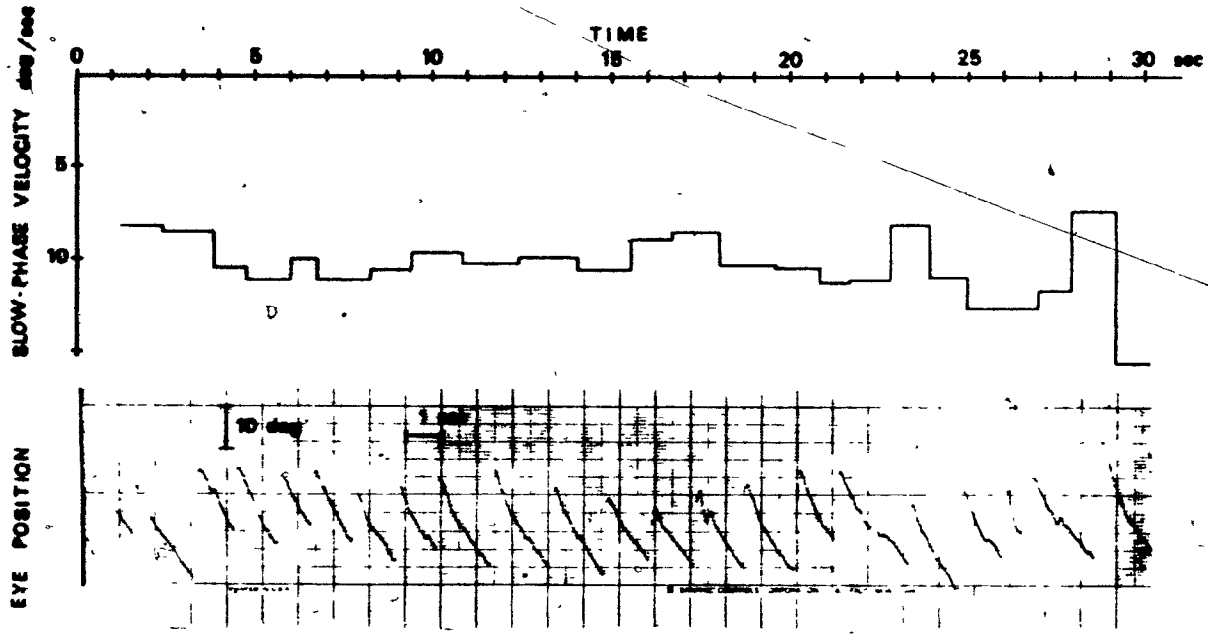

Fig. 4.7. Typical computer plot of slow-phase eye velocity shown with the original record from which it was obtained. The variability of slow-phase velocity between saccades is observable from the eye position tracing.

has been plotted as a stepwise varying function and is compared to the original eye position recording. The slow-phase velocity signal is "noisy" and variations of the slow-phase slope may be observed directly from the recording. For the sequence shown in figure 4.7, the mean slow-phase velocity is 10.2 deg/sec and the standard deviation ($m = 24$) is 1.8 deg/sec i.e. more than 17 percent of the mean value. All slow-phase velocity plots shown in this thesis exhibit such large deviations about the running average.

CHAPTER 5

EXPERIMENTAL STUDIES ON THE CALORIC VESTIBULAR RESPONSE: EXPERIMENTS AND RESULTS

5.1 Introduction

The experiments described in this chapter were designed to study the dynamics of the caloric vestibular response with particular reference to a hypothetical model relating slow-phase eye velocity to ear canal temperature. Temperature stimuli were applied during continuous water irrigation which consisted of simple elementary signals i.e. pure sinusoids, steps and pulses, so that the theoretical results of Chapter 3 might be directly applied to the analysis of the slow-phase velocity data. Caloric stimulation was performed in humans over much longer periods than in the classic caloric test in which irrigation times never exceeds one minute. In particular, sinusoidal input at frequencies as low as 0.00055 Hz and steps lasting over 20 minutes were applied. The purpose was to examine the long-term aspects of the caloric response in the low frequency range below 0.005 Hz where the peak of the "band-pass" equivalent system filter is located, according to the model.

Four different aspects were considered. First, the response to sinusoidal stimulation was investigated (section 5.2) before any other types of input waveform to obtain some indications of the system linearity and time invariance.

In the second set of experiments (section 5.3), the response to temperature step inputs was recorded since no adequate data could be found in the literature on the elementary step response. (The latter is particularly useful in systems analysis to identify the characteristic behaviour of processes). A quantitative analysis of the responses was made in terms of the general model and the relative influence of vestibular dynamics was studied.

The response to temperature pulse inputs was obtained (section 5.4) from a small group of subjects to provide some indication on the applicability of the model to short lasting caloric responses usually encountered in caloric testing. It also appeared important to determine the relative effect of forcing the return to body temperature by continuous irrigation as opposed to the usual procedure in which irrigation is simply stopped.

In experiments described in section 5.4, the effects of flow rate variation on step response were studied.

5.2 Sinusoidal Caloric Stimulation

5.2.1. Protocol

Five subjects were prepared and connected to the caloric stimulator as described in the previous chapter. Sinusoidally varying temperature changes around normal body temperature were applied at various frequencies between 0.00055 Hz and 0.05 Hz. Generally, several cycles of the response were recorded, but at very low frequencies it was sometimes possible to record only one full cycle. Stimulation was usually started at the beginning of a cycle when going from hot to cold temperatures. At low frequencies, the sinusoidal amplitude was set to around $2^{o}C$ to avoid nausea and excessive dizziness caused at larger amplitudes. Above 0.01 Hz, the amplitude was set to around $5^{o}C$ in order to compensate for marked response attenuation. However, at these high frequencies the temperature could not be raised beyond a certain limit above which the stimulation would become painful apparently due to failure of cutaneous receptors to adapt.

A different sequence of stimulation frequencies was followed for each subject to avoid any systematic trend. After stimulation was completed at a given frequency temperature was returned to $37^{o}C$ for about three to five minutes and the subject was allowed to relax mentally. The overall experiment lasted about three hours and midway through the irrigation was interrupted for a coffee break of ten minutes. Continuous attention was given to keep the subject alert and interested in the experiment.

5.2.2. The Caloric Response to Sinusoidal Stimulation: Qualitative Aspects

The response to sinusoidal temperature changes around body temperature was characterized by continuous nystagmus with periodic direction reversals according to the stimulation frequency. In most subjects, a sharp and brisk nystagmus was recorded with few interruptions or periods of arrhythmias even at very low frequencies. Short segments of the eye position recording at various phases of an 800 second cycle are shown in figure 5.1 to illustrate the variations of nystagmus intensity and direction reversals as a function of time. In this particular record, nystagmus was more intense at peak response on the hot side than on the cold, which is reflected as a bias in the slow-phase velocity replot (figure 5.2A)

The high frequency limit to caloric sinusoidal stimulation seems to lie in the interval 0.02 - 0.05 Hz. No measurable response was ever obtained at 0.05 Hz, but all subjects exhibited distinguishable nystagmus at 0.02 Hz.

The eye position records were analyzed by the semi-automated method described in the previous chapter and figure 5.2 shows typical replots of slow-phase eye velocity from subject C.M. at four different frequencies, 0.00086, 0.001, 0.003 and 0.01 Hz.

Slow-phase eye velocity appears as a continuous and approximately sinusoidal signal with superimposed high frequency "spike-like" noise. In two instances illustrated in curve A and B, data are missing because the recording could not be sampled due to artifacts. Typically

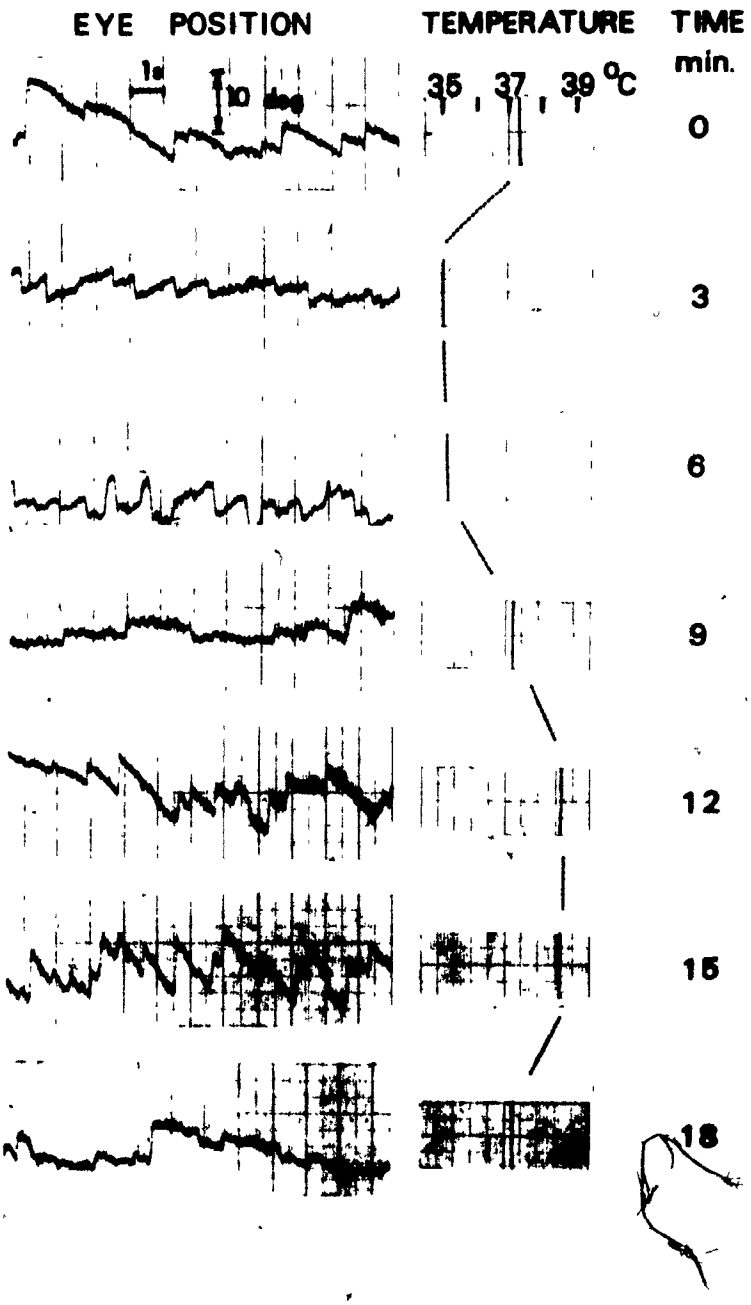

Fig. 5.1. The ocular response to a sinusoidal temperature stimulus applied during continuous irrigation of the external ear canal. The amplitude of the stimulus was 2°C about body temperature and the frequency was 0.00056 Hz. Segments of the eye position recording are shown at three minute intervals.

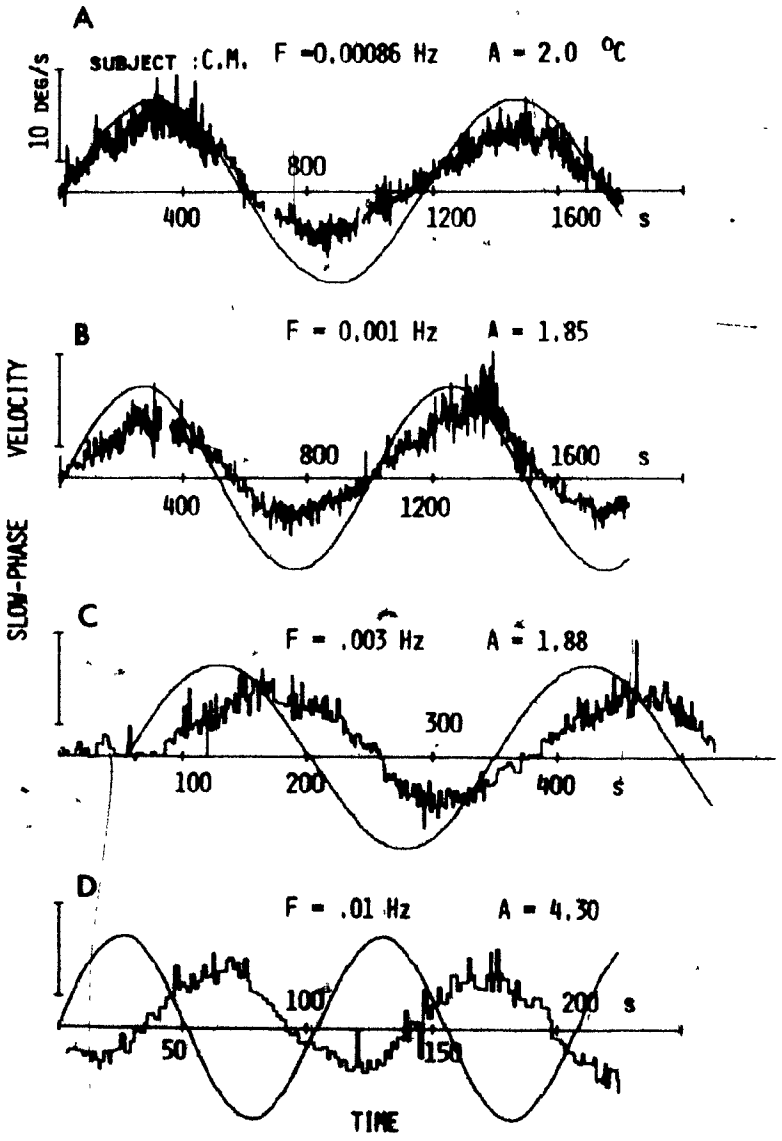

Fig. 5.2. Slow-phase velocity responses to sinusoidal temperature stimulation at various frequencies in the same subject. Temperature (smooth sinusoidal curves) has been normalized. A, amplitude of the temperature stimulus; F, frequency.

these blanks were of short duration compared to the period of the waveform and did not introduce major difficulties. The responses are biased towards the positive side (left direction) but in other subjects, the bias was not present or it appeared in the other direction. Increasing phase lag and attenuation occurred with increasing frequency. In the lower curve (D), recorded at 0.01 Hz, the phase shift approximates 180 degrees. Note that in this case the temperature input amplitude was more than double that in (A).

A marked distortion of the sinusoidal output waveform was found in one case (figure 5.3A) whereas the curves obtained at other frequencies in the same subject were symmetrical. The distortion may be explained by a time-varying factor (e.g. level of arousal) rather than by a static nonlinearity which would cause distortion at all frequencies.

Transient Analysis

The response of a linear system submitted to a sinusoidal input from initial resting conditions (e.g. uniform temperature throughout the temporal bone) undergoes a transient phase before steady state amplitude and phase values are reached. The aspects related to the transient are important in the present study since one is dealing with experimental responses that have been limited in duration to a few cycles because of particular constraints.

Young (1972) derived the time domain solution to a temperature sinusoidal input applied at zero phase of the cycle. The steady state component is immediately found from the transfer function derived in Chapter 3. The transient term is a complex expression involving a

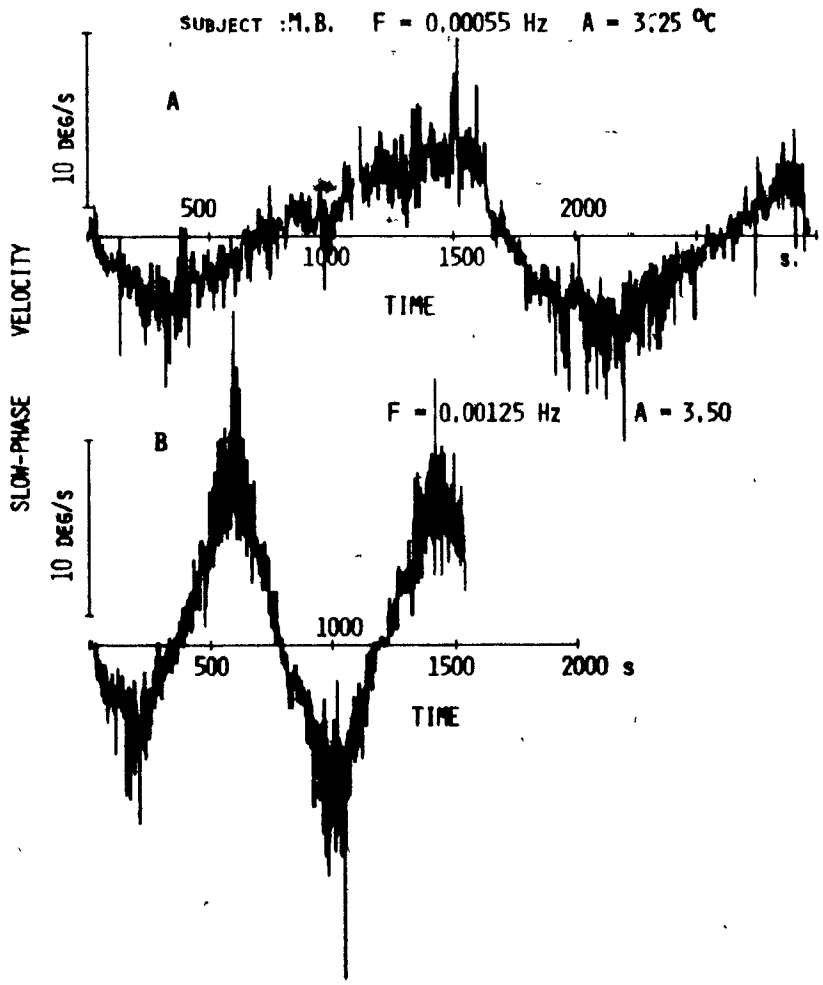

Fig. 5.3 A case of asymmetrical response (curve A) to sinusoidal stimulation. The distortion was not observed at other frequencies in the same subject (e.g. curve B). A, amplitude of the temperature stimulus; F, frequency.

double integral that we have calculated at various frequencies for normal parameter values with a computation method differing from the one used by Young (Appendix 3). Both the transient component and the overall torque response are shown at representative frequencies in figure 5.4, in which steady state components have been normalized to unity peak amplitude. The transient exhibits a fast phase lasting 200 seconds and it continues with a prolonged small amplitude tail. In theory, steady state is achieved only when time tends to infinity since this is the time required for the impulse response to vanish completely.

The effect of the transient on the overall response varies with frequency. Below 0.001 Hz, the transient introduces a short lasting positive bias, followed by a negative bias between 5 and 10 percent of peak amplitude with a slow drift towards the baseline. At intermediate frequencies between 0.001 and 0.009 Hz, the fast phase of the transient is observable on the first peak and the negative tail is less than 5 percent of peak amplitude. Above 0.01 Hz, the first cycle is shifted considerably above the baseline and a gradual return takes place during the subsequent cycles.

The observations made from the slow-phase velocity records are in general agreement with these theoretical curves. At very low frequencies, the fast phase of the transient was practically non-observable and up to 0.01 Hz it affected only the first peak. At frequencies above 0.01 Hz the predicted shift of the initial cycle could be observed (figure 5.5) and it was particularly pronounced at 0.0246 Hz. The prolonged tail of the transient could not be observed directly from

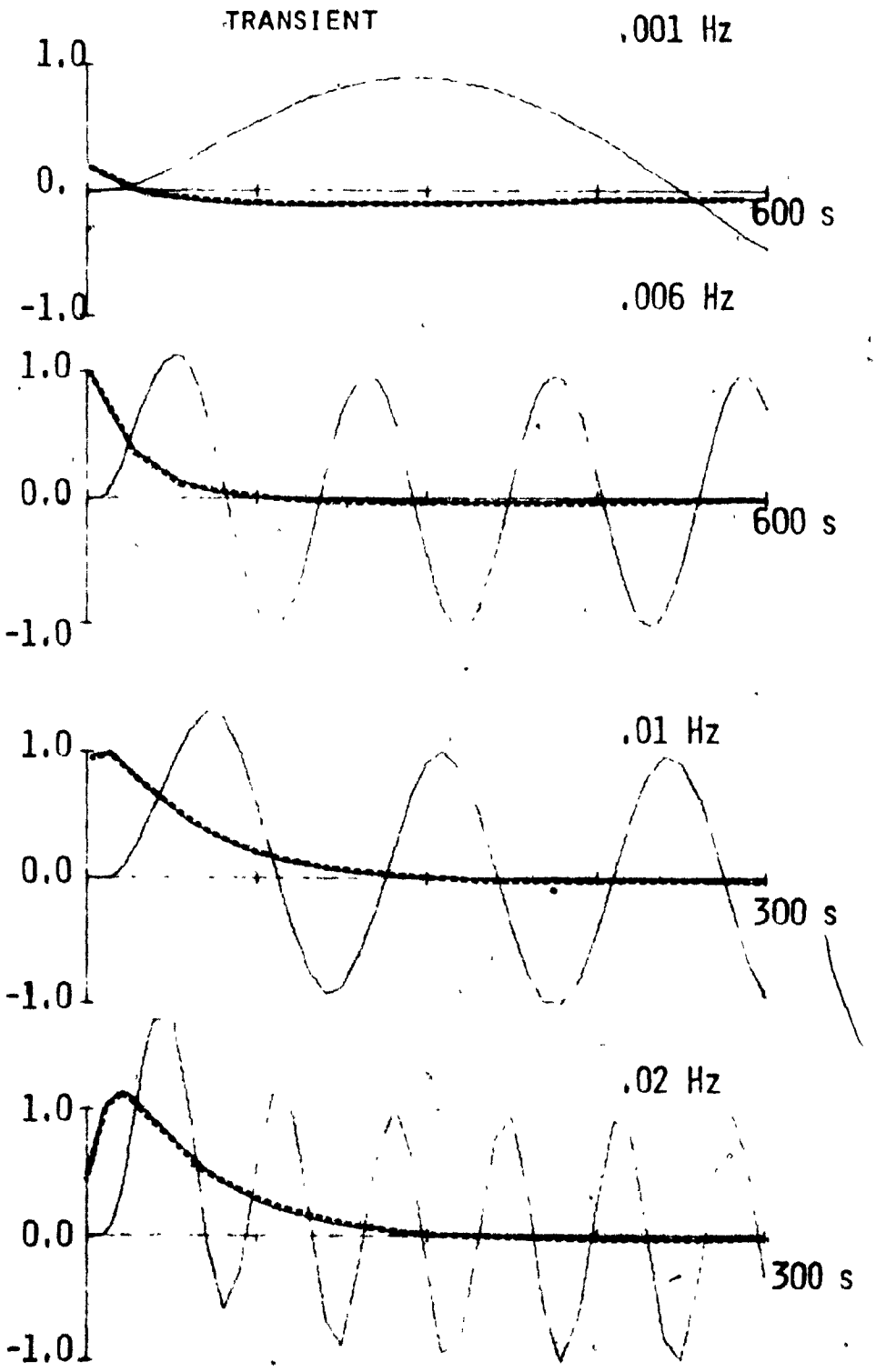

Fig. 5.4. Theoretical transient component (dotted line) and overall output torque (continuous line) to a sinusoidal temperature input applied at $t = 0$. The curves have been normalized relative to steady state amplitude.

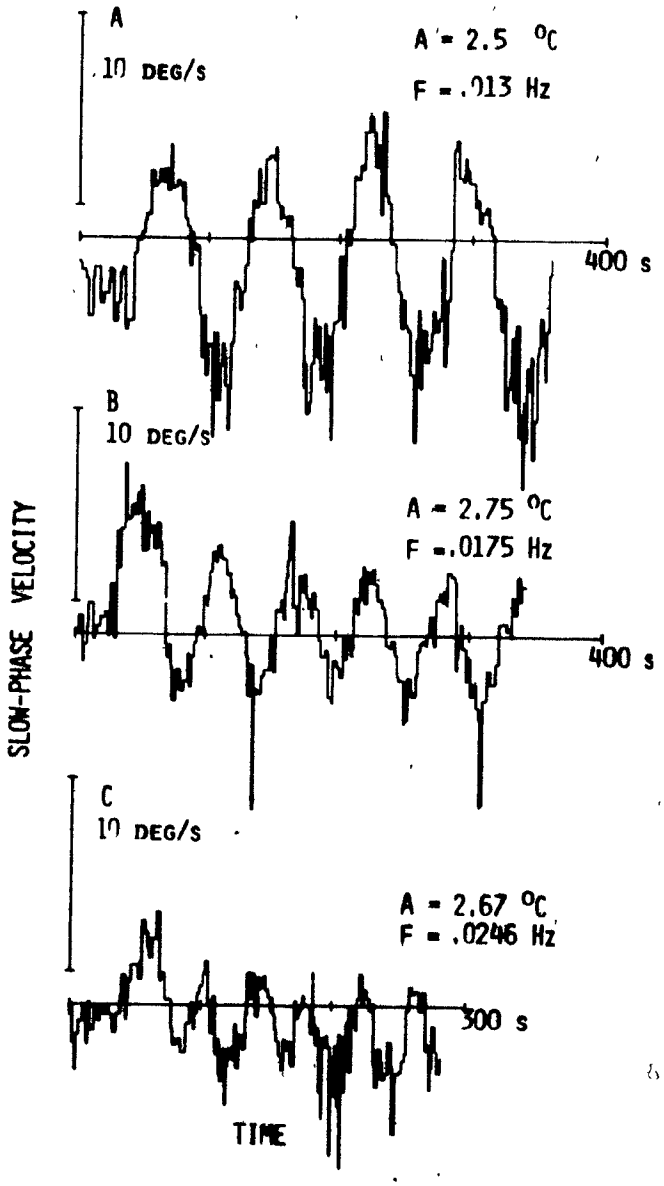

Fig. 5.5. **Slow-phase eye velocity responses illustrating the effect of the initial transient at high frequencies of sinusoidal stimulation. Compare with theoretical torque curves of fig. 5.4. F = frequency. A = amplitude.**

the slow-phase velocity replots because of noise. However, this tail should be viewed as a source of bias and drift for purpose of quantitative analysis.

5.2.3. Determination of Slow-Phase Velocity Amplitude and Phase; Bode Plot

In order to obtain estimates of phase and amplitude from the slow-phase velocity data, both Fourier analysis and statistical curve fitting were considered. Fourier decomposition provides least squares estimates of the fundamental component and the associated higher harmonics in one simple set of calculations but it requires equispaced data over a complete cycle. Data smoothing and reduction with conventional digital techniques was however a problem in our case because the data consisted of non-equispaced samples with occasional blanks.

Standard linear regression was easier to apply and was used here for this reason. The output slow-phase velocity (SPV) was represented by an equation of the form

$$SPV = a + b \sin (wt + \phi) + ct \qquad 5.1$$

where w is the stimulation frequency, b and ϕ the SPV amplitude and phase relative to the origin of the record. The terms a + ct were included to account for the bias directly observable from the replots and for linear drift due for example to the tail of the transient. Equation 5.1 may also be expressed as

$$SPV = a + b' \sin wt + b'' \cos wt + ct \qquad 5.2$$

where

$$b = (b''^2 + b'^2)^{\frac{1}{2}} \qquad 5.3$$

and

$$\phi = \tan^{-1} (b''/b') \qquad 5.4$$

Estimates of a, b', b" and c were obtained by standard linear regression. As an example, a best fitted sinusoid is shown in figure 5.6 superimposed on the raw data. The initial position of the data was judged by visual observation to contain the fast phase of the transient and hence was excluded from the regression. The residuals were also plotted and were found more or less randomly distributed along the time axis with little periodic trend. The regression equation obtained in this case was

$$SPV = 0.104 - 0.0028\ t + 10.14 \sin \frac{2\pi}{102} t + 3.81$$

The mean values b' and b" and the corresponding standard deviations $\Delta b'$ and $\Delta b''$ were

$$b' = -7.84 \qquad \Delta b' = 0.178$$

$$b'' = -7.20 \qquad \Delta b'' = 0.179$$

The amplitude b was determined within the limits of an error circle of radius Δb

$$\Delta b = \sqrt{\Delta b'^2 + \Delta b''^2}$$

and the maximum phase deviation $\Delta\phi$ was given by

$$\Delta\phi = \sin^{-1} \frac{\Delta b}{b} \approx \Delta b/b$$

In the above case $\Delta b = 0.256$ for a relative error of 2.4 percent

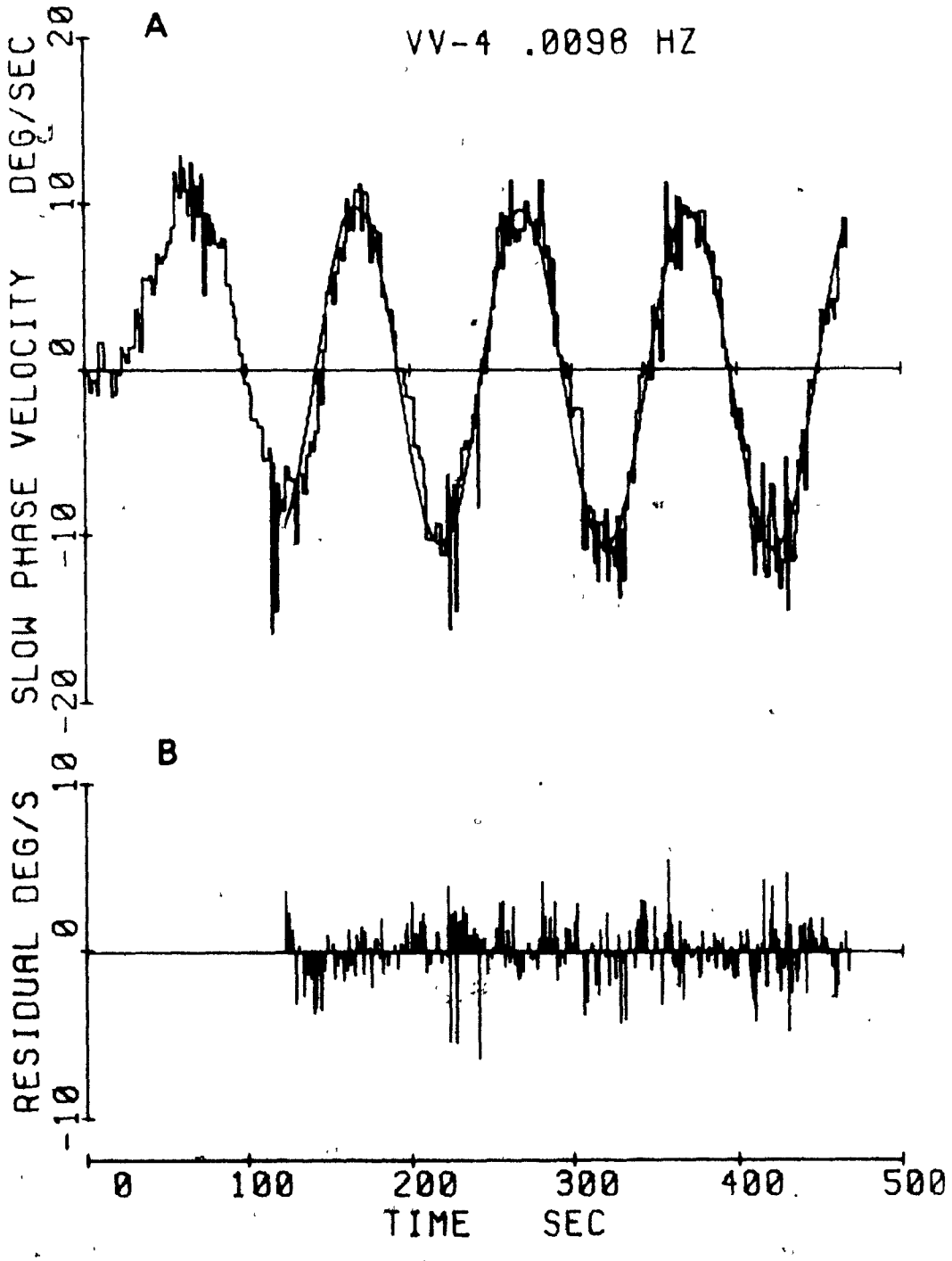

Fig. 5.6. Statistical curve fitting of slow-phase velocity response to sinusoidal stimulation. In A, the best fit curve is superimposed to the data. In B, the deviations from the best curve are plotted versus time. The initial cycle was not included in the regression analysis.

in amplitude, and a phase deviation of 1.4 degree.

The t statistics were computed for each coefficient in order to test the hypothesis that a given coefficient was significantly different from zero.

A total of 29 records from four subjects were processed by statistical curve fitting and numerical results are tabulated in table 5.1. The maximum amplitude ratios varied between subjects from 2.3 to 8.7 deg/sec/^{o}C and occurred in three cases between 0.001 and 0.002 Hz and in the other at 0.005 Hz. The range of relative phases extended from +17 degrees (lead) at 0.00055 Hz to -214^{o} (lag) at 0.0175 Hz.

At frequencies below 0.01 Hz, the amplitude deviations varied between 0.6 and 6 percent and the overall correlation coefficient was always above 0.90. At frequencies higher than 0.01 Hz, the amplitude deviations reached 9% and the correlation coefficients varied between 0.72 and 0.84. This deterioration of the goodness of fit at high frequencies was in part caused by the fewer number of points that could be sampled per cycle.

The drift coefficient was statistically non-significant in many cases; in the others, the drift rate ranged between small values of 0.009 and 0.00055 deg/sec/sec. The bias term was quite variable even in records from a single subject at various frequencies. In subject V.V., a marked shift towards negative bias values appeared mid-way through the experiment, probably due to a technical fault in the equipment since an offset was found in the temperature amplifier output after the experiment.

TABLE 5.1 STATISTICAL CURVE FITTING OF SINUSOIDAL RESPONSES

Subject and Pt No.	Frequency	Input amplitude	Amplitude ratio	Percent deviation	Relative phase	Drift coefficient	Bias	Correlation coefficient
V.V.	10^{-3} Hz	^{o}C	deg/sec/^{o}C		deg	deg/sec/sec	deg/sec	
1	3.3	1.9	7.24	2.2	- 65	N.S.	0.91	0.97
2	17.5	2.75	1.17	5.2	-214	-0.011	2.5	0.84
3	5.88	2.10	4.89	1.6	- 92	-0.0058	1.5	0.95
4	9.8	2.8	3.59	1.7	-152	N.S.	0.104	0.97
5	0.66	2.0	8.01	1.0	- 12	N.S.	-3.8	0.96
6	7.91	1.9	5.07	1.7	-114	-0.0046	-2.21	0.95
7	24.7	2.67	0.79	9.0	-208	N.S.	-	0.723
8	1.19	2.0	8.7	7.9	- 15.4	N.S.	-4.13	0.97
9	4.3	2.0	6.5	1.5	-106	N.S.	-4.35	0.96
10	13.2	2.5	2.2	3.0	-175	N.S.	-0.86	0.92
11	3.3	1.9	6.8	1.5	- 59	+0.005	-5.5	0.96

TABLE 5.1 continue

Subject and Pt No.	Frequency	Input amplitude	Amplitude ratio	Percent deviation	Relative phase	Drift coefficient	Bias	Correlation coefficient
M.A.B.	10^{-3} Hz	°C	deg/sec/°C		deg	deg/sec/sec	deg/sec	
1	5.42	1.9	2.29	2.2	- 81.5	N.S.	0.27	0.92
2	20.0	3.4	0.67	5.0	-206	N.S.	1.2	0.93
3	0.55	3.3	1.30	0.7	+ 17	-0.00055	1.06	0.89
4	3.25	3.0	2.2	1.4	- 53	-0.0033	2.4	0.94
5	9.63	3.2	1.16	2.8	-138	N.S.	0.69	0.93
6	1.25	3.5	2.2	0.8	- 17.6	-0.0019	2.7	0.95
C.M.								
1	3.97	1.9	2.77	1.3	- 54	-0.004	2.85	0.93
2	20.0	3.0	0.63	8.5	-205	N.S.	2.75	0.84
3	9.6	4.3	1.20	2.3	-136	-0.007	1.80	0.97
4	0.86	2.0	2.84	1.3	- 0.3	-0.0006	1.85	0.95
5	1.01	1.8	3.03	1.3	- 11.4	+0.0010	0.35	0.95

TABLE 5.1 continue

Subject and Pt No.	Frequency	Input amplitude	Amplitude ratio	Percent deviation	Relative phase	Drift coefficient	Bias	Correlation coefficient
M.B.	10^{-3} Hz	^{o}C	deg/sec/^{o}C		deg	deg/sec/sec	deg/sec	
1	9.26	5.04	1.66	3.1	-116	N.S	-1.60	0.92
2	19.5	4.6	0.694	6.9	-146	N.S.	0.989	0.88
3	19.46	4.2	0.484	7.9	-184	N.S.	0.796	0.76
4	9.8	4.6	1.53	3.2	-127	N.S.	0.98	0.93
5	5.39	5.2	2.92	0.6	-87	-0.0052	2.21	0.95
6	19.38	4.27	0.44	8.0	-177	-0.0093	0.65	0.79
7	1.85	5.30	5.64	3.3	-29	-0.06	11.6	0.97

The analysis was complemented by testing for the presence of second and third harmonics that are often generated from a pure sinusoidal input by systems with static nonlinearities. Thus, the regression analysis was repeated with additional terms proportional to cos 2wt, sin 2wt, cos 3wt and sin 3wt included in the regression equation. In general, the overall correlation coefficient increased little above the value obtained with the fundamental frequency alone. In a few cases harmonic terms were found to be significantly different from zero but there was no systematic occurrence of either the second or the third harmonic in any subject. Hence, these significant harmonics may be attributed to random factors that would probably be averaged out if more cycles could be recorded, especially at low frequencies.

Bode Plot

A Bode plot (figure 5.7) was constructed from the results of the regression analysis to study the caloric response in the frequency domain. The amplitude ratio is maximum in the frequency range 0.001 - 0.005 Hz and accelerated attenuation appears above 0.009 Hz. The very few points below 0.001 Hz indicate that amplitude probably decreases with decreasing frequencies.

The phase data from all subjects are remarkably grouped in a smooth curve. Around 0.02 Hz the phase reaches -210 degrees and extrapolates towards larger phase lags at higher frequencies. On the other hand, the phase curve reaches zero at 0.00086 Hz and is pointing towards positive phase values at lower frequencies.

Subject	Symbol
V.V.	●
M.A.B.	○
C.M.	■
M.B.	▼

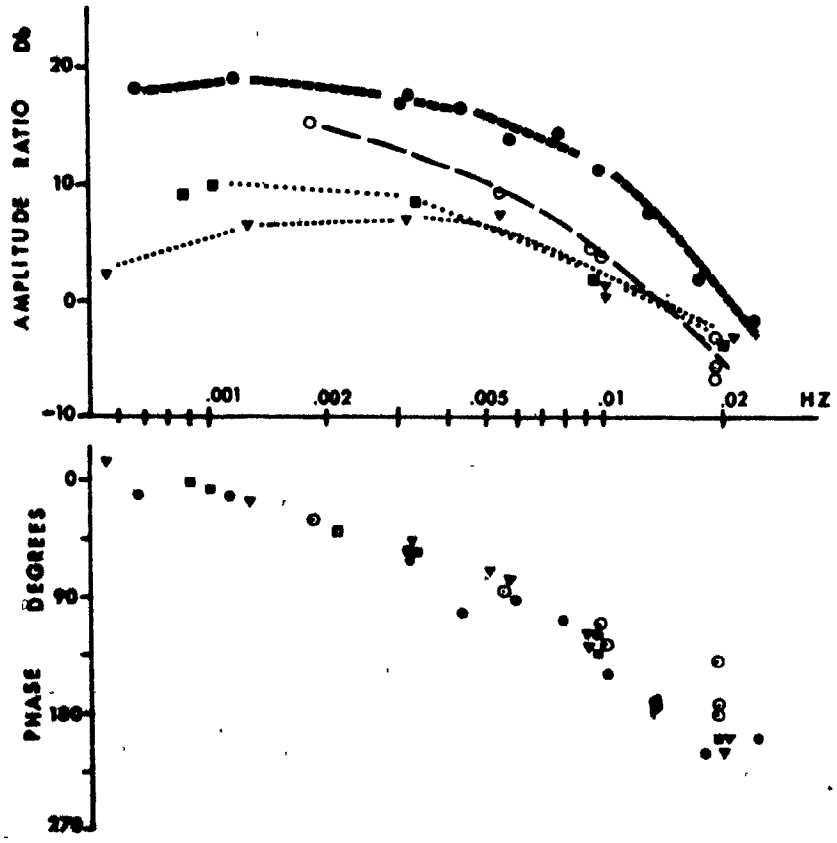

Fig. 5.7. Bode plot illustrating the frequency characteristics of the caloric response in four subjects. Each point was obtained from the response to a sinusoidal temperature input (table 5.1). The amplitude ratio is in deg/sec/°C.

5.2.4. Discussion

The only previous data on sinusoidal caloric stimulation were those obtained by Young (1972) who stimulated a number of subjects with air at frequencies around 0.007 Hz for approximately two complete cycles or approximately six minutes. Young's slow-phase velocity curves are comparable with those reported here.

However, Young's data suggest that there is a dead zone or vestibular threshold near zero eye velocity where nystagmus reverses its direction. The effect was probably due to a restricted definition of slow-phase velocity. Young sampled slow-phase between saccades only and did not estimate slow-phase velocity in the reversal period where no saccades occur. In the present work, the slope of the eye position signal was measured at convenient points during the null period so that measurements around zero slow-phase velocity could be obtained. With this method, no dead zone or threshold was found in any of the four subjects. This interpretation is in agreement with that of Malcolm and Melvill Jones (1970) who discussed similar data with slow-phase velocity going through zero when nystagmus reversed direction (figure 2.5, Chapter 2). According to these authors, their data suggested a continuous cupula signal lying between two lines representing the resolution limits and if a threshold existed, it could only be very small.

Young's work also deserves some comments concerning the transient aspects of the sinusoidal response. Young compared the time courses of both slow-phase velocity and theoretical pressure differential across the cupula, and noted that the nystagmus data did not exhibit an asymmetry as

large as that predicted by the model. However, the theoretical curve drawn by Young at 0.007 Hz probably pertains to a higher frequency located in the frequency range above 0.01 Hz according to our own calculations. Indeed, as shown in figure 5.4, around 0.007 Hz, the effect of the transient is pronounced only in the first peak and it is only above 0.01 Hz that asymmetry appears over several cycles. The computed curves have been confirmed qualitatively by the experimental data shown in figure 5.5. Contrary to what Young may have indicated, the model predicts well the time course of the sinusoidal response.

The sinusoidal character of the response was assessed by statistical curve fitting. A high correlation coefficient (> 0.9) was obtained for the fundamental frequency alone and higher order harmonics, second or third, were not present in any systematic fashion. The fact that a sinusoidal response was generated by a sinusoidal temperature input is far from being trivial since it provides a good indication that the system is linear and time invariant. Indeed, a great concern in these experiments has been that at such low frequencies of stimulation a number of time dependent factors could have perturbed the response, such as blood flow, direct thermal effects on the vestibular receptors or variations in the arousal level. A distorted output waveform was found in one case and has been tentatively explained by such influences. It is unlikely however that these factors would interact and balance out their effects so that the sinusoidal character of the output is preserved at all

frequencies. Hence, they probably played a minimal role during prolonged caloric stimulation.

The linearity of the caloric response has been investigated by a number of authors (Henrikkson, 1956; Torok, 1969; Litton and McCabe,1967) in experiments involving short irrigations at graded temperature levels usually in the direction of cold temperatures. In general, responses measured in terms of peak slow-phase velocity increased linearly with decreasing temperature down to 30°C, below which the linearity was often altered. The results of sinusoidal stimulation described here suggest that the system responds linearly in both hot and cold directions. It remains however to define more precisely the range of linear responses in caloric stimulation since a limited set of amplitudes and frequencies was examined in these experiments.

A great variability was observed in the bias term of the regression analysis, and is somewhat difficult to explain. As already shown, one source of bias may be the long tail of the response transient that can reach 10 percent of the steady state amplitude (at frequencies below 0.001 Hz).

Another cause of bias is the difference between the basic temperature level of the stimulator at zero signal (set as close as possible to 37°C) and actual body temperature. In principle, the bias slow-phase velocity due to any significant difference may be detected and corrected for by monitoring nystagmus at the resting level and trimming the stimulator basic temperature accordingly. Unfortunately,

this aspect was not given sufficient attention in the experimental protocol at that early phase of the work.

In any case, it would have required much longer control periods at body temperature between stimulation since accurate measurements at low slow-phase velocities are difficult.

The sinusoidal stimulation experiments were performed before the publication of Young's thesis, in order to test a tentative caloric response model using Steer's lumped parameter approach. If the canal time constant in Steer's model is changed from 10 seconds to the more realistic value of 20 seconds, a reasonable fit of the experimental phase curve can be obtained in the 0.002 - 0.01 Hz frequency range. However, Steer's model exhibits a maximum phase lag of 180^{o} in the frequency domain, hence it cannot explain measured phase lags exceeding 210 degrees at frequencies above 0.01 Hz that extrapolate towards greater phase lag at higher frequencies. Because of this discrepancy, Steer's model was abandoned in favour of the distributed parameter description of Young.

A brief comparison of the experimental Bode plot (figure 5.7) with the theoretical torque transfer function characteristics shown in figure 3.5 reveals a great deal of similarity in most details. On a more quantitative basis, transfer function curves were best fitted to the data yielding parameter values close to the normal values found in Young's work. The results provided some indication of the validity of the model but they had little statistical significance due to the scarcity of data points and they have not been reported here.

Another objective of sinusoidal stimulation was to test the

role of neural adaptation in the caloric response. It was originally argued on the basis of Steer's model that adaptation would cause positive phase shift at low frequencies. However, the introduction of Young's model to represent the thermal processes complicated the problem since the torque/temperature transfer function also predicted positive phase at low frequencies. For the sake of discussion, one may consider the frequency at zero phase shift, which is 0.00065 Hz and 0.002 Hz respectively for the torque model and for the overall transfer function with the adaptation filter ($m = 1$). Experimentally the cross over point was found at an intermediate frequency around 0.00086 Hz. This may in fact correspond to a case where the value of the parameter m is intermediate between 0 (no adaptation) and 1 (full adaptation), a possibility which will be raised again in the analysis of the step response in the next section.

It is evident that the measurements should extend further down in the frequency range perhaps as low as 0.0001 Hz (period = 166 minutes) to identify adequately the transfer function in terms of the caloric response model. To say the least, such measurements would be very difficult to obtain from human subjects. In any case, if system identification becomes the main objective in future experiments, one may then prefer other test signals more efficient than pure sinusoids that can only provide measurement at one frequency value. In this work, the sinusoidal stimulation experiments have provided a reasonable check of system linearity and time invariance that are required in the proper use of complex signals.

In conclusion, the data on sinusoidal responses have established

that the system responds linearly and is compatible with Young's torque model both in steady state and in transient aspects. However, the overall caloric response model cannot be tested adequately from these data.

5.3. Response to Temperature Step Change

5.3.1. Protocol

In eight subjects, a step change in temperature was applied either above (42 or 40°C) or below (30 or 32°) body temperature.* The steps lasted a minimum of ten minutes and sometimes exceeded twenty minutes. In a few cases, the response was also obtained for an additional ten-minute period after return to body temperature. The methods and set-up were as described before except that an AC amplifier with a time constant of three seconds was used to record eye position.

Another four step responses were taken from experiments on flow rate described below. Only the first response from each subject was then included in the study since it was obtained in the same conditions than for the above group of eight subjects i.e. at the same flow rate.

5.3.2. Results

In all subjects, sustained nystagmus was produced in response to step temperature changes, and lasted as long as the stimulus was applied (figure 5.8). The return to baseline temperature in a stepwise fashion caused a rapid decay of the response followed by an overshoot in the opposite direction.

A typical slow-phase eye velocity response is shown in figure 5.9. After an initial delay of 20-30 seconds, slow-phase velocity rose rapidly to a peak in about 100 seconds, then decayed more slowly during the first five minutes, after which the response either stabilized or

* We wish to acknowledge the assistance of Mr. M. Cheng in performing these experiments.

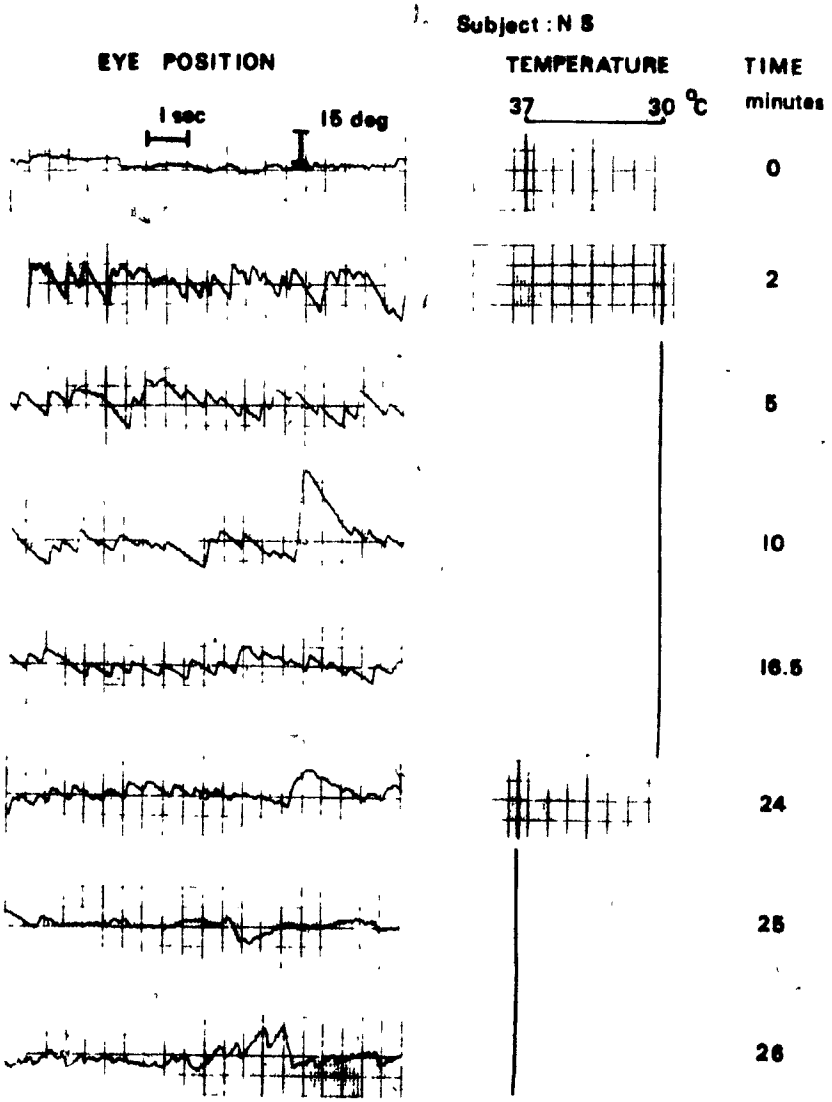

Fig. 5.8. The nystagmic response to a temperature step change applied during continuous irrigation of the ear canal and illustrated by 10 second segments of the eye position recording sampled at the time shown in the right-hand column. The off-step was applied 24 minutes after the on-step.

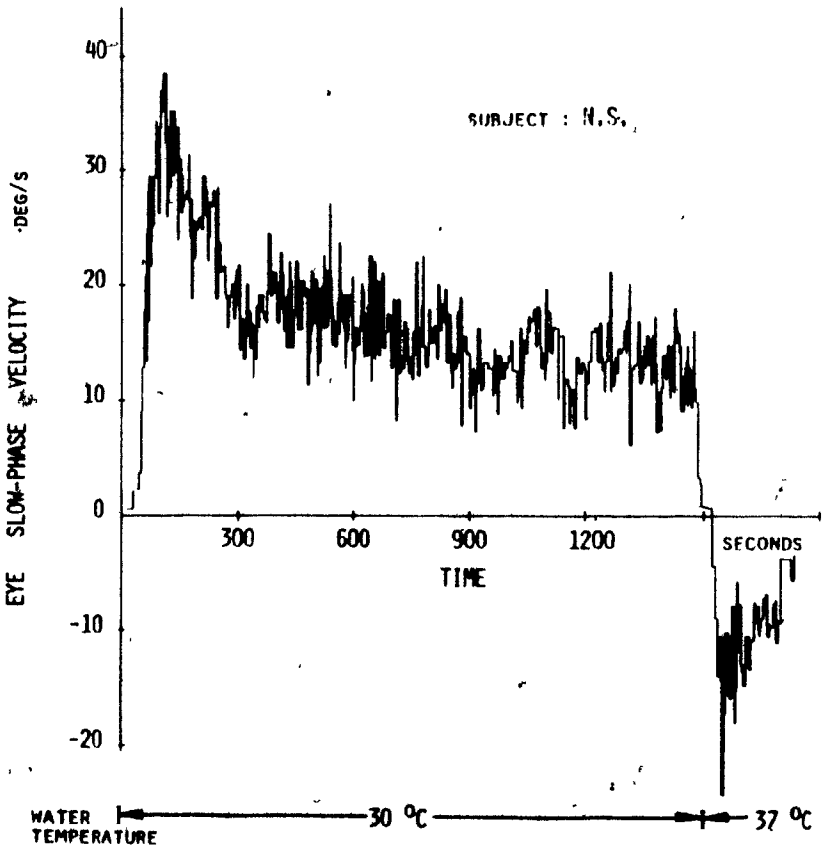

Fig. 5.9. The slow-phase eye velocity response following a temperature step change at the ear canal. The corresponding eye position recording is illustrated in fig. 5.8. Note the characteristic rise to a peak followed by a decay.

decayed very slowly, remaining significantly above zero over the last 15 minutes of stimulation. A similar reaction in the opposite direction was observed after the return to body temperature i.e. slow-phase velocity decreased quickly and reached a new peak in the opposite direction before gradually decaying to zero.

This characteristic response with an overshoot was observed in all subjects with some variations in the initial rate of rise and the time to peak. A number of fast and slow responses are illustrated in figure 5.10 (fast) and 5.11 (slow). The time to peak estimated directly from these plots varied between 92 and 270 seconds with an average of 159 seconds.

5.3.3. Quantitative Analysis of Step Response in Terms of the General Caloric Response Model

(a) Preliminary Remarks

Previous results of the theoretical model analysis were applied to interpret the step response data. A preliminary qualitative comparison with the model curves shown in figure 3.13 indicated that the sustained slow-phase velocity responses above zero required that the parameter m associated with the neural adaptation filter be given small values in the range of 0 - 0.5. Indeed, at higher values of m the response of the adapted model would attenuate rapidly within five minutes and would even reverse in the case where $m = 1$. Hence, the mathematical representation of neural adaptation pertaining to rotational responses ($m = 1$) could not be applied to the case of unilateral caloric stimulation.

When m was restricted to small values the differences between

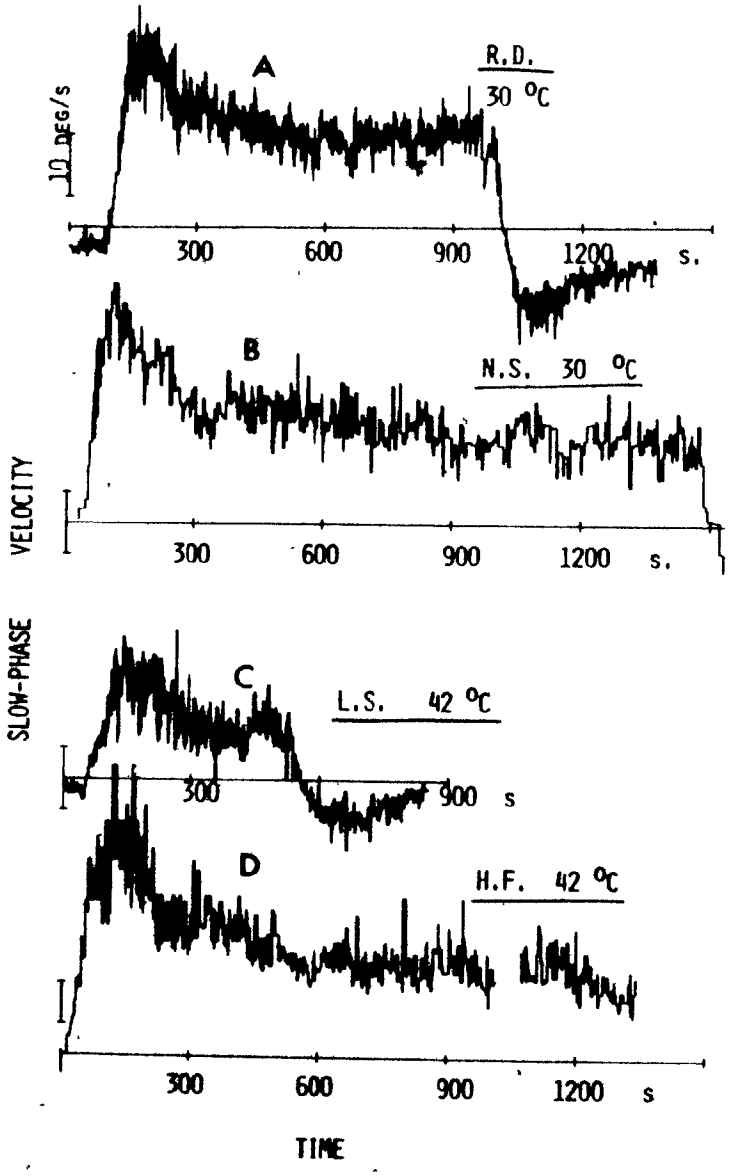

Fig. 5.10. Typical "overshooting" step responses.

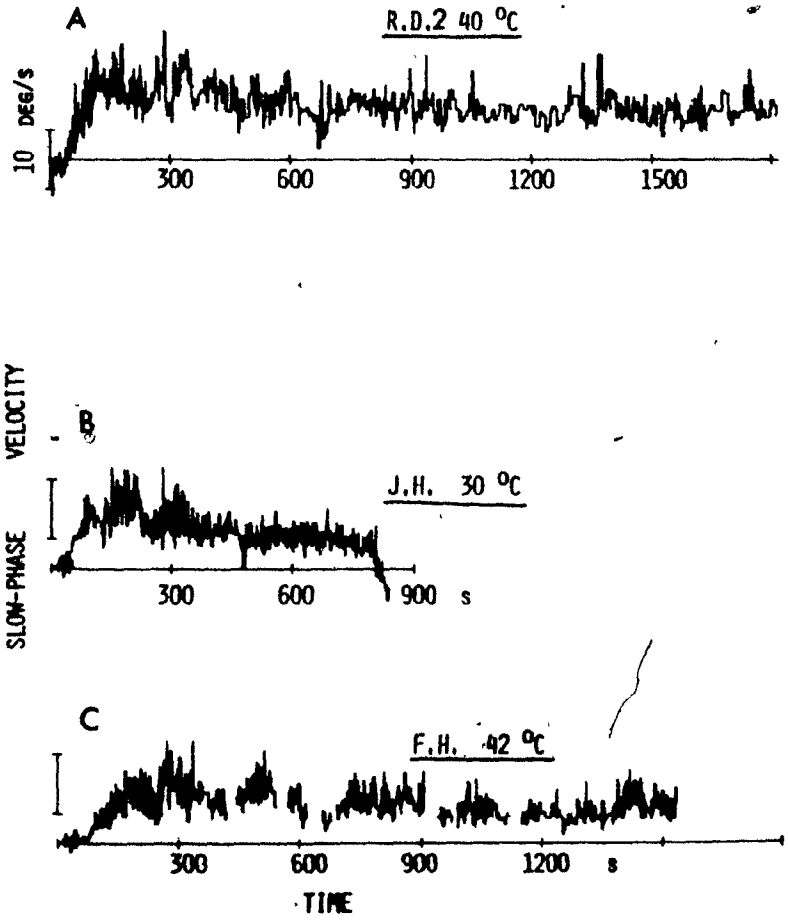

Fig. 5.11. Typical "sluggish" step responses.

the model variables (theoretical torque and theoretical adapted response in particular) were small so that in practice the noisy slow-phase velocity data curves could not be further evaluated on a qualitative basis. A quantitative analysis was therefore conducted to test whether the influence of canal dynamics and neural adaptation could be detected in these data. A method of stepwise curve fitting was adopted. The basic torque model was first fitted to the data and the model parameters were adjusted between certain limits to minimize the sum of squared deviations between slow-phase velocity data and theoretical torque. This was then repeated successively with the model cupula deflection and with the model adapted response. The improvement in the goodness of fit brought by additional components in the theoretical response was evaluated by a standard statistical test.

Statistical curve fitting could be used since the theoretical response was known analytically. However, the regression equations are highly nonlinear and an optimization procedure, very demanding in computer time and memory, is necessary in practice to obtain least squares estimates of the parameters. A simpler though less rigorous method based on an interactive computer program was devised to solve the problem.

(b) Curve Fitting Procedure

The curve fitting program displays simultaneously a slow-phase velocity record and a theoretical step response which can be modified and adjusted so that both curves are superimposed. To minimize

computing time, the theoretical response is obtained from a bank of precalculated theoretical torque curves stored on contiguous disc files, retrievable under program control. The basic torque model contains four parameters but one only needs a two-dimensional parameters grid in X_o and h, respectively the distance to canal center and the coefficient associated with heat transfer. Diffusivity can easily be simulated by increasing the basic time interval to stretch or compress the theoretical curve. The radius is neglected since as described earlier (section 3.3.) it affects only gain which is already included as a parameter. When the experimental response starts from a non-zero slow-phase velocity value, a bias must be added to the theoretical curve. Finally, to simulate canal dynamics and neural adaptation, the digital filters described in Appendix 2 are used on line. Further details on the program are given in Appendix 4.

Because of the program constraints, the parameters could only be varied between certain limits. X_o was varied between 0.45 and 1.14 cm i.e. approximately ±50% around the mean value 0.76 cm measured by Young (1972). This was required because of the absence of any hard data on the range of variation encountered in vivo. The lower and upper limits of h were 0.5 and 80 cm^{-1} respectively. The lower limit was 10 times smaller than the value of 5.0 suggested by Young for air. On the other hand, there was no advantage in further increasing the upper limit since the response changed little beyond that point, as already noted from theoretical considerations. Diffusivity could be varied continuously from zero to about 10 times the normal value

for bone (0.0025 cm^2/sec).

The relative goodness of fit was evaluated with the standard one-sided F test of variance ratio. The hypothesis was that the variance obtained in curve fitting the model adapted response was smaller than the variance obtained in fitting the model torque alone. The sum of squared deviations (SSQD) calculated from the program only provided an approximation to the variance since a zero-mean deviation could not be insured by visual fitting. However, the error was probably small since visually fitted curves were found very close to the optimum curve. A better procedure was implemented at a later stage of the analysis in which the variance was determined by linear regression with respect to the gain parameter so that a zero mean deviation could be obtained.

(c) Application to Experimental Responses

Fig. 5.12 illustrates a typical run of the program. In the first two photographs, the experimental data were compared to the torque variable. In one case, the theoretical torque curve was adjusted to fit the peak and the later part of the response whereas the initial rise and the decay immediately after the peak were poorly fitted. In the second case, the peak was left out to provide a better fit to the initial rise and to the major part of the response decay. Despite many attempts, it was not possible to find a combination of the torque response parameters that would fit all parts of the slow-phase velocity curve.

In figure 5.12C, the theoretical curve represents the output of the adapted response model with a canal time constant of 21 seconds

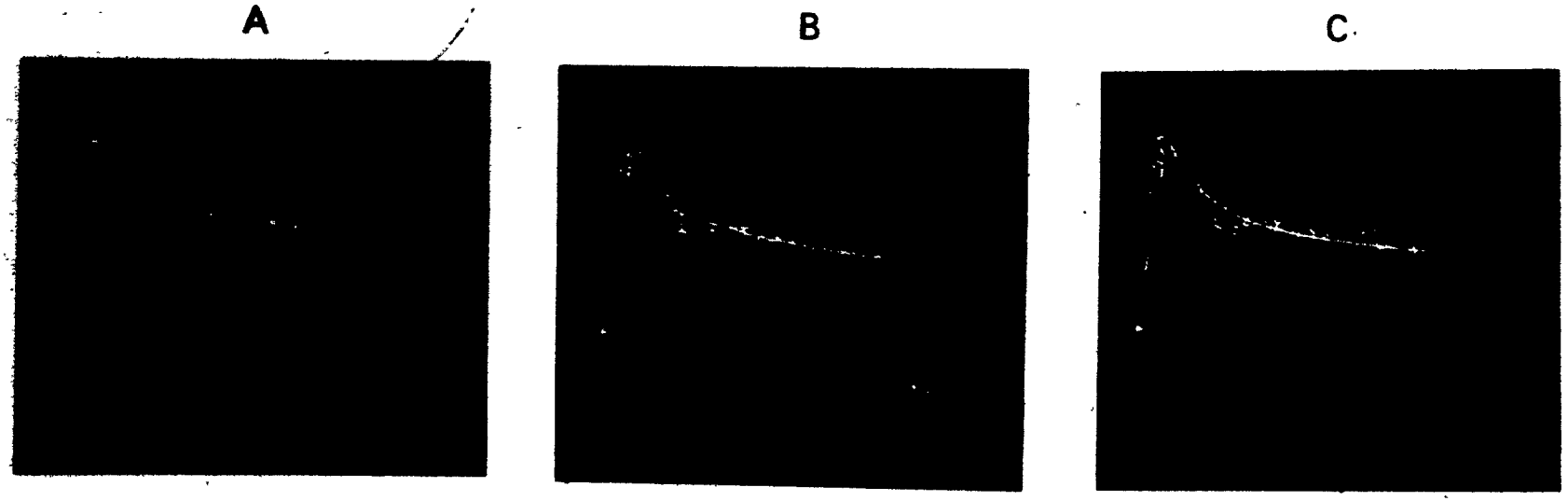

α = 0.00236

X_o = 0.608

α = 0.00129

X_o = 0.608

α = 0.00209 cm^2 / sec

X_o = 0.76 cm

τ_e = 21 sec

τ_a = 82 sec m = 0.5

Subject: J.McC

Fig. 5.12. Curve fitting the caloric response model. The model output (regular dotted curve) is superimposed to slow-phase eye velocity data from step response. In A and B, different attempts to fit the data by torque alone are shown. C illustrates the improvement in the fit given by the model which includes canal dynamics and "modified" neural adaptation. The parameter h was set to 80. cm^{-1} in all cases. Symbols defined in text.

and an adaptation time constant of 82 seconds with m = 0.5. A much better fit to all parts of the experimental response may be observed. The addition of the canal first order lag improved the fit mainly in the initial response rise whereas the lead-lag filter helped in reducing the discrepancy in the immediate post-peak decay which occurred at a faster rate than predicted by the model torque.

The goodness-of-fit observed visually was also confirmed by the decreasing SSQD value that successively dropped from 2.20 (arbitrary units) to 1.84 to 1.62 when considering successively the model torque, cupula deflection and adapted response. The rate of torque variance to adapted response variance yielded an F value of 1.35 which indicated a significant difference to the 0.01 probability level (n = 538).

Difficulties

Two basic difficulties were met in using the program. First, certain details of the experimental curves could not be fitted well by any of the three model variables. Sometimes, the responses reached a steady state rather than decaying smoothly as theoretically expected. One subject (figure 5.10A) exhibited a small but noticeable increase of slow-phase velocity after 10 minutes of stimulation. Differences were also noted between the initial peak and the second peak following the return to baseline. The second peak tended to be flatter and less steep than the initial one, with longer time to peak (figure 10C). These differences could not be explained by the residual effect of the on-step since the responses were decaying very slowly at the time the off-step was applied. These apparent changes in the system dynamic characteristics were not predicted by the model and the curve fitting

of the late part of the response was generally more difficult.

Another serious problem was met when several sets of parameter values yielded similar response shapes and sums of squared deviations that were very close to each other. The interactive program was not sufficiently accurate to allow identification of an absolute optimum set with any degree of confidence. This problem will be examined in more details after presenting the results.

The curve fitting procedure was simplified in order to deal with these difficulties. The responses were fitted only up to the point of return of the stimulus to body temperature and the later part of the response was neglected. The distance to canal center was also arbitrarily fixed at 0.76 cm (normal value) and only diffusivity, system gain and the parameter h were allowed to vary since most shapes could be reproduced with this reduced parameter set. It was thought that the distance to canal center was probably less variable than the other parameters.

Results

10 records were analyzed by visual curve fitting. The remaining two records were too noisy or contained too many blanks. Generally, the characteristic pattern observed in figure 5.12 was met in most curves i.e. a systematic improvement in the goodness of fit was observed as canal dynamics and neural adaptation were included in the simulation of the model responses. Additional examples of best fitted curves are shown in figure 5.13.

Table 5.2 summarizes the data on curve fitting. The time to peak given in the second column (measured directly from the slow-phase

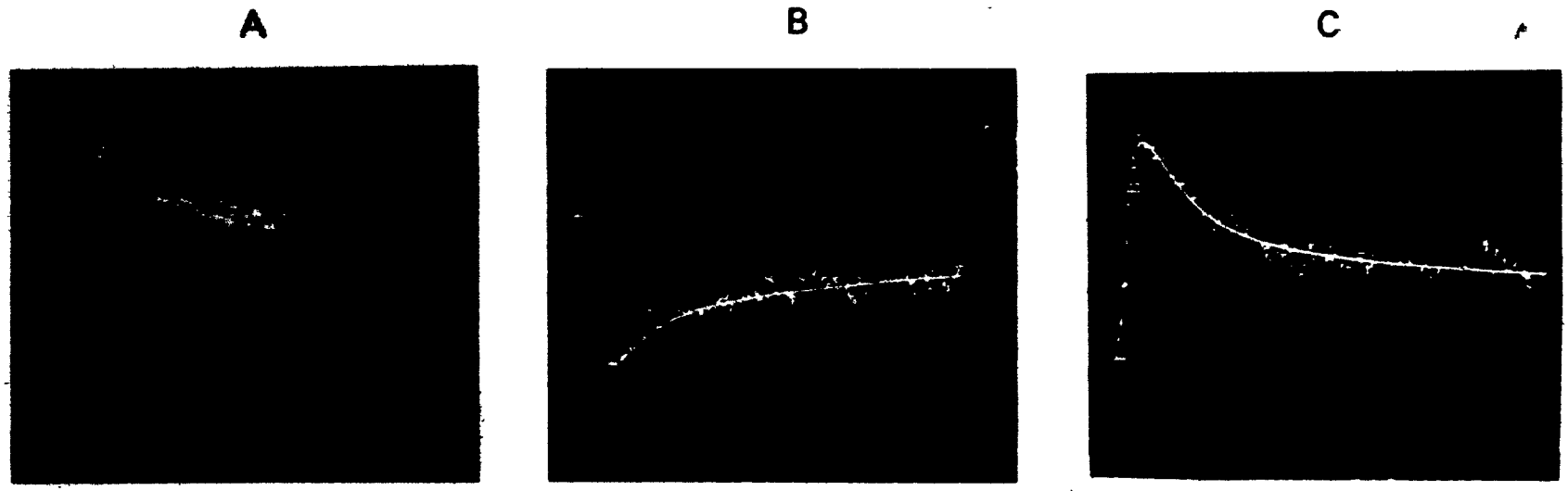

Subject : R.D.	N.S.	H.F.
α = 0.00218	α = 0.00299	α = 0.00209 cm^2 / sec
X_o = 0.76	X_o = 1.14	X_o = 0.76 cm

Fig. 5.13. Curve fitting the general caloric response model to slow-phase eye velocity data from step responses. Additional examples are given of best fitted curves of the model output including canal dynamics and neural adaptation. Parameter values common to all three cases: h = 80. cm^{-1} ; R = .3 cm; τ_c = 21 sec; τ_a = 82 sec; m = 0.5. Symbols defined in text.

TABLE 5.2 VISUAL CURVE FITTING OF STEP RESPONSES

Subject	Time to peak sec	h cm^{-1}	X_o cm	α 10^{-3} cm^2/sec	Variance ratio[(a)]	p level	Number of points
R.D.	92	80	0.76	2.18	1.65	< 0.01	566
J.McC	140	80	0.76	2.09	1.35	< 0.01	533
L.O.	120	80	0.76	2.45	1.53	< 0.01	670
N.S.	115	80	1.14	2.99	1.28	< 0.01	431
J.H.	210	5	0.76	1.79	1.18	< 0.05	670
H.F.	130	80	0.76	2.09	1.60	< 0.01	424
D.K.	122	80	0.76	2.14	1.14	N.S.	860
F.H.	270	5	0.76	1.34	1.295	< 0.01	539
R.D.2	160	80	0.95	3.03	0.97	-	500
L.S.	240	10	0.76	1.60	0.96	-	295
Mean	160			1.96*			
±S.E.	18.8			0.126			

(a) $\frac{\text{Variance (torque model)}}{\text{Variance (adapted response)}}$

* excluding subjects N.S. and RD2

velocity plot) gives an indication on the basic character of the response - sluggish or overshooting. The h parameter varied between 80.0 and 5.0 cm^{-1} and diffusivity between 0.00303 and 0.00134 cm^2/sec. Low values of these two parameters were found associated with sluggish responses in which the time to peak exceeded 200 seconds. On the other hand, responses with small time to peak had larger diffusivities (> 0.0020) and the h coefficient was usually 80.0. In two cases (N.S. and RD2) distance was inadvertently set to 1.14 and 0.95 cm respectively, but this was apparently compensated by much higher diffusivity values than those obtained for the rest of the group. These two cases were excluded when an average diffusivity value was computed that yielded 0.00196 ± 0.000126 .

In eight out of ten subjects, the variance ratio is larger than 1.0 i.e. the SSQD obtained with model torque decreased with the addition of the vestibular dynamic components. In all but one of these cases, the improvement in the goodness of fit is statistically significant (6 cases at $p < 0.01$). The other two subjects had responses for which neural adaptation did not provide a better fit. In these two cases there was no significant difference between the variances of all three model output variables.

5.3.4. Analysis in the parameter space

A different procedure was developed to check the curve fitting results and to investigate further the aspects related to parameter identification. The sums of squared deviations (SSQD) were calculated for each point of the X_o - h parameter grid at five diffusivity values

above and below normal diffusivity. The data of subject J.H. (figure 5.11) were used. Gain was determined by linear regression and bias was set to the value previously determined by visual curve fitting.

In figure 5.14A, diffusivity is constant and SSQD is shown as a function of distance X_o for different h values. A minimum is clearly visible for each curve and as h takes lower values, there is a decrease in the value of X_o at which the minimum occurs, as expected from previous theoretical considerations. The lowest SSQD value is observed at $X_o = 0.76$, $h = 80.0$ which differs by only 3% from other minima at $X_o = 0.6$.

The coordinates of this minimum SSQD point in the X_o - h grid (plane) vary with diffusivity (Table 5.3). As already noticed in several occasions, the effects of increasing diffusivity may be compensated by decreased heat transfer coefficient or by increased distance. Distance increases steadily with increasing diffusivity but the variations of the h parameter are somewhat irregular which is probably due to the coarseness of the grid. The actual path followed in the three dimensional space by the minimum SSQD function is probably a smooth curve for each coordinate.

TABLE 5.3 X_o-h COORDINATES OF MINIMUM SSQD AT VARYING DIFFUSIVITY

Diffusivity	$cm^2/sec \times 10^{-3}$	1.5	2.0	2.5	3.0	3.5
h	cm^{-1}	10.0	40	10	80	20
X_o	cm	0.45	0.60	0.60	0.76	0.76
minimum SSQD in the plane h - X_o	arbitrary units	0.7724	0.7545	0.7543	0.7466	0.7467

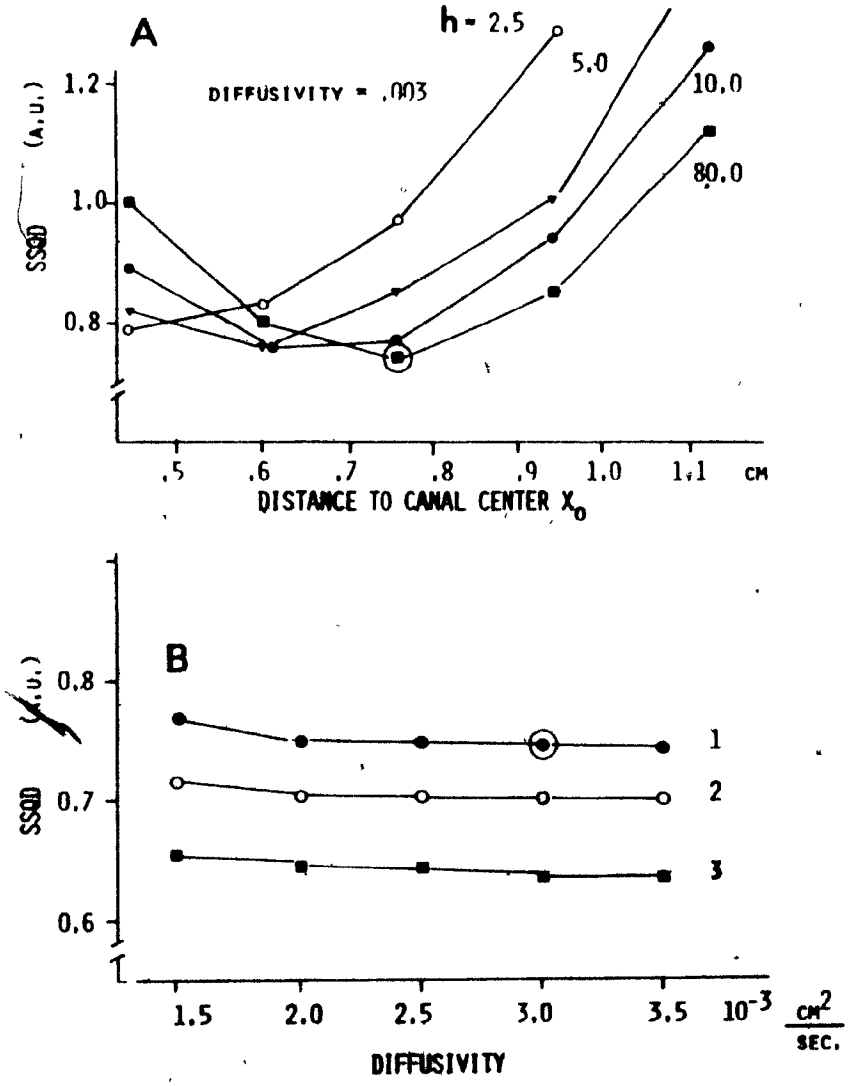

Fig. 5.14. The sum of squared deviations (SSQD) between model and data in the parameter space. A: SSQD (in arbitrary units) is plotted as a function of canal distance at constant diffusivity. B: SSQD as a function of diffusivity. Each point is the minimum SSQD obtained in the plane X_o - h at constant diffusivity. e.g. the circled point of curve 1 corresponds to the circled minimum SSQD of the top plot. Curve 1, 2 and 3 respectively relate to model torque, theoretical cupular deflection and model adapted response. Data from subject J.H.

The SSQD minimum points of Table 5.3 are shown plotted against diffusivity in figure 5.14B (curve 1). The latter pertains to the output of the torque model. Curves 2 and 3 were obtained for the theoretical cupula deflection and the theoretical adapted response. Note that above a diffusivity of 0.002 the SSQD functions vary by less than 1%. An absolute minimum is found in curve 1 at 0.003 diffusivity but in curves 2 and 3, SSQD steadily decreases with increasing diffusivity. The differences between the SSQD levels of the model variables are much larger than the variations seen along any given curve. The SSQD level is the highest for torque and the lowest for adapted response.

This analysis in the parameter space confirms two important observations made in visual curve fitting. First, it is obvious that a large number of parameter sets fit equally well the experimental data which cannot be differentiated by visual observation. Second, a significant improvement in the goodness-of-fit is obtained with the theoretical adapted response i.e. when the basic torque model is extended by addition of canal dynamics and neural adaptation.

Ideally, all experimental curves should have been fitted using the parameter scanning method but this has not been possible in practice because of the required computer time. Fortunately, it has been found relatively easy to "land" in the valley of the minima by visual fit alone. For instance after completing the visual fit for subject J.McC. (figure 5.15) the SSQD were obtained for model torque at different X_o - h values and constant diffusivity, using the visual curve fitting program only. Both the SSQD values previously obtained for theoretical

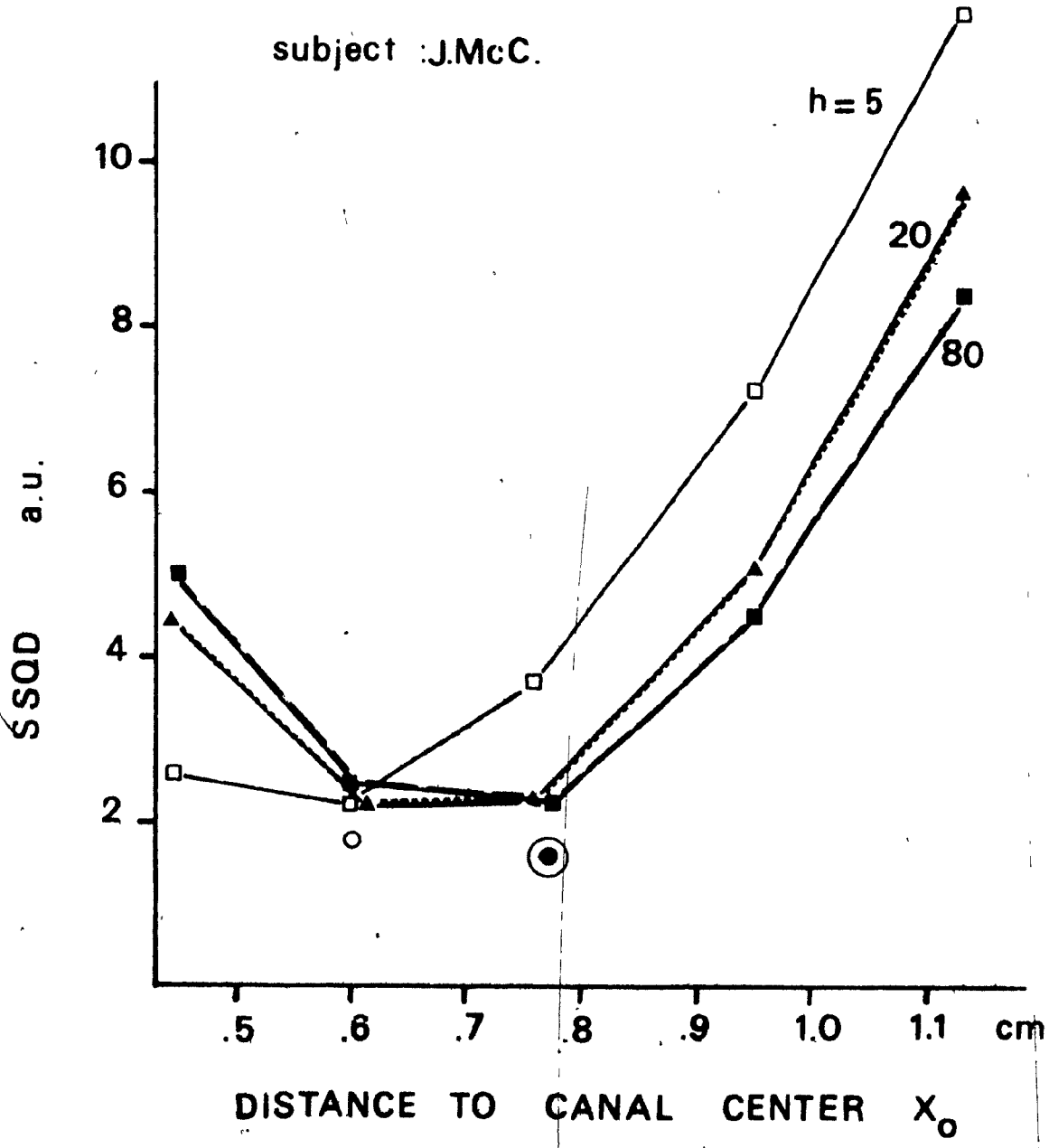

Fig. 5.15. To check results of visual fitting against SSQD data in the parameter space. In A, the points joined by lines relate to model output torque. The open circle at $X_o = 0.60$ and the circled dot at $X_o = 0.76$ respectively relate to theoretical cupular deflection and to model adapted response. These latter points were obtained by visual fit before scanning the parameter space for the torque model.

cupula deflection (open circle at $X_o = 0.6$) and adapted response (circled dot at $X_o = 0.76$) were smaller than any of the minima found around X_o values 0.76 and 0.6 for the output of the torque model.

5.3.5. Discussion

Sustained nystagmus is produced in response to a temperature step input applied at the external ear canal. This experimental fact has been documented in humans by recording step responses in several subjects over 15 minute periods.

Another fundamental result has been obtained concerning the time course of slow-phase eye velocity, which is characterized by a peak occurring between one and four minutes after the beginning of the step and followed by a slow decay. van Egmond and Tolk (1954) expressed the opinion that a constant temperature stimulus in the external ear should produce a constant slow-phase velocity. However, these authors made that statement without any supporting data.

In the interpretation of the step response variations of arousal, indirect thermal effects on blood flow and on vestibular receptors must again be considered as possible causes of the post-peak decay. On the basis of previous results on sinusoidal caloric stimulation one may reasonably assume that the influence of these factors was probably small in the step response as well.

The dynamic characteristics of the response have been explained in terms of a general caloric response model used as a working hypothesis. The model is an extension of the basic torque model of Young (1972) that is coupled to models of canal dynamics and neural adaptation. From a quantitative analysis of the data important conclusions have been reached:

1. The semicircular canal component is reflected in the response by an additional lag in the initial rise. Part of the lag was in fact due to the caloric stimulator that had a time constant of 3 seconds. The latter is small relative to the 20 seconds time constant used in curve fitting and would not invalidate the above conclusion concerning the role of canal dynamics.

2. The decay of slow-phase velocity after the initial peak is best fitted by the model adapted response.

The adaptation effect was not so pronounced as the one observed in rotational responses since the caloric response did not vanish after 5 minutes as predicted from analysis of the model. However, the decay phenomenon could be related to a more general form of the adaptation filter suggested by Malcolm and Melvill Jones (1970). This filter contains a so-called directional preponderance parameter m which was set to the value 0.5 (instead of 1 for rotational response) to fit adequately the response decay. The choice of the value $m = 0.5$ was made arbitrarily as the best choice between a "fully adapting" and a "non-adapting response".

Note that the phase data in the Bode plot obtained from sinusoidal stimulation were tentatively explained on a qualitative basis by a transfer function of the adapted response in which m also took an intermediate value between 0 and 1. In figure 5.15.2, the sinusoidal data are compared to frequency response curves of the general model that correspond to best fitted step responses. The two sets of data from step and sinusoidal caloric inputs are compatible with each other and appear to be adequately described by the model.

The attenuation of the adaptation effect is probably related

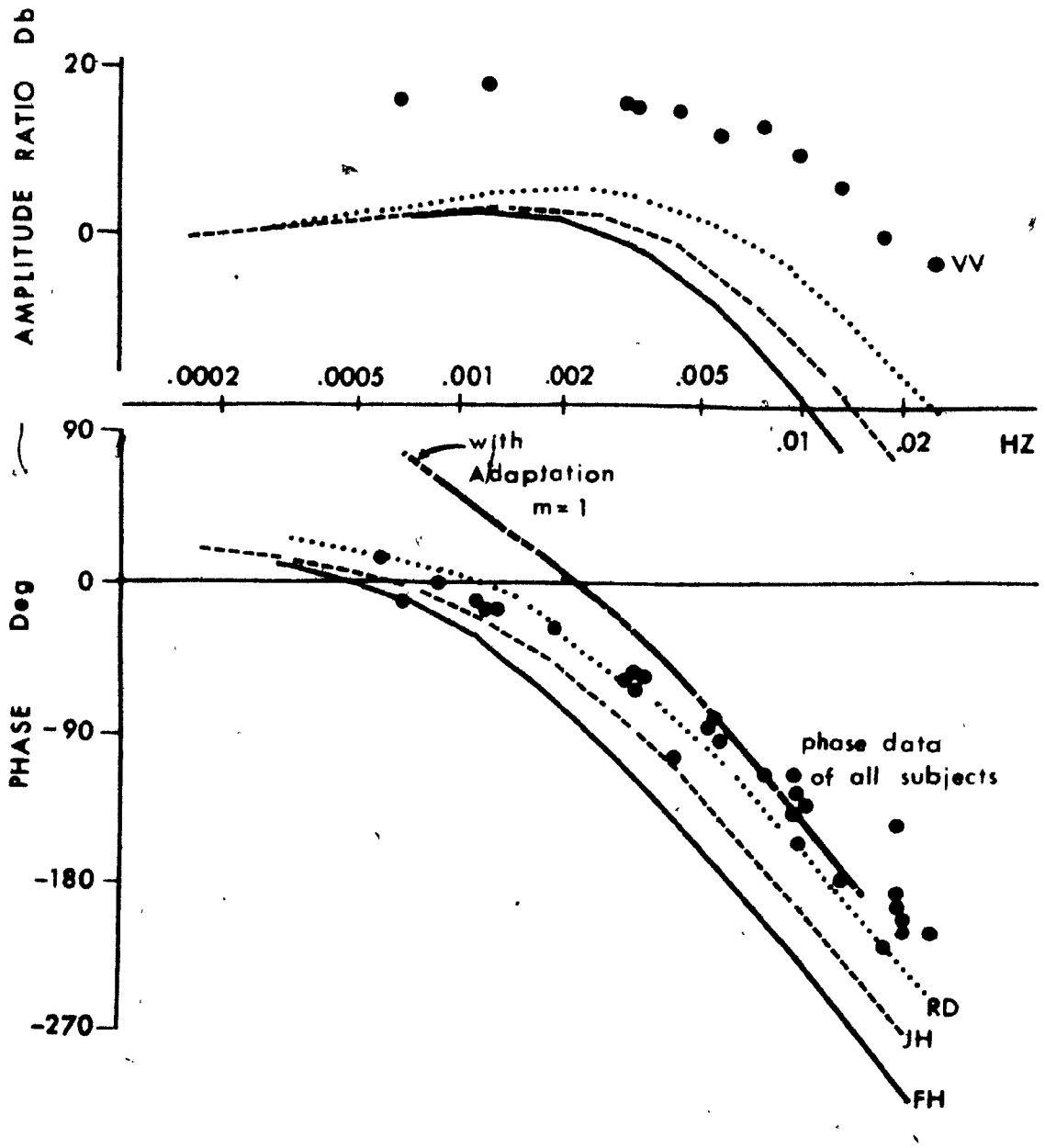

Fig.5.15.2. Comparison of step and sinusoidal data in the frequency domain. Curves RD,JH and FH were calculated from the general model with canal dynamics ($_c$ = 21 s) and adaptation ($_a$ = 82 s and m = .5). The other parameters were set to the values obtained from the corresponding fitted step responses (table 5.2). The data points (dots) are from sinusoidal stimulation . For clarity, amplitude data from only one subject are shown and the amplitude level was set arbitrarily. The phase pertaining to the case of "full" adaptation is also shown (thick broken line).

to the fact that only one side of the vestibular system was activated. However, one can hardly speculate about the nature of the modification brought about by unilateral caloric stimulation since the mechanism of vestibular adaptation is still poorly understood. Nevertheless, one may suggest a useful experiment to further investigate the question. In this experiment, equal temperature steps of opposite direction would be applied in both ears simultaneously. By activating the semicircular canals on both sides a "fully" adapting response should be obtained as if a rotational stimulus were applied.

The analysis has been based on the assumption that the torque model, the first component of the general caloric response model, is a valid representation of the thermal processes generating the torque acting on the endolymph. Since the torque model has not yet been verified directly, the results of step response analysis can only be considered as providing good evidence of the significant role played by the vestibular dynamics in the caloric response.

A number of discrepancies of the model have been left unexplained that may require a reappraisal of the step response data in terms of a different model. For the sake of discussion, consider the infinite slab model where the solid bone is limited at some distance from the ear canal by an infinite plane surface at constant temperature. Such a representation is quite acceptable physiologically since at some undetermined depth (e.g. in the brain), blood flow is presumably large enough to maintain a constant temperature. Intuitively, it would seem that the slab should exhibit a lead characteristic enhanced relative to the semi-infinite solid and furthermore a steady state

should be reached in a finite time. Such a physical model would perhaps fit the nystagmic data without the addition of an adaptation component. Furthermore, it might explain the post-peak plateau of constant slow-phase velocity seen in a few cases. The solution of the slab model involves infinite series that add considerable complexity to the mathematical description and the available data have not justified further theoretical development on this aspect.

Parameter identification has been somewhat unsuccessful because of the rather flat valley where the optimum parameter set lie in the parameter space. However, parameter values close to the normal values obtained by Young (1972) were found in that valley of minima, which indicated the basic correctedness of the model. The curve fitting results have shown that the dynamic parameters may vary considerably between subjects.

Diffusivity varied over a range of 0.00134 - 0.00303 which is not unexpected in view of the wide spread observed in the time-to-peak values of slow-phase velocity (92-270 seconds). The mean diffusivity value 0.00196 cm^2/sec compares reasonably well with the values 0.0025 and 0.0017 respectively obtained by Young (1972) and by Schmaltz (1924).

The h coefficient, the ratio of heat transfer coefficient to bone thermal conductivity, is much higher in most cases than the mean value of 5.0 cm^{-1} measured by Young (1972) with an air stimulator in cadaver skulls. According to our data, water irrigation provides better heat transfer than air, which is expected on the basis of the different thermal properties of the two fluids. Other factors must also be considered such as bone characteristics and flow rate. This latter

factor has been investigated experimentally and the discussion on heat transfer will be resumed below in section 5.5.

5.4. The Caloric Response to Temperature Pulse Input

5.4.1. Protocol

The study was performed in five subjects prepared as described before and connected to the stimulator. The caloric input consisted of a 20 second duration temperature pulse followed by a return to body temperature for a minimum of 5 minutes. The initial stimulus was cold (30°C) in three cases and hot (44°C) in the two others. A second stimulus was always applied in the direction opposite to the first one. The experiment was terminated by a third 20 second pulse, at the end of which the irrigation was stopped by turning off the pump while the recording was continued for another five minutes. This latter manoeuvre was intended to simulate the stimulus provided by the standard short irrigation used in caloric testing. The irrigation stimulus differs from a true temperature pulse in that the temperature in the external ear canal decays slowly towards body temperature.

5.4.2. Results

Slow-phase velocity responses to pulse input temperature are shown in figures 5.16 and 5.17. Peak slow-phase velocity and response duration were measured directly from the plots (Table 5.4). Response duration was estimated as the time interval between the initial rise and the point at which the response met the baseline during the decay following the initial peak. The response durations of the two pulses averaged 118.4 sec ± 6.1 S.E. and peak slow-phase velocity 7.74 deg/sec ±0.45 S.E. (n = 10). The response to

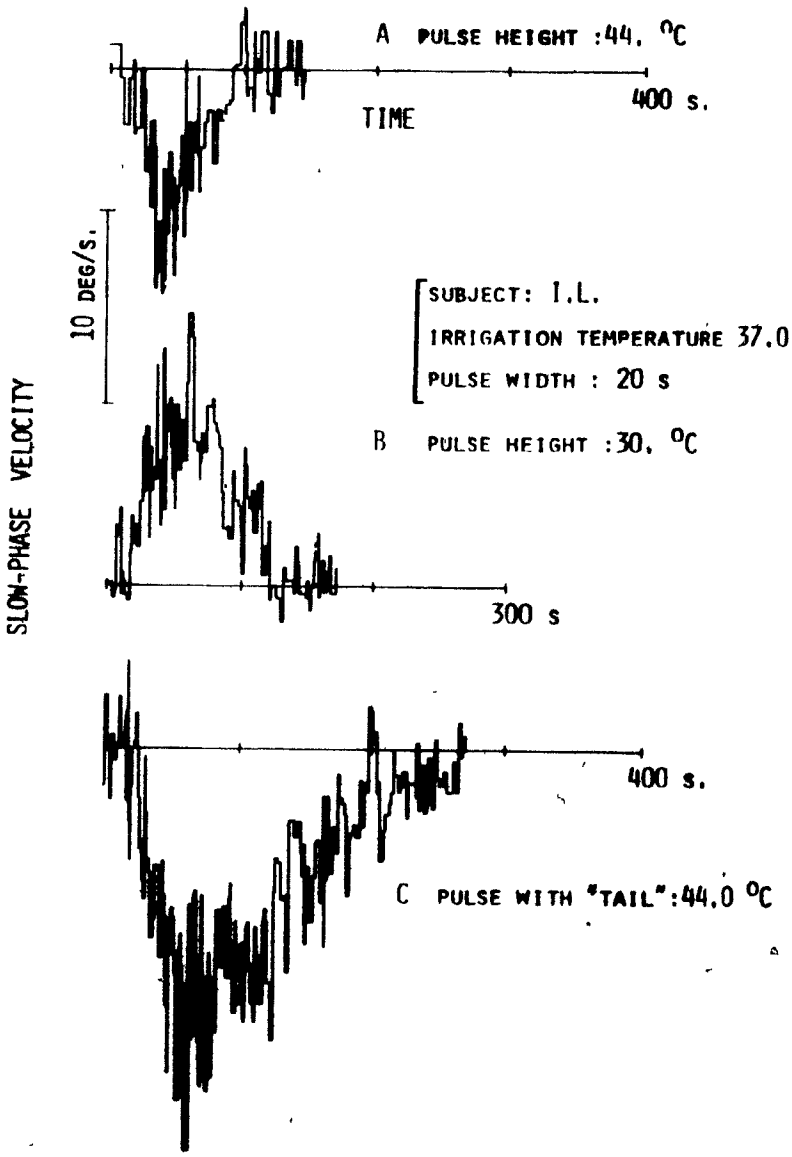

Fig. 5.16. **Responses to hot (A) and cold (B) 20 second temperature pulses in the same subject. In C, the irrigation was stopped at the end of the pulse. The response duration and peak increased relative to the true pulse response.**

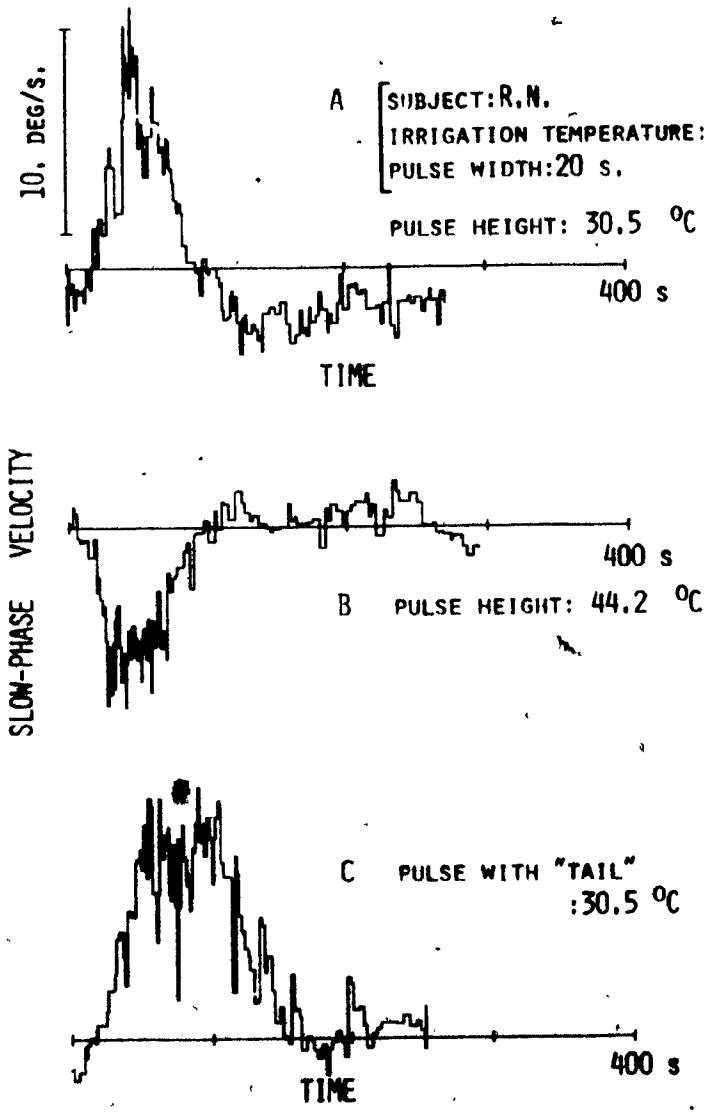

Fig 5.17. Same as in fig. 5.16 except that the cold pulse was administered first. In this subject, the model response with adaptation and canal dynamics provided a best fit to the cold pulse response (curve A).

TABLE 5.4

Subject	Stimulus (Hot H, Cold C)	True 20s pulse Duration	True 20s pulse Peak SPV	Pulse w. tail Duration	Pulse w. tail Peak SPV
		sec	deg/sec	sec	deg/sec
R.N.	C	104	9.2	160	10.6
	H	92	6.4		
I.L.	C	120	9.0	220	11.4
	H	96	9.0		
L.Y.	C	144	8.0	180	10.0
	H	128	6.0		
F.D.	C	120	7.0	160	9.0
	H	100	5.4		
S.H.	C	140	8.4	240	14
	H	140	9.0		
Mean ± S.E.		118.4±6.2	7.74±0.45	192±16	11.0±0.84

SPV: slow-phase eye velocity

pulses with a temperature "tail" lasted much longer (192 sec ± 16.2 S.E.) and reached higher peaks (11.0 deg/sec ± 0.80 S.E., n = 5) than the true pulse responses.

The true pulses responses were also analysed in terms of the caloric response model. Visual fitting was found difficult to use because of noise. Instead, the analysis was done using the program developed to study the SSQD function of the step response in the parameter space. This could be done in a reasonable time because of the smaller number of points in each record.

Table 5.5 gives the minimum SSQD value obtained for each of the model variable in 10 responses. The theoretical variable which best fitted the data is indicated by a star in the appropriate column. The theoretical cupula deflection provided the best fit in 6 cases, model torque in 2 and model adapted response in 2 also. A variance ratio was calculated by relating the variance of the model torque to the variance of the theoretical variable that yielded the minimum SSQD. From a statistical viewpoint, the improvements in the fit brought by addition of canal dynamics and neural adaptation were not significant except for the cold response of subject R.N. illustrated in figure 5.17A. In the latter case, the adapted response provided the best fit and the corresponding experimental slow-phase velocity exhibited a characteristic overshoot of the post-peak response decay.

TABLE 5.5 VARIANCE OF THE MODEL VARIABLES FITTED TO PULSE RESPONSES

Subject		Torque	Cupula Deflection	Adapted Response	F[1]	Probability level
R.N.	COLD	0.61	0.47	0.34*	1.81	$p < 0.01$
	HOT	0.135	0.134*	0.152	1.00	N.S.
F.D.	COLD	0.840	0.693*	5.14	1.21	N.S.
	HOT	0.409 *	0.448	0.560	1.00	N.S.
L.Y.	COLD	0.781	0.723	0.602*	1.29	N.S.
	HOT	0.388*	0.431	0.530	1.00	N.S.
S.H.	COLD	0.414	0.412*	0.435	1.00	N.S.
	HOT	0.428	0.409*	0.417	1.03	N.S.
I.L.	COLD	0.525	0.509*	0.543	1.01	N.S.
	HOT	0.493	0.481*	0.481	1.02	N.S.

1. $F = \dfrac{\text{variance (output of torque model)}}{\text{variance (} * \text{ model variable)}}$

5.4.3. Discussion

It has been found difficult in general to document the shape of the pulse response especially after the initial peak because of the noise level and the lack of measuring accuracy near zero slow-phase velocity. Statistical analysis of the data in terms of the general caloric response model showed no significant differences between the theoretical variables of the model. These results would seem to contradict previous results obtained from step response analysis but they probably reflect the poor quality of the data more than anything else.

An interesting case is the one in which the adapted response model exceptionally provided a significant better fit than the other model variables. The noise level was much smaller (figure 5.17A) and a characteristic overshoot could be recognized by visual observation. However, the hot response from the same subject did not exhibit adaptation and the overshoot of the post-peak decay was not so pronounced (figure 5.17B). In the latter case, the wavy appearance of slow-phase velocity near the baseline indicates that other factors may have influence the response. Young (1972) also studied the response to cold air pulses and similarly noted a lead of recorded slow-phase velocity relative to the theoretical pressure difference across the cupula (which is equivalent to torque). Young suggested that the lead could be modelled according to the adaptation model of Young and Oman (1969) but he did not fit his data to that model.

The results have also shown that in the ordinary clinical irrigation procedure for caloric stimulation a considerable portion of the caloric response is due to the temperature tail. The length of this tail depends among other factors on the amount of water left in the ear cavity after removing the cannula. According to Henriksson's data (1955) the temperature in the ear canal drops exponentially with a time constant of about one minute. Since the temperature decay is totally uncontrolled it may vary between subjects and even between consecutive irrigations in a given subject. From a clinical viewpoint, this raises the important question of how such a variable factor affects the quality of the vestibular function measures, directional preponderance and canal sensitivity, that are obtained from the responses to a number of successive irrigations. A study should be conducted to evaluate the advantages of the true temperature pulse compared to the standard irrigation in terms of an improved reproduction.

Obviously, further studies will be necessary to define the characteristics of the pulse response. The preliminary experiments discussed here, indicate the need to revise the protocol to study the pulse response. The caloric response model predicts a prolonged response at low amplitudes after the initial peak. Therefore, the stimulus amplitude should be made as large as possible to yield measurable slow-phase velocities for prolonged periods after the peak. Secondly, one might consider the advantages of response averaging by obtaining several responses separated by an appropriate time interval. The aspects related to habituation become important in that case but

the work of Collins (1965) has shown that habituation may not influence the caloric response if the latter is recorded in the dark without visual fixation.

5.5. The Effect of Flow Rate Variations on the Caloric Step Response

5.5.1. Protocol

In this experiment, the stimulation consisted of three consecutive step inputs at 32°C, of 15 minute duration each followed by a 10 minute period at body temperature. The irrigation flow rate was set to 150 cc/min during the first stimulus and to 30 and 300 cm/min during the two others. The low flow rates were achieved by pumping a fraction of the normal stimulator outflow at the junction of the subject cannula and the outlet tube. The high flow rates were obtained by increasing the stimulator pump speed.

A different protocol was followed in one subject (L.S.) to study the effect of flow rate variations in both the hot and the cold directions. Five consecutive steps were applied for 8 minutes followed by 8 minutes at baseline temperature. The response to both cold (32°C) and hot (42°C) stimuli were obtained first at 150 cc/min then at 30 cc/min. The last stimulus was identical to the first one (32°C - 150 cc/min).

5.5.2. Results

Results were obtained from four subjects. As already mentioned, the first step response (at 150 cc/min) from each subject was included in the group of experimental responses analyzed in section 5.3.

In figure 5.18, the slow-phase velocity responses recorded at 150 and at 30 cc/min from the same subject illustrate the effects of decreased flow rate. At the lower flow rate, the initial rate of rise diminished, the peak occurred at a later time and the response amplitude

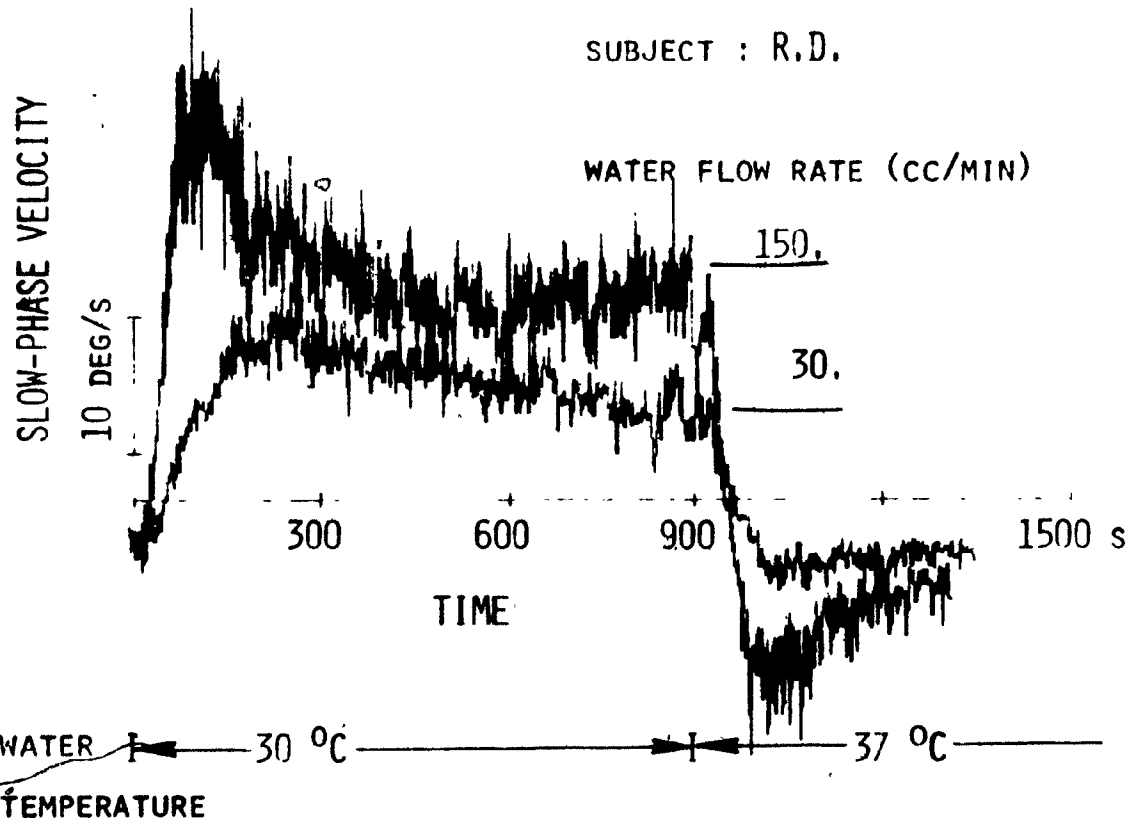

Fig. 5.18. The effect of flow rate on the dynamic aspects of the slow-phase eye velocity response to a step temperature change. The curves obtained at 150 and at 30cc/min have been superimposed.

was generally smaller.

Two responses only were obtained at high flow rate (300 cc/min). They showed no major differences from the responses recorded at 150 cc/min.

The effects of decreasing flow rate were the same for both hot and cold stimuli (figure 5.19).

Presumably, the changes in the dynamic aspects of the step response brought about by flow rate variations correspond to changes in the value of the model parameter h. Indeed, the latter is defined by the ratio of heat transfer coefficient H to bone conductivity k_B and H is known to be dependent on fluid flow rate although the mathematical relationship between the two parameters must often be derived empirically. Since k_B and all other parameters were constant in a given subject, the model was used to estimate the changes in h due to changes in flow rate.

Using the parameter values obtained by curve fitting the normal flow response for the adapted response model (section 5.3) the curve fit was repeated for the low flow response allowing only h to vary. In 3 cases, h dropped from 80.0 to 2.5 cm^{-1}. In the other case (L.S.) the response was already sluggish at normal flow rate and h only changed from 5.0 to 2.5 cm^{-1}.

The flow rate experiments have provided useful information on the step response obtained repeatedly from the same subject. In particular, figure 5.20 illustrates the hot and cold step responses recorded in subject L.O. at 150 cc/min flow rate. A remarkable

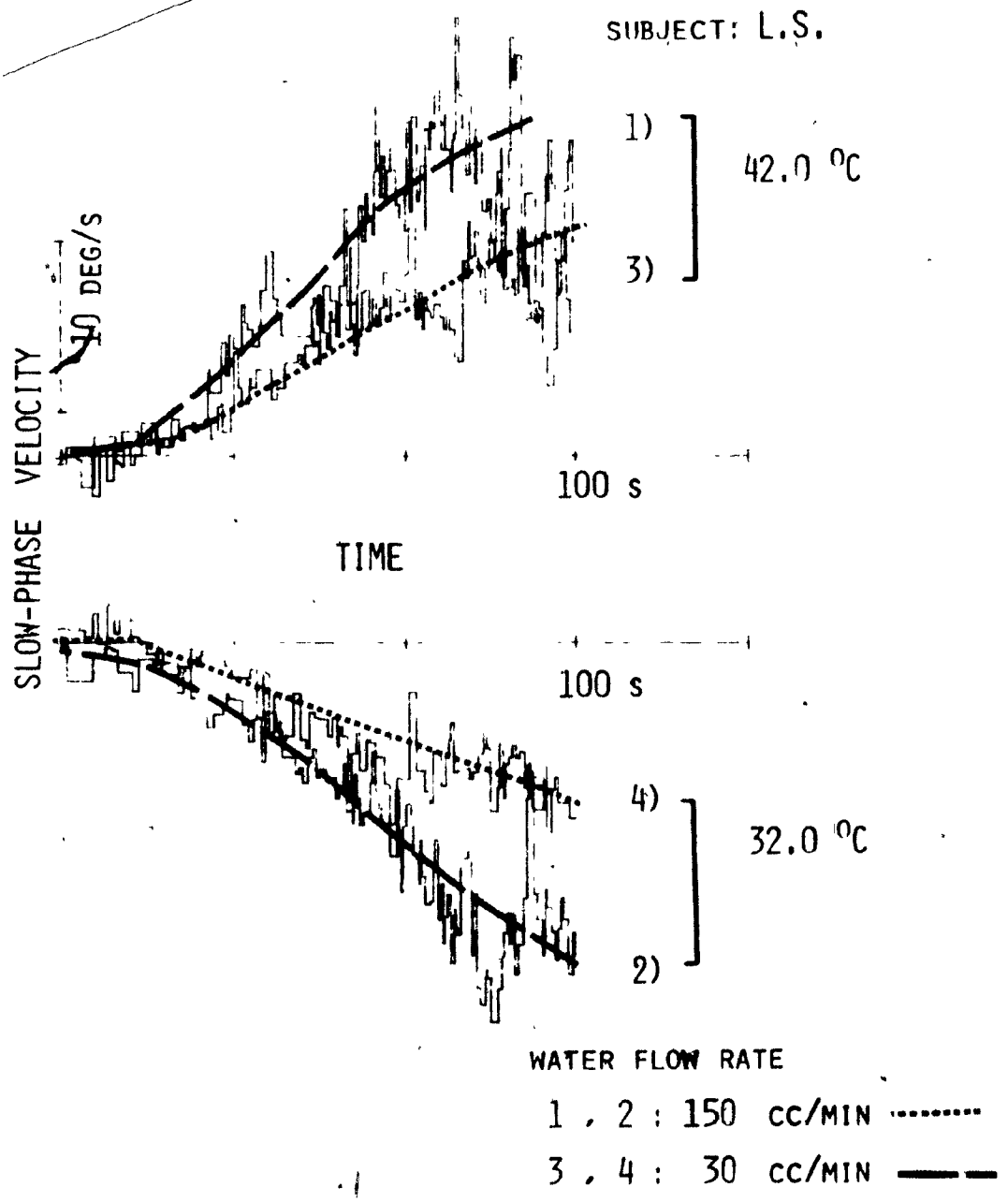

Fig. 5.19. **The effect of decreased flow rate on the initial rise of slow-phase velocity following a temperature step change. The effects were the same for both the hot and the cold stimuli.**

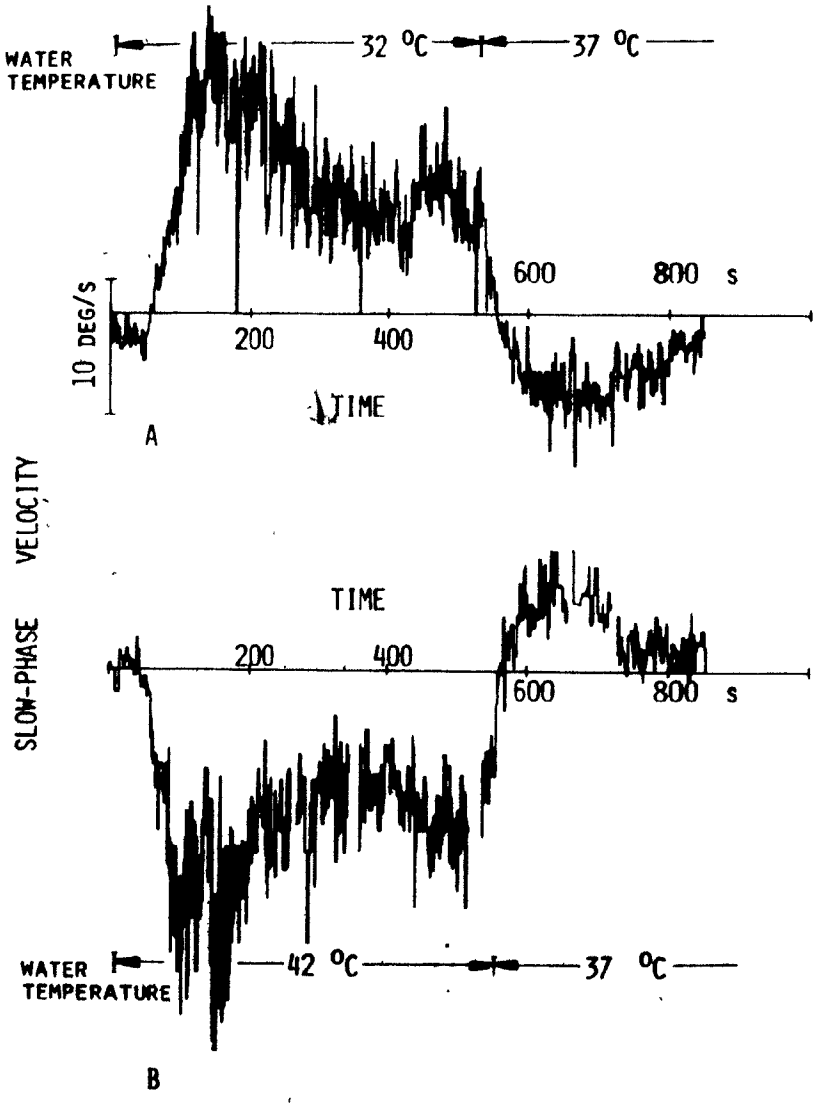

Fig. 5.20. Slow-phase eye velocity responses obtained at five minute interval from the same subject. Note the remarkable symmetry of the hot and cold responses and the difference in the dynamic aspects of the off-step response compared to the initial peak.

similarity may be observed between the two curves. Note especially a significant rise of slow-phase velocity that started at 400 seconds and the widened peak of the off-step response. These latter details could not be fitted by the model and figure 5.20 shows that they were not caused by time-varying factors but that they arose as part of the basic step response.

5.5.3. Discussion

The experiments involved a sequence of stimuli applied in the same temperature direction but at varying flow rates. The question may then be raised that the overall decrease of the response at low flow rate could have been caused in part by habituation to the repeated stimulus. However, nystagmus was recorded with the eyes closed and without visual fixation. According to Collins (1967), under these conditions the caloric response does not show habituation. Even if one accepted that habituation reduced the gain of the response, the changes in the response shape must still be related to the variation in flow rate. Note that in subject L.S. the direction of the stimuli were alternated and the effects of flow rate were not significantly different from those observed in other subjects. Therefore, habituation probably did not play any major role in this study.

The flow rate experiments here confirmed the validity of Young's assumption of a limited heat transfer process at the temporal bone surface in the external ear canal. Changes in the dynamic characteristics of the response with changes in flow rate were predicted on the

basis of the general relationship existing between heat transfer coefficient H and flow rate F in heat transfer processes. Only the direction of change could be predicted since the particular relationship between F and H is unknown. Young (1972) used models borrowed from heat transfer technology to estimate H from gas flow rate. However, the assumptions required to apply these models are difficult to justify and further studies are needed to investigate the problem of heat transfer in the ear canal. An interesting application is the determination of bone conductivity from the knowledge of H and experimental values of h.

The experiments have established that major changes in the response occur between 30 cc/min and 150 cc/min flow rate. The h values are probably sufficiently high at 150 cc/min to consider that the theoretical limit case ($h \to \infty$) applies in practice in which further increases of h do not modify any further the step response. This conclusion is also supported by the fact that the responses at 150 and at 300 cc/min did not differ significantly.

When using water at high flow rates, Young's theoretical model can probably be simplified by eliminating the process of limited heat transfer. The boundary condition at the bone surface is then reduced to one in which the surface temperature is made equal to the irrigating water temperature. The problem of parameter identification is of course simplified considerably since both the model solutions become simpler and the number of parameters is reduced by one.

When air is used as a medium, the heat transfer process must be

taken into account since h is only 5.0 cm^{-1} at 5 L/min gas flow rate (Young, 1972). Although gases have many important practical advantages in terms of manipulation specially, water appears to be a better medium for heat exchange and is preferable for quantitative studies of the type done in this thesis.

CHAPTER 6

SUMMARY AND CONCLUSIONS

In the preceding chapters, the dynamic aspects of the caloric response have been investigated. A mathematical model has been used to estimate the relative influences of the various thermal and physiological processes involved in the caloric response. In the following paragraphs, the results of the study are summarized and their significance is discussed.

Theoretical Results

The physical events of the caloric reaction phenomenon were described by Barany in terms of a heat wave generated by the temperature stimulus that travelled in the temporal bone and perturbed the equilibrium of gravity forces acting on the semicircular canal endolymph. On the basis of Barany's description Schmaltz developed a model in which the classic unidimensional heat conduction equation was applied to calculate endolymph velocity in response to a temperature input. Schmaltz's model was neglected until Young's recent work (1972) in which specific time domain solutions were reported that account for limited heat transfer at the bone surface and were expressed in terms of the pressure differential across the cupula. However, there was no attention given to the general

characteristics of the model response and the implications of the model were not fully elaborated.

The distributed parameter model of Schmaltz and Young has been reexamined theoretically in this thesis using a frequency domain approach. A transfer function has been derived from the model equations to relate output torque $M(s)$ on the endolymph to input temperature $T_w(s)$ of the irrigating medium, i.e.:

$$\frac{M(s)}{T_w(s)} \;\triangleq\; \frac{h}{(h + \sqrt{s/\alpha})} \cdot \exp\left(-X_o \sqrt{s/\alpha}\right) \cdot I_1\left(R \sqrt{s/\alpha}\right)$$

where h ($= H/k_B$) depends on the heat transfer coefficient H and bone conductivity k_B; and where X_o is the distance to the canal center, R the large semicircular canal radius and α, the thermal diffusivity of bone.

The above function is mathematically separable into three components associated with distinct physical processes. The first component corresponds to the boundary conditions of linear heat transfer at the surface. The exponential term is a so-called diffusion operator associated with heat conduction within the semi-infinite solid and relates the temperature at X_o to the temperature at the surface. The third component involves a modified Bessel function I_1 and relates torque generated by the temperature distribution around the canal

to the temperature at X_o. This Bessel term has the characteristics of a "differentiating" process with positive phase and attenuation which decreases with increasing frequency.

The overall transfer function has the appearance of a wide band-pass filter dominated at low frequencies ($f < 0.001$ Hz) by the $R\sqrt{s/\alpha}$ asymptote of the Bessel term and at frequencies above 0.01 Hz, by the attenuation of the exponential term. Peak amplitude is met around 0.001 Hz.

The dynamic characteristics of the torque step response to a temperature step input have been studied over a wide range of parameter values using a simplified mathematical expression derived from the complex formula given in Young's work. At normal parameter values, ($R = 0.3$ cm, $X_o = 0.76$ cm, $h = 5$ cm^{-1}, $\alpha = 0.0025$ cm^2/sec), the step response exhibits a peak at 120 s with a 50 percent overshoot relative to the amplitude at 20 minutes. After the initial peak, torque decays and tends asymptotically to zero as time tends to infinity.

Increasing h values and thermal diffusivities as well as decreasing distances to canal center accentuate the characteristic overshoot and the opposite effect is produced by changes of these parameters in the other direction. The radius affects the response gain only and torque (M) varies with the cube of R. The equivalent angular acceleration M/I is independent of R since I, the moment of inertia of endolymph, varies with R^3 also.

A limiting case is reached as h tends to very large values

(small bone conductivity and large heat transfer coefficient). The response tends to the one obtained when the surface temperature is made equal to the irrigating medium temperature. In practice, this condition is met with $h = 80\ cm^{-1}$ and other parameters at normal values.

An integration of the temperature distribution around the canal is required to compute torque. It has been shown that over a wide range of parameter values, torque is approximately proportional to the temperature difference across the canal.

A New Caloric Response Model

Young's torque model only represented the thermal processes of the caloric reaction and it could not be applied directly to the analysis of caloric responses usually recorded in terms of slow-phase eye velocity.

In order to study the relationship between slow-phase eye velocity and input temperature at the ear canal, a caloric response model has been proposed as a working hypothesis which incorporates models of vestibular dynamics developed by others. The torque model has been tentatively coupled to a first order lag representing canal dynamics ($\tau_c = 21$ sec) in series with a first order lead-lag filter describing neural adaptation ($\tau_a = 82$ sec). The hypothesis is an important one since it gives the possibility of separating the thermal and the vestibular components from the overall caloric response.

Experimental Results

The possible influence of neural adaptation in caloric vestibular response made it necessary to explore the response characteristics at very low frequencies below 0.005 Hz. However, most data in the literature were obtained from such stimuli as the short lasting irrigations of the standard test that could not provide the required information. Experiments are described in this thesis in which subjects were connected to a specially designed caloric stimulator and the responses to sinusoidal and to step temperature inputs were recorded using electro-oculography.

Slow-phase eye velocity has been found to vary sinusoidally in response to sinusoidal temperatures at frequencies extending from 0.00055 to 0.02 Hz. The data could be fitted with high correlation coefficients ($r > 0.9$) to a regression equation including a sine function plus linear drift and bias terms. No significant harmonic could be detected systematically at all frequencies in any given subject.

Calculations of the torque transient from sinusoidal inputs showed that below 0.01 Hz the effects of the transient were limited to the first half cycle and that after three minutes one needed only be concerned with a residual component similar to a bias plus drift. Above 0.01 Hz, the fast initial phase of the transient was reflected by a shift of the first cycles above the steady state mean output level. These predictions have been qualitatively verified from the data.

In the Bode plot, amplitude was maximum in the frequency range

0.001 - 0.005 Hz and accelerated attenuation occurred above 0.01 Hz with phase lag exceeding 200 degrees. Extrapolating the frequency response data the amplitude ratio probably decreases and the phase becomes positive at low frequencies below 0.001 Hz. This behaviour is in agreement with both the torque and the general caloric response model, but the data do not allow one to make definite conclusions on the contribution of the vestibular components.

The response to temperature step changes were recorded in several subjects over periods extending to 20 minutes and in some cases the off-step responses were also monitored.

Typically, the slow-phase velocity response to a temperature step change exhibited a peak at 159 seconds + 18.8 S.E.(n = 10) followed by a slow decay. The response level was maintained significantly above zero throughout the on-step phase. The off-step response was characterized by an overshoot of the response to a new peak in the opposite direction before the response vanished. Slow-phase velocity followed a time course similar to that of the model torque step response and it did not adapt to the extent predicted by the current model of vestibular adaptation based on rotational responses.

The caloric step responses were analyzed in terms of the new caloric response model with the help of a curve fitting program that allowed adjustments of the parameters within certain limits. A different form of the adaptation filter was used in which the

zero of the lead-lag was shifted halfway between the pole and the origin ($m = 0.5$ in the model of Malcolm & Melvill Jones (1970)). A best fit was obtained for the model output variable that included both canal dynamics and the modified adaptation filter. The improvement over the fit obtained with torque was statistically significant in seven out of ten cases. However, the off-step part of the response could not be included in the fitting procedure for any of the model variables because of apparent changes in the dynamic aspect of the response.

The frequency response data similarly indicated an attenuated form of adaptation since the point of zero phase shift recorded at 0.00086 Hz corresponds to an intermediate theoretical curve between torque alone and fully adapted response.

The experimental work also involved preliminary studies on the pulse response and on the effect of water flow rate.

The response to 20 second hot and cold temperature pulses were recorded in five subjects. The mean response duration was 118 sec and mean peak slow-phase velocity was 7.4 deg/sec. The same group of subjects was stimulated with a 20 second "flow pulse" that simulated the standard irrigation of the clinical test: mean peak slow-phase velocity reached 11.8 deg/sec and response duration 198 sec. The differences between the temperature pulse and the "flow pulse" responses can be attributed to the long temperature tail that accompanies the stopping of irrigation in the latter.

The pulse responses were curve fitted with the caloric response

model but inconclusive results were obtained except in one case in which the model output with adaptation and canal dynamics provided a better fit than torque alone.

In three cases, a change in the irrigation flow rate from 150 to 30 cc/min modified the dynamic character of the step response from an overshooting type to a sluggish type. Correspondingly, the h values obtained by curve fitting the model to the data dropped from 80 to 2.5 cm^{-1}. In a fourth case, the response was already sluggish at the standard flow rate ($h = 5$) and little change was observed in the response at the low flow rate. In two cases, increasing flow rates from 150 cc/min to 300 cc/min did not alter significantly the character of the response, which indicates that, in practice, the theoretical limiting case of heat transfer ($h \rightarrow \infty$) prevailed at 150 cc/min.

Conclusions

From these results, the following important conclusions have been reached.

(i) The system is probably linear and time-invariant even at very low frequencies below 0.001 Hz, as shown by the data from sinusoidal stimulation.

(ii) The gross dynamic features of the caloric slow-phase velocity response are well predicted by the torque model which indicates that the overall response is dominated by the thermal processes. This conclusion is supported (a) by the general appearance of the step response, (b) by the frequency response characteristics, derived from

sinusoidal stimulation, (c) by the behaviour of the transient to sinusoidal inputs and (d) by the changes in the dynamic character of the response due to changes in flow rate.

(iii) The current representation of neural adaptation derived from rotational studies does not apply to unilateral caloric stimulation, and it must be modified to account for the reduced adaptation observed in the latter.

(iv) From a quantitative curve fitting of the step responses, both canal dynamics and neural adaptation in an attenuated form are significantly reflected in the slow-phase eye velocity response. Therefore, the relationship between slow-phase velocity and input temperature alone is better represented by the general caloric response model than by the torque model alone.

On the Validity of the Physical Model

The semi-infinite solid model of the caloric process has provided good estimates of the torque acting on the endolymph following caloric stimulation since the basic dynamic characteristics of the system have been verified from the general agreement between predicted torque and slow-phase velocity data. However, the physical model has been used as a basic assumption to demonstrate by dynamic analysis and stepwise model comparison that significantly distinct and reproducible deviations from the theoretical torque response could be attributed to vestibular dynamics. These deviations are relatively small and one cannot a priori exclude other

explanations based on different and more complex mathematical representations that would take into account the limit dimensions and the intricate geometry of the temporal bone. Furthermore, discrepancies have been found between model output and data which cannot be arbitrarily attributed to an inadequate physical model or to time-varying neural processing of the cupula signal. Finally, the challenging work of Harrington (1969) suggested that other heat pathways are involved through the air-filled vestibule and would require an extensive revision of the torque model based on the heat conduction through the temporal bone only.

In that context, the direct validation of the torque model of Young appears now as a critical step in the continuation of this work. Torque or pressure cannot be directly measured in the semicircular canals and to appreciate the technical difficulties, one may quote the estimate of 10^{-3} dyne/cm^2 (10^{-5} cm H_2O) obtained by Oman & Young (1972) for the pressure variations in the canal due to caloric stimuli. Torque may be estimated from the known distribution of temperature around the semicircular canal. Techniques are available (Dohlman, 1925, Cawthorne & Cobb, 1954, Ishiyama & Keels, 1973) that were successfully applied in animals, cadavers and even in anesthetized human subjects to measure temperature in the perilymphatic space. New data are needed concerning the dynamics of the temperature distribution around the canal and the simplest approach might involve recording the temperature difference across the semicircular canal, which has been shown to provide a good

approximation to calculated torque.

On Vestibular Adaptation in Caloric Responses

The conclusions concerning neural adaptation of the caloric response are of particular significance to the basic concepts of vestibular functioning. It has been suggested (Malcolm & Melvill Jones, 1970) that the functional role of neural adaptation is to maintain the balance of the differential inputs to the central nervous system from the vestibular receptors of both sides of the head. These receptors exhibit a resting neural discharge and adaptation would act as an "automatic balancing circuit" insuring zero output at the very low frequencies, well below the frequency range in which the system operates under the action of normal head movements. The current vestibular adaptation model cannot differentiate between shifts in the resting discharge of one side only and a differential signal generated by sustained cupula deflections on both sides. It is now clear that this model must be modified to take into account the reduced adaptation capacity exhibited by the caloric response to a unilaterally applied temperature step change.

An intriguing question is whether the mild adaptation observed in the step response involves the same pathways as the adaptation seen in rotational responses. This is somewhat implied by the use of a unique filter to represent these two different phenomena that can be differentiated by adjustment of a single gain parameter. However, such a general representation of vestibular adaptation must still be considered as a working hypothesis and needs further testing. In this

respect, a critical experiment has been suggested in which prolonged accelerations might be simulated by caloric stimuli of equal magnitude but opposite direction applied simultaneously to both sides. If the model is correct, a "fully adapting" response should be recorded.

The question of a unique mathematical model of adaptation may also be raised concerning such adaptation phenomena observed in the pulse response by us and by Young (1972) and also recorded by Hood in the standard caloric test (1973). In particular, Hood concluded that the stimulus applied to the endolymph probably persisted for more than ten minutes but that nystagmus disappeared after 4 - 5 minutes presumably because of adaptation. Qualitatively, Hood's data can be explained in terms of the basic adaptation high pass filter pertaining to rotational responses. However this interpretation conflicts with the earlier conclusion of this work based on step response data. As discussed later, such data from standard irrigation stimuli cannot be easily applied to the torque model and further studies are needed to clarify their significance.

Another important component of the caloric response is the perceived sensation of angular rotation. The latter has not been discussed so far mainly because no attempt was made to measure subjective response in the experimental work reported here. Nevertheless, it may be worthwhile mentioning that in all subjects, a sensation of turning was experienced which completely disappeared some time after the temperature step change was applied. This observation would indicate

that "full adaptation" still takes place along the subjective pathways in unilateral caloric stimulation. The subjective response adapts much more rapidly than slow-phase velocity (Young & Oman, 1969) and an interesting question proposed for future investigation is whether the same time constant characterizes the process in unilateral caloric stimulation as in bilateral caloric stimulation or in rotational inputs.

It is obvious that the integration of these various phenomena of vestibular adaptation in a coherent picture will require a systematic investigation along some of the lines proposed here. The main motivation to pursue this fundamental research may come not only from the increased understanding of vestibular functioning but also from the clinical implications of the findings.

Clinical Application of the Caloric Response Model

The objectives of this research have been to apply systems methodology to the evaluation and to the development of clinical caloric testing. A promising avenue opened to clinical researchers is the use of a caloric response model as a tool to interpret caloric test data. An important step has been to establish that the vestibular dynamics are significantly reflected in the slow-phase velocity response to prolonged stimulation with step inputs. Attempts to identify model parameters gave somewhat disappointing results except for the encouraging fact that a best fit of the model could be obtained for many sets of parameters within the expected range around normal values. It was not considered appropriate to complicate the optimization search

by varying the canal time constant and the adaptation time constant. In future studies, the identification of vestibular parameters should be an important objective since these are the main parameters of interest to the clinician concerned with vestibular function.

The work done on the problem of parameter identification has served to point out basic difficulties which must be overcome before considering direct clinical applications. These difficulties may be broadly related to two general aspects, namely, the number of parameters estimated from the nystagmic response and the quality of the slow-phase velocity data.

Four basic parameters characterize the torque temperature transfer function and four additional parameters are necessary to represent the vestibular dynamics. It is obvious that any reduction in the number of dimensions of the parameter space considerably simplifies the analysis of data in terms of the overall caloric response model. Two possibilities have been discussed, namely, the separate measurement of the distance to canal center (by X-ray techniques) and the elimination of heat transfer parameter from the model equation by using sufficiently high water flow rates.

Another important aspect is the definition of practical boundaries limiting the domain of optimization. There is a lack of data concerning the parameters of the thermal processes. Extensive data could only be found for the canal radius (which does not influece the response). Other parameters have been estimated but little is known

about the corresponding deviations to be expected in a normal population. In order to obtain such basic data, studies of the type already suggested to validate the torque model are required and this may provides further justification to orient research efforts in this direction.

A traditional approach has been used in representing the cupula related signal by slow-phase eye velocity. Our slow-phase velocity data were characterized by a high noise level which undoubtedly contributed to the difficulties in parameter estimation. The "noise" appeared as an inherent component of caloric nystagmus and the question of smoothing and filtering was not discussed mainly because the measuring process involved some kind of sampling and visual filtering which is not simply expressed in terms of commonly used techniques of signal analysis.

In the broad context of nystagmus analysis, the basic problem is the separation of the continuous signal related to cupula deflection and the saccadic component. The saccadic component involves some kind of stochastic process as evidenced by the random occurrence of saccades and by the variability of saccade amplitudes. The nature of the stochastic process is not fully understood. Cheng (1972) suggested that a multi-model phenomenon in interval distribution may be seen at the beginning and at the end of the caloric response. There is probably some interaction between the saccadic and the continuous components of nystagmus as suggested by the work of Sugie & Melvill Jones (1966) but that aspect has not been investigated for caloric nystagmus.

Slow-phase velocity remains a simple and useful concept. A reexamination in depth of the characteristics of caloric nystagmus is required to deal with such aspects as slow-phase eye velocity "noise". With respect to the objectives of this research, a new approach to nystagmus analysis is highly desirable because the interpretation of caloric response on the basis of slow-phase velocity alone is necessarily limited and other information with potential clinical value is neglected.

Clinical Applications: Modification of the Hallpike Test

The experience gained in developing techniques for prolonged caloric stimulation may be called upon to offer specific suggestions to modify the procedure of the Hallpike test and to increase the reliability and the accuracy of the test. The application of the model has made it necessary to define precisely the temperature stimulus and to keep conditions of heat transfer as constant as possible. We have noted that the simple "flow pulse" or irrigation of the Hallpike standard test provides an inadequate input test signal because the conditions of heat transfer are abruptly changed at the end of irrigation. An uncontrolled temperature decay is added to the initial temperature pulse which has been shown to contribute significantly to the response. The component of the response due to the "temperature tail" is somewhat variable and can be identified as a source of error.

Caloric stimulation applied during continuous irrigation has been found advantageous from two points of view. First, the temperature in the ear canal could be controlled accurately and the rate of heat

transfer considered constant. Secondly, the subjects seemed to habituate rapidly to water irrigation and presumably the state of arousal was maintained at a more constant level than could be achieved in a standard test. In the latter procedure, the surprise due to sudden flushing of the ear is added to the effect of the stimulus itself and may cause wide variations of arousal.

The sequence of four irrigation in the standard test was designed to provide measures of the sensitivities to hot and cold in each ear. These basic measures could be obtained equally well from one adequately chosen temperature stimulus successively applied to each ear. For instance, the stimulus might be a temperature sine function of limited duration say at a frequency of 0.006 Hz. The steady state responses to hot and cold waves are normally symmetrical and the peak values should provide sound measures of hot and cold sensitivities. Of course, these measures could be used to derive directional preponderance and canal preponderance as is usually done.

The use of a sinusoidal stimulus may be justified in practice since it has been shown that steady state is achieved rapidly (except for a bias that can be accounted for). Indeed, the effects of the transient are relatively small below 0.01 Hz contrary to the previous indication of Young (1972). The influence of the transient could probably be further reduced by appropriately selecting the initial angle of the input function as may be done for other linear systems. One should also consider the off-transient and determine the optimal

return to initial conditions which would allow testing the other side with a minimum waiting time interval.

The above technique should not only reduce the test duration but insure a more steady level of arousal for both hot and cold responses. It should also make it possible to offset (during an initial stabilization period) any significant bias due to individual differences in body temperature.

Concluding Remarks

Traditionally, caloric stimulation has been used largely on an empirical basis and mostly in clinical vestibular function testing. The present study has demonstrated that the caloric response can be analysed quantitatively in terms of a model representing the chain of thermal processes and vestibular dynamics. Techniques have been developed to provide precisely controlled temperature stimulation during continuous irrigation.

It is felt that caloric stimulation should be considered as a quantitative tool of research in vestibular physiology and it appears particularly suitable to study the phenomenon of vestibular adaptation. The need of basic research on the thermal processes has been pointed out which should increase the confidence in the model and allow its use in the evaluation of clinical responses.

REFERENCES

AANTAA, E. (1967). Caloric test with air. Acta Otolaryng. Suppl. 224: 82-85.

ALBERNAZ, P.L. & GANANCA, M.M. (1972). The use of air in vestibular caloric stimulation. Laryngoscope 82: 2198-2203.

ASCHAN, G., BERGSTEDT, M. & STAHLE, J. (1956). Nystagmography, recording of nystagmus in clinical neuro-otological examinations. Acta Otolaryng. Suppl. 129.

BAERTSCHI, A. & ALLISON, J.L. (1972). A servo-controlled air stimulator for vestibular function testing. Proceedings of 25th Annual Conference on Engineering in Medicine and Biology (25th ACEMB) Bar Harbour, Florida.

BARANY, R. (1906). Untersuchungen über den vom Vestibularapparat des Ohres reflektorisch ausgelösten rythmischen Nystagmus und seine Begleiterscheinungen. Machr. Ohrenheik 43: pp. 191. (cited by Camis, 1930).

BARBER, H.O., WRIGHT, G. & DEMANUELE, F. (1971). The hot caloric test as a clinical screening device. Arch. Otol. 94: 335-337.

BERNSTEIN, L. (1965). Simplification of clinical caloric test. Arch. Otolaryng. 81: 347-349.

BRUNER, A. & NORRIS, T.W. (1971). Age related changes in caloric nystagmus. Acta Otolaryng. Suppl. 282.

BUYS, E. (1924). Rev d'oto-neuro-ocul. 2: 641. Cited by Henrikkson 1956.

CAMIS, M. (1930). The Physiology of the Vestibular Apparatus. Oxford University Press, London, England.

CAPPS, M.J., PRECIADO, M.C., PAPARELLA, M.M. & HOPPE, W.E. (1973). Evaluation of the air caloric test as a routine examination procedure. Laryngoscope 83: 1013-1021.

CARSLAW, H.S. & JAEGER, J.C. (1959). Conduction of Heat in Solids, Oxford University Press, London, England.

CAWTHORNE, T. & COBB, W.A. (1954). Temperature changes in the perilymph space in response to caloric stimulation in man. Acta Otolaryng. 44: 580-588.

CHENG, M. (1972). Point process analysis in the physiological study of human nystagmus. Ph.D. Thesis, McGill University, Montreal, Canada.

COLLINS, W.E. (1963). Manipulation of arousal and its effect on human vestibular nystagmus induced by caloric irrigation and angular acceleration. Aerospace Med. 34: pp. 134.

COLLINS, W.E. (1965). Subjective responses and nystagmus following repeated unilateral caloric stimulation. Annals Otology Rhinology and Laryng. 74: 1034-1055.

DAS, S.K. & MEHRA, Y.N. (1969). Caloric tests in passive vascular congestion of the labyrinth. An electronystagmographic study. Acta Otolaryng. (Stockholm) 67: 43-48.

DAYAL, V.S., FANKASHIDY, J. & KUZIN, B. (1973). Clinical evaluation of the hot caloric test as a screening procedure. Laryngoscope 83: 1433-1439.

DEMERS, R. & OUTERBRIDGE, J.S.O. (1974). Theoretical analysis of vestibular response to caloric stimulation. 5th Canadian Medical and Biological Engineering Conference, Montreal, Canada.

DE RUSSO, P.M., ROY, R.J. & CLOSE, C.M. (1965). State Variables for Engineers. John Wiley & Sons.

DOHLMAN, G. (1925). Physikalische und Physiologische Studien zur Theorie des Kalorischen Nystagmus. Acta Otolaryng. Suppl. 5.

van EGMOND, A.A.J., GROEN, J.J. & JONGKEES, L.B.W. (1949). The mechanics of the semicircular canal. J. Physiol. 110: 1-17.

van EGMOND, A.A.J.& TOLK, J. (1954). On the slow-phase of caloric nystagmus. Acta Otolaryng. 44: 589-593.

FITZGERALD, G. & HALLPIKE, C.S. (1942). Studies in human vestibular function: I. Observations on the directional preponderance ("Nystagmusbereitschaft") of caloric nystagmus resulting from cerebral lesions. Brain 65: 116-137.

FLUUR, E. & MENDEL, L. (1962a). Habituation, efference and vestibular interplay. I. Monaural caloric habituation. Acta Otolaryng. 55: 65-80.

FLUUR, E. & MENDEL, L. (1962b). Habituation, efference and vestibular interplay. II. combined caloric habituation. Acta Otolaryng. 55: 136-144.

FORSMANN, B., HENRIKSSON, N.G. & DOLOWITZ, D.A. (1963). Studies on habituation of vestibular reflexes. VI. Habituation in darkness of calorically induced nystagmus laterotorsion and vertigo in man. Acta Otolaryng. (Stockh.) 56: 663-674.

GATES, G.A., YOUNG, J.H. & WINEGAR, L.K. (1970). The thermoelectric air stimulator. Arch. Otolaryng. 92: 80-84.

GENTLES, W. & BARBER, H.O. (1974). Human vs. automated techniques in analysis of post-caloric nystagmus. C.J. Otolaryng. 3: 27-36.

GONSHOR, A. & MALCOLM, R. (1971). Effect of changes in illumination level on electro-oculography (EOG). Aerospace Med. 42: 138-140.

GUSEV, V.M., KISLYAKOV, V.A., LEVASHOV, M.M., ORLOV, I.V. & POLONNIKOV, R.I. (1970). Investigations on the receptors of the vestibular apparatus as angular acceleration sensors. From "Technical and biological problems of control a cybernetic view". Iberal A.S., & Reswick, J.B. Eds.

HALAMA, A. & HINCHCLIFFE, R. (1970). Studies on a clinical caloric test. Journal of Laryngology and Oxology. Vol. 84 No. 2 pp. 149-153.

HALLPIKE, G.S. & HOOD, J.D. (1953). The speed of the slow component of ocular nystagmus induced by angular acceleration of the head: its experimental determination and application to the physical theory of the cupular mechanism. Proc. Roy. Soc. B. 141: 216-230.

HARRINGTON, J.W. (1969). Caloric stimulation of the labyrinth experimental observations. Laryngoscope 79: 777-793.

HASTINGS, C. Jr. (1955). Approximation for Digital Computers. Princeton University Press, Princeton, New Jersey.

HENRIKKSON, N.G. (1956). Speed of slow component and duration in caloric nystagmus. Acta Otolaryng. Suppl. 125.

HENRIKKSON, N.G., KOHUT, R. & FERNANDEZ, C. (1961). Studies on habituation of vestibular reflexes. I. Effect of repetitive caloric test. Acta Otolaryng. 53: 333-349.

IGARASHI, M. (1966). Dimensional study of the vestibular end organ apparatus. In 2nd Symposium on the Role of Vestibular Organs in Space Exploration. NASA SP-115, 47.

ISHIYAMA, E. & KEELS, E.W. (1970). Preliminary results in intra-labyrinthine temperature changes in the vestibular labyrinth during caloric stimulation. Pract. Oto-rhino-laryng. 32: 231-239.

HOOD, J. (1973). Persistence of response in the caloric test. Clinical Aviation and Aerospace Medicine 44: 444-449.

JONES, G.M. & MILSUM, J.H. (1965). Spatial and dynamic aspects of visual fixation. IEEE Trans.Bio.Med.Eng. BME-12 54-62.

JONES, G.M. & SPELLS, K.E. (1963). A theoretical and comparative study of the functional dependence of the semicircular canal upon its physical dimensions. Proc. Roy. Soc. B 157: 403-419.

JONES, R. (1969). Biological Central Mechanisms in Biological Engineering (Ed. P.H. Schwan) McGraw Hill, New York.

JONGKEES, L.B.W. (1948). Value of the caloric test of the labyrinth. Arch Otolaryng. 48: 402-417.

KLEINFELDT, D. & DAHL, D. (1969). Temperaturmessungen am menschlichen bogengang Nach Thermischer Reizung. Acta Oto-laryng. 68: 411-419.

LEBOVITZ, R.M. (1973). Caloric vestibular stimulation via UHF microwave irradiation. IEEE Trans.Bio.Med.Eng. BME-20 119-126.

LIDVALL, H.F. (1961a). Vertigo and nystagmus responses to caloric stimuli repeated at short intervals. Acta otolaryng. 53: 33-44.

LIDVALL, H.F. (1961b). Vertigo and nystagmus responses to caloric stimuli repeated at short and long intervals. Acta otolaryng. 53: 507-518.

LITTON, W.B. & MCCABE, B.F. (1967). Thermal vestibulometry: technique and clinical aspects. From International Symposium on Sensorineural Hearing Processes and Disorders. Henry Ford Hospital, Detroit. (A.B. Abraham Ed.) Little Brown Boston.

MAFFEI, G., ZINI, C. & BOTTAZI, D. (1967). Stimulatore termico labrintico a controllo automatico della temperatura. Arch ital. otol. 78: 668-772.

MALCOLM, R. & MELVILL JONES, G. (1970). A quantitative study of vestibular adaptation in humans. Acta Otolaryng. 70: 126-135.

MAYNE, R. (1965). The "match" of the semicircular canals to the dynamic requirements of various species. In The Role of Vestibular Organs in the Exploration of Space. NASA SP-77: 57-67.

MCLACHLAN, N.W. (1955). Bessel Function for Engineers. Oxford University Press, London, England 2nd Edition.

MILLER, K.S. (1956). Engineering Mathematics. Holt Reinhart & Winston, New York.

MONEY, K.E., BONEN, L., BEATTY, J.D., KUEHN, L.A., SOKOLOFF, M. & WEAVER, R.S. (1971). Physical properties of fluids and structures of vestibular apparatus of the pigeon. Am.J.Physiol. 220(1): 140-147.

MONNIER M. (1967). Central mechanisms of vestibular and optokinetic nystagmus. In Myotatic, Kinesthetic and Vestibular Mechanisms CIBA Foundation Symposium (A.V.S. de Reuck & J. Knight Eds.) Churchill, London, England.

MONNIER, M., BELIN, I. & POLE P. (1970). Facilitation, inhibition and habituation of the vestibular responses. In Advances in Oto-Rhino-Laryngology 17 pp. 28-55. Karger, Basel/München/New York.

MONRO, D.M. (1970). Digital filters for digital simulation. Unpublished report Engineering in Medicine Laboratory, Department of Electrical Engineering, Imperial College of Science and Technology, London, England.

MILSUM, J.H. (1966). Biological Control Systems Analysis. McGraw Hill Inc., New York.

OLVER, F.W.J. (1964). Bessel functions of integer order. In Handbook of Mathematical Functions with Formulas, Graph and Mathematical Tables. M. Abramowitz and I.A. Stegun (Eds.) National Bureau of Standards. Superintendent of Documents, Washington D.C.

OMAN, C.M. & YOUNG, L.R. (1972). The physiological range of pressure difference and cupula deflection in the human semicircular canal. Acta Otolaryng. 74: 327-331.

RALSTON, A. (1965). A First Course in Numerical Analysis. McGraw Hill Inc., New York.

SCHACKEL, B. (1967). Eye movement recording by electrooculography. From A Manual of Psychophysiological Methods. North Holland Pub. Co.

SCHMALTZ, G. (1932). The physical phenomena occurring in the semicircular canals during rotatory and thermic stimulation. Proc. Roy. Soc. Med. 25: 359-381.

SCHMALTZ, G. & VÖLGER, G. (1924). Ueben die Temperaturbewegung im Felsenbein ber der kalorischen Reizung des Vestibularapparates. Pflüg Arch. f.d.ges.Physiol. 204: 708-717. Cited by Camis 1930.

SPIEGEL, E.A. & ARONSON, L. (1933). Continuous stimulation of the labyrinth with sustained nystagmus. Arch Otolaryng. 17: 311-320.

STEER, R.W. (1967). The influence of angular and linear acceleration and thermal stimulation on the human semicircular canal. Sc.D. Thesis, M.I.T., Cambridge, Mass.

STEFFEN, T.N. & LINTHICUM, F.H. (1970). Continuous thermal vestibulometry and new technique of caloric examination. Annals of Otology Rhinology and Laryngology 79: 619-633.

STOCKWELL, Ch.W., GILSON, R.D. & GUEDRY, F.E.Jr. (1973). Adaptation of horizontal semicircular canal responses. Acta Otolaryng. 75: 471-476.

SUGIE, N. & MELVILL JONES, G. (1966). The mechanisms of eye movements Part II eye movements elicited by head rotation. Bull. Electrotechnical Lab. (Tokyo) Vol. 30 pp 574-586.

TOLE, J.R. & YOUNG, L.R. (1971). Mitnys. A hybrid program for on-line analyses of nystagmus. Aerospace Med. 42: 508-511.

TOROK, N. (1969). Nystagmus frequency versus slow-phase velocity in rotatory and caloric nystagmus. Ann. Oto 78: 625-639.

TOROK, N. (1970). The effects of arousal upon vestibular nystagmus. In Adv. Oto-Rhino-Laryng. Vol. 17 pp. 76-89. Karger, Basel/München/New.York.

YOUNG, J.H. (1972). Analysis of vestibular system responses to thermal gradients induced in the temporal bone. Ph.D. Thesis, University of Michigan.

YOUNG, L.R. & OMAN, C.M. (1969). Model for vestibular adaptation to horizontal rotation. Aerospace Med. 40: 1076-1080.

APPENDIX 1

COMPUTATION OF THE STEP RESPONSE

The step response of Young's torque model involves the co-error function (or 1 minus the error function). The latter can be approximated by a rational expression taken from Hastings (1955) and found in most mathematical handbooks. Thus the error function erf is given by

$$\text{erf}(u) = 1 - e^{-u2} \sum_{j=1}^{5} d_j \left[\frac{1}{1 + pu} \right]^j + e(u)$$

where

$$|e(u)| \leq 1.5 \times 10^{-7}$$

The values of p and d_j may be found in the following FORTRAN program listing, denoted respectively by p and array A. The program was used to calculate the theoretical step response of Young's torque model.

```
C- TO COMPUTE STEP RESPONSE OF TORQUE MODEL
C- EVALUATE INTEGRAL ONLY TO GET TORQUE MULTIPLY BY 2*C1
C-VERSION GRID TO BE USED WITH EVBAL PROGRAM
C-40 POINTS @ H=.5 AND .5 /@ .5
C
C-      X0      DISTANCE TO CANAL CENTER
C-      HTR     HEAT TRANSFER COEFFICIENT/BONE CONDUCTIVITY
C-      RAD     CANAL RADIUS
C
C       NORMALIZED TIME DIF 1   INTERVAL=.200*DT
C
C-SUBROUTINE CALLED DSF  TO INTEGRATE
C-      SEE IBM SSP MANUAL
C
        DIMENSION A(5),FACH(8),FACX(5),R(13),Z(13),Y(302)
        DOUBLE PRECISION Y1,Y2,YY,ARG,P,A
C
C       VECTOR A CONTAINS COEFFICIENTS OF APPROXIMATING POLYNOMIAL
C
        DATA A/ .25828592D0,-.28449673D0,1.42141374D0,
        1-1.45315202D0,1.06140542D0/
        DATA P/ .32759110D0/
        DATA RAD,X0N,HTRN/.3, .76,.5 /
        DATA FACH/ .125, .25, .5,1 ,2 ,4 ,8 ,16 /
        DATA FACX/ .6, .8,1 ,1 .25,1 .5/
C
        NREC=40
        NDAT=302
        NDATM2=NDAT-2
        NDATX=NDAT*2
        CALL SETFIL(1,'STEPT2',IERR,'DK ')
        DEFINE FILE 1(NREC,NDATX,U,IV)
        IV=1
        PI=3.141592653
        DT=.02
        LIM=13
        HA=PI/(LIM-1 )
        DIF=1
        DO 15 II=1,5
        X0=X0N*FACX(II)
        DO 16 JJ=1,8
        HTR=HTRN*FACH(JJ)
        T=0
        DO 11 J=1,NDATM2
        T=T+DT
        XT=SQRT(T*DIF)

C
C-CALCULATE 13 POINTS AROUND THE CANAL CIRCUMFERENCE FROM -PI/2 TO +PI/2
C
        DO 30 K=1,LIM
        AI=K-1
        ANGLE=-PI/2 +AI*PI/(LIM-1 )
        XSTAR=X0+RAD*SIN(ANGLE)
        Y1=(XSTAR/2 /XT)
        ARG=Y1**2
        Y2=(XSTAR/2 /XT+HTR*XT)
        Y1=1.D0/(1.D0+P*Y1)
        Y2=1.D0/(1.D0+P*Y2)
        YY=0.D0
        DO 100 I=1,5
100     YY=YY+A(I)*(Y1**(I)-Y2**(I))
        IF(DABS(ARG) LT 87.D0)GO TO 50
        R(K)=0
        GO TO 30
50      R(K)=YY*(EXP(-ARG)*SIN(ANGLE)
30      CONTINUE
C-
C-INTEGRATE
C-
        CALL DSF(HA,R,Z,LIM)
        Y(J)=Z(LIM)
11      CONTINUE
C
C-STORE ON CONTIGUOUS FILES ON DISK
C
        Y(NDATM2+1)=HTR
        Y(NDATM2+2)=X0
        WRITE(1'IV)(Y(I),I=1,NDAT)
16      CONTINUE
15      CONTINUE
        END FILE 1
        STOP
        END
```

APPENDIX 2

CALCULATION OF CANAL CUPULAR DEFLECTION AND SLOW-PHASE EYE VELOCITY FROM TORQUE

The canal cupular deflection θ_c and the eye slow-phase velocity $\dot{\theta}_e$ have been calculated from torque M by recurrence formulae which are equivalent digital filters for a first order lag and a first order lead-lag. The method has been described by Monro (1970) to simulate simple transfer functions.

Consider sequences of the variables M, θ_c and $\dot{\theta}_e$ sampled at times $t_i = i\Delta t$, $i = 1, 2....N$ where Δt is the basic time interval between samples. θ_{c_i} is obtained from M by

$$\theta_{c_i} = \theta_{c_{i-1}} e^{-\gamma_1} \pm M_i \left[\frac{1 - e^{-\gamma_1}}{\gamma_1} \right] \qquad \text{(A.2.1)}$$

where

$$\gamma_1 = \Delta t/\tau_1 \qquad \text{(A.2.2)}$$

$\dot{\theta}_e$ is obtained from θ_c by

$$\dot{\theta}_{e_i} = \dot{\theta}_{e_{i-1}} e^{-\gamma_2} + G\left[\theta_{c_i} - \theta_{c_{i-1}} e^{-\gamma_2(1-m)}\right] \qquad (A.2.3)$$

where $$\gamma_2 = \Delta t/\tau_a \qquad (A.2.4)$$

and

$$G = \frac{1-m}{\left(1 - e^{-\gamma_2(1-m)}\right)} \left(1 - e^{-\gamma_2}\right) \qquad (A.2.5)$$

with $0 \leq m < 1$

For $m = 1$, G tends to the limit

$$G = \frac{1 - e^{-\gamma_2}}{\gamma_2} \qquad (A.2.6)$$

```
C-SUBROUTINE LAG APPLY FIRST ORDER LAG TO VECTOR Y
C-OUTPUT Y. NDAT IS VECTOR LENGTH
C-       TLAG=TIME CONSTANT
C
C-METHOD DEVELOPED BY MONRO SEE REPORT IMPERIAL COLLEGE, LONDON
C                                   BIOMEDICAL ENGINEERING PROGRAM
C                                   ELECTRICAL ENGINEERING
        SUBROUTINE LAG(DT, TLAG, Y, NDAT)
        DIMENSION Y(1)
        IF(TLAG EQ 0 )RETURN
        A2=1 /TLAG
        COEF2=EXP(-A2*DT)
        GAIN=(1 -COEF2)/A2
        YLAST=Y(1)
        DO 10 I=2, NDAT
        X=Y(I)
        Y1=YLAST*COEF2+X*GAIN
        YLAST=Y1
        Y(I)=Y1
10      CONTINUE
        RETURN
        END


C-SUBROUTINE TO SIMULATE ADAPTATION IN CALORIC RESPONSE MODEL
C-APPLY LEDLAG FILTER TO SEQUENCE Y ; OUTPUT IS Y
C-NDAT IS LENGTH OF VECTOR Y
C-       TA=ADAPTATION TIME CONSTANT
        SUBROUTINE LEDLAG(DT, TA, ZERO, Y, NDAT)
        DIMENSION Y(1)
C
        A1=ZERO/TA
        A2=1 /TA
        COEF1=EXP(-A1*DT)
        COEF2=EXP(-A2*DT)
        IF((1 -COEF1) LT 1 E-6)GO TO 4
        GAIN=A1/A2*(1 -COEF2)/(1 -COEF1)
        GO TO 5
4       GAIN=(1 -COEF2)/(A2*DT)
5       YLAST=0
        XLAST=Y(1)
        DO 2 I=2, NDAT
        Y1=YLAST*COEF2+(Y(I)-XLAST*COEF1)*GAIN
        XLAST=Y(I)
        YLAST=Y1
2       Y(I)=Y1
        RETURN
        END


$
```

APPENDIX 3

TORQUE TRANSIENT TO A SINUSOIDAL INPUT

The formula derived by Young (1972) to calculate the transient torque response to a sinusoidal input is given by

$$M = C_1 \frac{2\alpha h}{\pi} \int_0^{\pi} \int_0^{\infty} \cos\theta \cdot f(u) \; e^{-\alpha u^2 t} \; u \, du \, d\theta \qquad \text{A3.1}$$

$$\text{where} \quad f(u) = \frac{\omega \; u \cos(ux^*) + h \sin(ux^*)}{(d^2 u^4 + \omega^2)(h^2 + u^2)} \qquad \text{A3.2}$$

$$\text{and} \quad x^* = X_o + R \cos\theta \qquad \text{A3.3}$$

The other symbols are defined in the main text (see Chapter 3.0). The formula is valid if the input is a sine function applied at

$t' = 0$ with zero phase. In our work, Equation A3.1 was evaluated by direct integration using a standard subroutine QSF*.

Young used a faster technique based on a Gauss-Laguerre quadrature (DQL32).* However, it was found difficult to assess the accuracy of the quadrature technique which depended on the value of very high order derivatives ($n = 32$ in this case) (Ralston, 1965).

---

* system/360 Scientific Subroutine Package (360 - cm 03X) Version II International Business Corporation, 1966.

APPENDIX 4

VISUAL CURVE FITTING PROGRAM

The computer system was a medium size laboratory computer (PDP-11/20, Digital Equipment Corporation) with 16K core memory, a scope display, an analog-digital interface and a 1.2 M-word cartridge disc. The system operated with DOS (Disc Operating System) and all programs were written in FORTRAN IV. The system software included a number of special FORTRAN callable subroutines to operate the analog-digital interface and the scope display.

In a preliminary phase, torque step responses were calculated in the normalized time interval 0 - 3.0 divided in 300 steps. The responses were calculated for a grid of values in the X_o - h plane. In order to accommodate longer data files and larger diffusivity values, another bank of torque responses was obtained over the interval 0 - 6.0. For pulse responses, a 0 - 0.05 interval was used.

The curve fitting program listed at the end of this appendix is briefly explained. Experimental data are first read and a bank of theoretical responses is selected. A set of 6 potentiometers (P1 to P6) is sampled. The X_o - h coordinates are set by P1 and P2 and, if necessary, a new torque response is read in array Y from the disc. The array YOUT is used to represent the fitted response. According to the requested options, YOUT is modified to yield the response to a pulse of a given width and/or is filtered through the "canal" lag and the "adaptation" lead-lag filter (Appendix 2). The modified YOUT are then fitted to the data by appropriate adjustment

of bias P5 and gain P4. A time array (ITIM) is also computed according to diffusivity value set by P3. The theoretical response is displayed on the scope along with the experimental data point. During computation, the display is blanked out to avoid poor interaction with the user.

P6 acts as a switch that returns the program to potentiometer sampling or to keyboard control for selection of options.

Because of core limitation, a second program is chained to the curve fitting program to compute the mean squared deviation (SSQD) between experimental and theoretical curves. The times of the experimental points fall randomly between the equispaced points (y_i) of the theoretical sequence. Hence for any slow-phase velocity value SPV_j at time t_j between t_i and t_{i+1}, a new value y_j is obtained by linear interpolation from the values y_i and y_{i+1}.

SSQD is calculated according to

$$SSQD = \frac{1}{n} \sum_{j=1}^{n} \left(SPV_j - (GAIN \cdot y_j + BIAS) \right)^2$$

and is minimized with respect to GAIN by linear regression. Gain optimization was added at a later stage of program development to perform the analysis of SSQD in the parameter space.

```
C-TO EVECALL FIT EXP DAT TO THEOR CURVES FROM MODEL
C-THEORETICAL STEP RESPONSES IN STEP10 OR STEP12
C-"                "          "        GENERATED BY GRID PROGRAM 40 POINTS
C-DATA POINTS IN FILE EVDAT DAT
C-PARAMETER VALUE SELECTED BY MANIPULATING POT 1 TO 6
C-MODEL TIME=ITIM  OUTPUT=IFIT
C-DATA  TIME=IT    S P VELOCITY=ISPV
C
C-
C-SUBROUTINE CALLED      ADCRT SYSTEM SOFTWARE BY C G
C-                       RIDIS     "
C-                       PULSE     SEE APPENDED LISTING
C-                       LAG
C-                       ADAPT
      DIMENSION V(302),IFIT(302),ITIM(302),ICH(8),POT(8),NBIAS(8)
      DIMENSION IT(1300),ISPV(1300),IU(10)
      DIMENSION VOUT(202)
      DATA NBIAS/0.0,2E0,0.0,0.0,0.0,0/
      DATA POT/12 ,13 ,56 ,56 ,1 ,1 ,0 ,0 /
      DT= 01
C-READ EXP DATA
      CALL SETFIL(1,'EVDAT DAT',IERR,'OK')
      NREC2=1
      NDF2=2C&0
      DEFINE FILE 1(NREC2,NDF2,U,IW)
      IW=1
      READ(1'IW)TBEG,TMA),TIMCAL,SPVSCA,MPTS,(IT(I),ISPV(I),I=1,MPTS)
C
      ENDFILE 1
      NHIGH=200
      DIFN= 0025
      SIGNE=-1
      IFACT=8
      IVN=1
      NREC=40
      IDAT=20
      NDAT=302
      NDATM2=NDAT-2
      NDATX=NDAT+2
C-SELECT BANK OF THEORETICAL RESPONSES
C-READ IN FIRST RESPONSE
195   CALL SETFIL(2,'STEP10',IERR,'OK')
      GO TO 198
196   CALL SETFIL(2,'STEP12',IERR,'OK')
198   DEFINE FILE 2(NREC,NDATX,U,IV)
      IV=1
      NEW=1
      READ(2'IV)(V(I),I=1,NDAT)
C
      NDX=10
C-
C-
C-SAMPLE POT 1-6 ONLY ONCE
26    CALL ADCRT(IFACT,ICH,1,0,1,2,3,4,5,6)
C-READ ON DISK ONLY IF NEW VALUES OF P1,P2
      IF(NEW.EQ.1)GO TO 160
      IF(IABS(ICH(1)-ICH1LD) GT 1)GO TO 160
      IF(IABS(ICH(2)-ICH2LD) GT 1)GO TO 160
      IF(IABS(ICH(3)-ICH3LD) GT 1)GO TO 51
      GO TO 162
C-COMPUTE FILE INDX
160   NEW=1
      CALL RIDIS(ITIM,IFIT,20,2)
      ICH3LD=ICH(1)
      ICH2LD=ICH(2)
      IN=(NBIAS(1)+ICH(1))/POT(1)+1.
      IX=(NBIAS(2)+ICH(2))/POT(2)+1.
      IF(IX.LT.1 OR IX GT.5)GO TO 35
      IF(IN LT 1 OR IN GT 8)GO TO 35
      IVN=(IX-1)*8+IN
      IF(IVN.EQ IVOLD)GO TO 51
      IVOLD=IVN
      IV=IVOLD
      IF(IV.GT.NREC OR. IV.LE 0)GO TO 35
      GO TO 38
35    WRITE(6,21)IN,IX,IV
21    FORMAT(1H ,'OUT ORID',2I6)
      GO TO 26
38    READ(2'IV)(V(I),I=1,NDAT)
```

```
C--NEW DIFFUSIVITY ADJUST  ITIM VECTOR
51      DIF=(NBIAS(3)+ICH(3))/POT(3))*DIFN
C-BLANK DISPLAY WHILE RESETTING VECTORS
        CALL RTDIS(ITIM,IFIT,20,2)
        ICH_LOG=ICH(3)
        DO 48 I=1,NDATM2
        TIM1=(TBEG+I*DT,DIF)
        IF(TIM1 GT TMAX)GO TO 47
48      ITIM(I)=TIM1*TIMCAL
47      IF(I LT 20)I=20
        IDAT=I
C-ADJUST YOUT VECTOR ACCORDING TO OPTION
C-
49      DO 120 I=1,NDATM2
120     YOUT(I)=Y(I)
C-TO FIT A PULSE OF WIDTH WPULS
        IF(NPULS EQ 1)CALL PULSE(DIF,WPULS,YOUT,Y,DT,NDATM2,TMAX)
C-TO ADD CANAL DYNAMICS OR ADAPTATION
        DT1=DT/DIF
        IF(NADA EQ 1)CALL LEDLAG(DT1,TADAPT,ZERO,YOUT,NDATM2)
        IF(NCAN EQ 1)CALL LAG(DT1,TCAN,YOUT,NDATM2)
C-ADJUST FOR BIAS AND GAIN AND DIRECTION
162     GAIN=10 **(ICH(4)/POT(4))
        BIAS=(NBIAS(5)+ICH(5))/POT(5)
C-DISPLAY CONTINUOUSLY ON SCOPE REFRESH RATE SET BY EXTERNAL TRIGGER
C-
C-DISPLAY IN X-Y MODE (ITIM,IFIT) AND (IT,ISPV)
        CALL RTDIS(ITIM,IFIT,IDAT,2,IT,ISPV,MPTS,2,NDX,IU,10,1)
C-COMPUTE NEW IFIT
        DO 50 I=1,NDATM2
        IF(I LE 10)IU(I)=BIAS*SIGNE
        YX=YOUT(I)*GAIN+BIAS
        IF(YX GT 4096)YX=4096
50      IFIT(I)=YX*SIGNE
        NEW=0
C-POT 6 RETURN CONTROL TO CONSOLE FOR OPTIONS
27      IF(ICH(6) LT NHIGH)GO TO 26
14      WRITE(6,101)
101     FORMAT('& -$SQ-1  PAR 2 EYBAL-3 NW FIL 4 PULS 5 ADA-6 REV-7
        1 QR 0 1-0'/)
        READ(6,130)MARK
        GO TO(10,11,26,12,125,126,185,190),MARK
C-TYPE  PARAMETER VALUES
11      RELGEN=GAIN/SPVSCA
        BIASRL=BIAS/SPVSCA
        WRITE(6,102)Y(NDATM2+1),Y(NDATM2+2),DIF,RELGEN,BIASRL
102     FORMAT('& WTR    X0     DIF     GAIN     BIAS'//
        11H ,5G15 6///)
        GO TO 14
C-PULSE OPTION ENTER RESET TIME
125     WRITE(6,127)
127     FORMAT('&1 -PULS,TEND'/)
        READ(6,128)NPULS,TEND
128     FORMAT(I1,F6.0)
        WPULS=TEND-TBEG
        NEW=1
        GO TO 49
C-CANAL DYNAMICS AND ADAPTATION TIME CONSTANT
126     WRITE(6,129)
129     FORMAT('&NADA-NCAN-TADAPT-ZERO-TCAN- 211---2F6.0'/)
        READ(6,130)NADA,NCAN,TADAPT,ZERO,TCAN
130     FORMAT(2I1,2F6.0)
        NEW=1
        GO TO 49
C-FOR A NEW BANK OF STEP RESPONSE
190     WRITE(6,191)
191     FORMAT('&GRID NO,$PACE,DT'/)
        READ(6,130)MARK,NDUM,DT
        ENDFILE 2
        IF(MARK.NE.0)GO TO 193
        GO TO 196
C-DATA OUTPUT TO CHAIN TO $SQD PROGRAM
18      WRITE(6,172)
172     FORMAT('&TO GET $SQ RU,$SQ PRO WITH PARAM'/)
        WRITE(6,173)DT,DIF,GAIN,BIAS,TCAN,TADAPT,ZERO,SIGNE,NPULS
173     FORMAT(E13.6)
        WRITE(6,174)IV
174     FORMAT(I3)
        GO TO 14
C-TO REVERSE DIRECTION OF MODEL RESPONSE
185     SIGNE=-SIGNE
        GO TO 14
63      STOP
        END
```

```
C-TO COMPUTE PULSE RESPONSE FROM STEP RESPONSE
C-SUBROUTINE TO EYBALR PROGRAM
C
      SUBROUTINE PULSE(DIF,WPULS,YOUT,YGRID,DT,NMAX,TMAX)
      DIMENSION YOUT(1),YGRID(1)
      DO 1 I=1,NMAX
1     YOUT(I)=YGRID(I)
      NEND=WPULS*DIF/DT
      NEND=NEND+1
      IF(NEND GT NMAX)GO TO 5
      DO 2 I=NEND,NMAX
      YOUT(I)=YOUT(I)-YGRID(I-NEND+1)
2     CONTINUE
      RETURN
5     WRITE(6,3)
3     FORMAT(' &WIDTH EXCEED BASIC VECTOR LENGTH'/)
      RETURN
      END
```